Journal of Hydraulic Engineering

A Two-Dimensional Two-Phase Depth-Integrated Model for Transients over Mobile Bed

--Manuscript Draft--

Manuscript Number:	HYENG-8852R3
Full Title:	A Two-Dimensional Two-Phase Depth-Integrated Model for Transients over Mobile Bed
Manuscript Region of Origin:	ITALY
Article Type:	Technical Paper
Abstract:	Fast geomorphic transients may involve complex scenarios of sediment transport, occurring near the bottom as bed load (i.e. saltating, sliding and rolling) or as suspended load in the upper portion of the flow. The two sediment transport modalities may even coexist or alternate each-other during the same event, especially whenever the shear stress varies considerably. Modeling these processes is therefore a challenging task, for which the usual representation of the flow as a mixture may result unsatisfactory. In the present paper a new two-phase depth-averaged model is presented, which accounts for variable sediment concentration both in bed and suspended loads. Distinct phase velocities are considered for bed load, while the slip velocity between the two phases is neglected in the suspended load. It is shown that the resulting two-phase model is hyperbolic and the analytical expression of the eigenvalues is provided. The entrainment/deposition of sediment between the bottom and the bed load layer is based on a modified van Rijn transport parameter, while for the suspended sediment a first-order exchange law is considered. A numerical finite-volume method is employed for the simulation of three literature dam-break experiments, which are effectively reproduced in terms of both free surface elevation and bottom deformation, confirming the key role played by the solid concentration variability even for two-phase models.
Corresponding Author:	Massimo Greco University Federico II of Naples Napoli, ITALY
Corresponding Author E-Mail:	grecom@unina.it
Order of Authors:	Cristiana Di Cristo, Ph.D
	Massimo Greco
	Michele Iervolino, Ph.D
	Angelo Leopardi, Ph.D
	Andrea Vacca, Prof., Ph.D
Suggested Reviewers:	Ana Maria A.F. da Silva amsilva@civil.queensu.ca Expertise in the field covered by the manuscript
	Mustafa S. Altinakar altinakar@ncche.olemiss.edu Expertise in the field covered by the manuscript
	Catherine Swartenbroekx catherine.swartenbroekx@uclouvain.be Expertise in the field covered by the manuscript
Opposed Reviewers:	
Additional Information:	
Question	**Response**
Is the article being considered for more than one journal?	no

The Journal of Hydraulic Engineering does not review manuscripts that are being submitted simultaneously to another organization or ASCE journal for publication.	
Is this article already published? Material that has been previously published cannot be considered for publication by ASCE. A manuscript that has been published in a conference proceedings may be reviewed for publication only if it has been significantly revised. If you answer YES, please explain.	no
Have all the authors contributed to the study and approved the final version? All authors must have contributed to the study, seen the final draft of the manuscript, and accept responsibility for its contents. It is unethical to list someone as a coauthor who does not want to be associated with the study and who has never seen the manuscript.	yes
Was an earlier version of the paper previously considered and declined by ASCE? Declined manuscripts are sent through the review process again. If your manuscript has been submitted to us before under a different title, please provide that title in the space provided below. It is our policy to inform an editor that a manuscript has been previously reviewed, even when it has been reviewed by a different Division, Institute, or Council within ASCE.	no
Do your table titles/figure captions cite other sources? If you used a figure/table from another source, written permission for print and online use must be attached in PDF format. Permission letters must state that permission is granted in both forms of media. If you used data from another source to create your own figure/table, the data is adapted and therefore obtaining permission is not required.	no
Does your paper exceed 10,000 words? If YES, please provide justification in your cover letter. If you need help estimating word length, see our sizing worksheet at this link: Sizing Worksheet. If you have questions about the Sizing Worksheet, please see the Sizing Worksheet Instructions.	yes

Estimates for color figures in the printed journal begin at $924. Cost increases depend on the number and size of figures. Do you intend for any figure to be printed in color? If YES, how many and which ones? Please provide a total count and also list them by figure number.	no
Is this manuscript a companion to one already submitted/or being submitted? If yes, please note whether this is part I, II, or III. Please make sure all related papers are uploaded on the same day and provide the date of submission, title, and authors of each.	no
Is this manuscript part of a Special Issue? If yes, please provide the Special Issue title and name of the guest editor.	no
To read ASCE's Data Sharing Policy, please click on the "Instructions" link associated with this question. According to this policy, you are required to report on any materials sharing restrictions in your cover letter. Are you restricted from sharing your data & materials? If yes, did you report on these in your cover letter?	no

Dear Editor in Chief,

Please find below the revised version of manuscript HYENG-8852R2, now titled "A Two-Dimensional Two-Phase Depth-Integrated Model for Transients over Mobile Bed" by Cristiana Di Cristo, Massimo Greco; Michele Iervolino, Angelo Leopardi and Andrea Vacca.

We thank you, the Associate Editor and the reviewers for the important comments, which helped us to improve the quality of the paper.

Following your formal recommendation and referees' suggestions, we have revised the manuscript, complying with all of the comments and concerns.

Best regards,

Massimo Greco

Massimo Greco - Università di Napoli "Federico II"
Dipartimento di Ingegneria Civile, Edile e Ambientale - VIA CLAUDIO 21
80125 Napoli - ITALY

A Two-Dimensional Two-Phase Depth-Integrated Model for Transients over Mobile Bed

Cristiana Di Cristo[1]; Massimo Greco[2]; Michele Iervolino[3]; Angelo Leopardi[4]; Andrea Vacca[5]

Abstract: Fast geomorphic transients may involve complex scenarios of sediment transport, occurring near the bottom as bed load (i.e. saltating, sliding and rolling) or as suspended load in the upper portion of the flow. The two sediment transport modalities may even coexist or alternate each-other during the same event, especially whenever the shear stress varies considerably. Modeling these processes is therefore a challenging task, for which the usual representation of the flow as a mixture may result unsatisfactory.

In the present paper a new two-phase depth-averaged model is presented, which accounts for variable sediment concentration both in bed and suspended loads. Distinct phase velocities are considered for bed load, while the slip velocity between the two phases is neglected in the suspended load. It is shown that the resulting two-phase model is hyperbolic and the analytical expression of the eigenvalues is provided. The entrainment/deposition of sediment between the bottom and the bed load layer is based on a modified van Rijn transport parameter, while for the suspended sediment a first-order exchange law is considered. A numerical finite-volume method is employed for the simulation of three literature dam-break experiments, which are effectively reproduced in terms of both free surface elevation and bottom deformation, confirming the key role played by the solid concentration variability even for two-phase models.

Key words: Two-phase depth-integrated model, Variable concentration, Bed load, Suspended load, Finite-Volume Method.

INTRODUCTION

Morphological evolution in river, estuarine and tidal environments involves the interplay of fluid flow, sediment transport and loose bed deformation. During extreme events, as flash-floods, avalanche-induced floodwaves, debris-flows or dam collapses, the above processes may evolve with comparable time-scales. The resulting morphological evolution may lead to dramatic consequences in terms of damages and losses of human lives (Brooks and Lawrence, 1999). Analysis and prediction of these fast morphological transients are therefore mandatory for hazard assessment (Sturm, 2013). The present paper aims to contribute in this field presenting a two-phase depth-integrated model suitable for fast unsteady flows, involving sediment transport and bed deformation.

[1] Assistant Professor, Università di Cassino e del Lazio Meridionale, Cassino, Italy. Email: dicristo@unicas.it
[2] Full Professor, Università di Napoli “Federico II”, Napoli, Italy. Email: grecom@unina.it
[3] Assistant Professor, Seconda Università di Napoli, Aversa, Italy. Email: michele.iervolino@unina2.it
[4] Assistant Professor, Università di Cassino e del Lazio Meridionale, Cassino, Italy. Email: a.leopardi@unicas.it
[5] Associate Professor, Seconda Università di Napoli, Aversa, Italy. Email: vacca@unina.it

During unsteady morphological processes the sediment entrained from the bed is transported through bed load and suspended load. The former occurs under moderate bottom shear stress, the latter pertains to higher bottom shear stress.

The bed load motion is strongly affected by particle-bottom and particle-particle collisions and by the drag received by the fluid. The suspended load is mainly characterized by the convection by the carrying fluid, often with negligible slip velocity and particle contacts. In presence of a strong spatial and/or temporal variability of the bed shear stress, the two transport modalities may coexist or alternate each-other.

Experimental modeling of fast geomorphic transients encounters strong difficulties. In fact, high-resolution measurements in both time and space of flow field, sediment transport and bottom deformation are tremendously expensive, beyond the capabilities of most laboratories. With the growing availability of computational resources, the mathematical modeling of these processes is becoming a more and more interesting alternative for practitioners and researchers.

The present study follows a deterministic approach, describing the main features of the sediment transport in terms of time-averaged flow properties only. This approach has the great advantage that the sediment dynamics may be analyzed without the detailed knowledge of the whole process, at the price of losing some information concerning the turbulence dynamics. Although this approach is the most used in engineering applications, different analyses have been alternatively developed accounting for the turbulence effect on the sediment transport. For instance, starting from experimental evidences and following a stochastic approach, Papanicolaou et al. (2002a) developed a theoretical model for the inception of sediment motion, accounting for near-bed turbulent structures and bed micro-topography. Wu and Chou (2003), incorporating the probabilistic features of the turbulent fluctuations and of the bed-grain geometry, investigated the probability of rolling and lifting for the sediment entrainment. Cheng (2006) showed that the mobility probability of a bed particle may be either enhanced or weakened by an increase of the shear stress fluctuation. In case of low sediment entrainment, the mobility probability is increased by the turbulence, while it is reduced by the shear stress fluctuation if the average bed shear stress becomes relatively high. Wong et al. (2007) designed a detailed experiment to predict the probability density function for the particle virtual velocity and the thickness of the active layer, showing that the statistics of tracer displacements can be related to the macroscopic aspects of the bed load. Furbish et al. (2012) provided a probabilistic definition of the bed load sediment flux. Their formulation is shown to be consistent with experimental measurements and simulations of particle motion. Additionally, either numerical solution of the Reynolds Averaged Navier-Stokes (e.g. Duran et al., 2012; Marsooly and Wu, 2014) equations or of the Direct and Large Eddy Simulations (e.g. Keylock et al., 2005, Soldati and Marchioli, 2012) of the turbulent flows coupled with sediment particle motion provided useful insights about the role of the coherent structures on erosion / deposition dynamics.

In the following only depth-integrated models are considered and discussed. These models do not explicitly account for the dynamics of the very near-bed zone, i.e. the roughness layer. In such a layer, since the flow around sediment particles is strongly three-dimensional and influenced by wakes shed by grains, the velocity profile can significantly deviate from the logarithmic one (Byrd and Furbish, 2000; Wohl and Thompson, 2000). Considering that the mixing from wakes shed by particles induces a change in the eddy viscosity (Lopez and Garcia, 1996; Nikora and Goring, 2000; Defina and Bixio, 2005), Lamb et al. (2008) assumed a mixing length proportional to the roughness height and derived a parabolic velocity profile, instead of a logarithmic one, in the layer.

Depth-integrated models may be further distinguished between coupled and de-coupled ones. In the coupled models it is assumed that the sediment transport and the bottom evolution synchronously develop (Cao and Carling, 2002). On the other hand, de-coupled models assume a time-scale hierarchy, by which hydrodynamics is usually considered to be faster than the sediment transport and the bottom evolution.

Common examples of de-coupled models are those built up by supplementing a proper fixed-bed hydrodynamic model with a sediment continuity equation (the so-called Exner equation). In the simplest formulation (Graf, 1998), the solid discharge is further assumed to instantaneously adapt to the transport capacity, which is estimated by means of empirical relationships proposed for uniform flow conditions (Graf, 1998; Wang and Wu, 2005). In many real situations this hierarchy is not respected and the application of these models is questionable. Limitations of the de-coupled approach have been discussed in literature (Cao et al., 2002, Garegnani et al. 2011), along with the drawbacks of models based on immediate adaptation of the solid discharge to the transport capacity (Simpson and Castelltort, 2006; Di Cristo et al., 2006; Singh et al., 2004; Xia et al., 2010).

Among the existing coupled (i.e. non-equilibrium) morphological models, a further distinction arises from the representation of the fluid-sediment motion. They may be classified either as mixture or two-phase models, which is the type employed herein. To highlight the features of two-phase models, it is useful to firstly discuss the more popular mixture models. For relatively low solid concentrations, the rheological behavior of the mixture may be represented through a clear-water friction law (Wu, 2007; Wu and Wang, 2007; Sabbagh-Yazdi and Jamshidi, 2013). As far as hyperconcentrated mud flows are considered, non-Newtonian constitutive relations able to describe the shear-thinning behavior of the flow are employed in model based on full (Ancey, 2012) or simplified (Di Cristo et al., 2014a,b,d) wave dynamics.

The description of a stratified flow with clear-water above the mixture leads to the two-layer models, with equal (Fraccarollo and Capart, 2002) or distinct (Capart and Young, 2002, Li et al., 2013) velocities in the layers. However, within the transport layer no distinction is made between the motion regime of sediments and water. The interaction between mixture and clear-water layers is expressed through an interface shear-stress based on the analogy with the multi-layer shallow water models. Furthermore, most of these models (Capart and Young, 2002, Savary and Zech, 2007; Swartenbroekx et al., 2013) assume constant sediment concentration in the transport layer. These models are effective in the analysis of fast morphological transients (Spinewine et al., 2007, Chen and Peng, 2006), but the assumption of constant concentration under highly unsteady conditions has been recently questioned. Li et al. (2013) suggested that sediment concentration has to be considered as one of the unknowns of the numerical model, proposing an enhanced two-layer formulation through the application of the fundamental mass conservation law for sediment. Their numerical tests support the conclusion that bed load concentration variability has to be taken into account, if a detailed description of the sediment routing is sought for. It is worth of noting that the mixture models lack any explicit representation of the features of different transport regimes, i.e. bed load and suspended load, which are comprehensively lumped in the behavior of the mixture layer. Furthermore, in these models a hyperbolicity loss may occur in both subcritical and supercritical flow regimes (Savary and Zech, 2007; Greco et al., 2008b; Savary and Zech, 2008).

Two-phase modeling is an effective alternative for analyzing the morpho-hydrodynamics of rivers, debris flows and snow avalanches (Armanini, 2013). Usually, these models are deduced by averaging the conservation principles of mass and momentum for the liquid-solid mixture, considered as an equivalent continuous fluid characterized by unique physical characteristics and a unique velocity value, obtaining a phase-averaged system of equations with an unknown variable concentration (e.g. Dewals et al., 2011; Canelas et al., 2013). The system of partial differential equations is hyperbolic and it may be solved through standard finite volume schemes (Garegnani et al. 2011; Rosatti and Begnudelli, 2013). Alternatively, Greco et al. (2012a) proposed a two-phase model which separately considers the liquid and solid phases, accounting for the difference between their velocities and preserving the hyperbolic nature of the system (Evangelista et al., 2013). However, in Greco et al. (2012a) the hypothesis of a constant bed load concentration has been assumed and the suspended load has not been considered. Recent researches suggest that these two assumptions should be reconsidered. Indeed, the results by Li et al. (2013), even if referred to mixture models, suggest that the hypothesis of constant bed load concentration may represent a strong limitation. On the other hand, Zhang et al. (2013) recommend that the simulation of both bed load and suspended load may be required to analyze transients with a wide range of shear stress.

In the present paper a two-phase depth-integrated model is proposed, which is an extension of the preliminary version presented at the River Flow international conference (Di Cristo et al., 2014c). The model accounts for both the bed and suspended load. As far as the former is concerned, both the liquid-solid velocities difference and the concentration variability are considered. The suspended load is still described assuming the concentration variability, but neglecting the slip velocity between the two phases. The entrainment\deposition of sediments between the bottom and the bed load is evaluated by a formula based on the modified Van Rijn mobility parameter, while a diffusive vertical flux is assumed to drive the sediments towards the upper region of flow, where the suspended sediment transport occurs. The model is numerically integrated using a finite volume method and its performance is tested against literature experimental test cases, reporting also the comparison with other existing models.

The paper is structured in the following way: the proposed model is presented in next Section. In the first Subsection the governing equations are given, while the closures, the model mathematical characterization, i.e. its hyperbolic nature, and a concise presentation of the numerical model are reported in the last two Subsections. Then, the results of the model in reproducing experimental data are presented, along with the comparison with other literature models. Finally, the conclusions are drawn.

THE TWO-PHASE MODEL

Governing Equations

In the proposed two-phase model the following hypotheses are assumed:

- the liquid (ρ_l) and solid (ρ_s) densities are constant;
- the sediment is uniformly graded (with diameter d) and non-cohesive;
- there is no inflow/outflow from side-walls and free-surface;
- standing bed is saturated with a porosity p.

In the depth-integrated framework, the following shallow-water assumptions are also considered: the vertical components of both acceleration and velocity are neglected; the hydrostatic pressure distribution along the vertical axis is assumed. Despite these conditions are not strictly verified in the near-field of fast geomorphic transients (e.g. during the first instants and in the tip region of a dam-break), shallow-water depth-integrated models are widely applied also for simulating such events (e.g. Soares-Frazão et al., 2012; Li et al., 2013). In addition it is supposed that the volume concentration, $C_{s,b}$, along the vertical axis of the bed load region is constant and that the suspended sediment passively follows the motion of the fluid phase (Greco et al., 2012b).

It is worth of remarking that the bed load dynamics is described considering separately the liquid and solid phase, with distinct velocities and accounting for the momentum exchange between them, instead of assuming an equivalent homogeneous fluid with an unique velocity value, i.e. as a water-sediment mixture. Similarly to almost all of the geophysical flow models (e.g. Pitman and Le, 2005; Pudasaini et al., 2005; Pelanti et al., 2008), the lift and virtual (added) mass forces are neglected. As far as the latter force is concerned, Pudasaini (2012) has shown that its introduction in a two-phase model produces a strong coupling (in both time and space) between the stream-wise and cross-stream velocity components in the differential terms. However, the inclusion of this force allows only a slight improvement of the model performance in predicting fast processes. On the other side, it has been shown that this additional term, modifying the differential structure of the model, may cause a loss of hyperbolicity and therefore the mathematical well-posedness of the system equations is not guaranteed.

The governing equations, reported in the following, derive from the mass and momentum conservation for the liquid phase (Eq.1 and Eq.4) and solid phase, which moves as bed load (Eq.2 and Eq.5). Eq.3 represents the mass conservation of sediment moving as suspended load. Since it is assumed that the sediment velocity is equal to the liquid one in the region where suspended transport occurs, there is no drag between the two phases and therefore the momentum conservation equation for the suspended sediment is not needed. Finally, Eq.6 is the equation for predicting bed deformation. The complete set of equations reads:

$$\frac{\partial \delta_l}{\partial t} + \nabla \cdot \left(\delta_l \mathbf{U}_l \right) - p e_B = 0 \tag{1}$$

$$\frac{\partial \delta_{s,b}}{\partial t} + \nabla \cdot \left(\delta_{s,b} \mathbf{U}_s \right) - \left(1 - p\right) e_B + e_{s,b-s} = 0 \tag{2}$$

$$\frac{\partial \delta_{s,s}}{\partial t} + \nabla \cdot \left(\delta_{s,s} \mathbf{U}_l \right) - e_{s,b-s} = 0 \tag{3}$$

$$\frac{\partial \delta_l \mathbf{U}_l}{\partial t} + \nabla \cdot \left(\delta_l \mathbf{U}_l \mathbf{U}_l \right) + \nabla \left(\frac{g h^2}{2} \right) + g h \nabla \left(z_B \right) + \mathbf{S}_l = 0 \tag{4}$$

$$\frac{\partial \delta_{s,b} \mathbf{U}_s}{\partial t} + \nabla \cdot \left(\delta_{s,b} \mathbf{U}_s \mathbf{U}_s \right) + \frac{r}{r+1} \nabla \left(\frac{g {\delta_{s,b}}^2}{2 C_{s,b}} \right) + g \delta_{s,b} \frac{\Delta}{\Delta + 1} \nabla \left(z_B \right) + \mathbf{S}_{sb} = 0 \tag{5}$$

$$\frac{\partial z_B}{\partial t} + e_B = 0 \tag{6}$$

in which t is the time, g is the gravity acceleration; $r = (\rho_s - \rho_l)/\rho_l$ and $h = z_w - z_B$, where z_w and z_B are the free surface and bottom elevation, respectively. In Eqs.(1)-(5) δ_l denotes the liquid phase volume for unit bottom surface, $\delta_{s,b}$ (resp. $\delta_{s,s}$) is the solid phase volume transported as bed (resp. suspended) load for unit bottom surface so that $h=\delta_l+\delta_{s,b}+\delta_{s,s}$. $\mathbf{U}_l$ (resp. $\mathbf{U}_s$) is the phase-averaged water (resp. solid) velocity vector, e_B is the bottom erosion/deposition rate and $e_{s,b\text{-}s}$ is the sediment mass exchange between bed and suspended load. The second-order tensor $\mathbf{U}_l\mathbf{U}_l$ (resp. $\mathbf{U}_s\mathbf{U}_s$) represents the diadic product of the phase-averaged water (resp. solid) velocity with itself. Finally, denoting with $\mathbf{D}$ the stress due to drag exchanged between the two phases, the source terms of momentum equations $\mathbf{S}_l$ and $\mathbf{S}_{s,b}$ are:

$$\mathbf{S}_l = \frac{\boldsymbol{\tau}_{B,l}}{\rho_l} + \frac{\mathbf{D}}{\rho_l} \tag{7}$$

$$\mathbf{S}_{s,b} = \frac{\boldsymbol{\tau}_{B,s}}{\rho_s} - \frac{\mathbf{D}}{\rho_s} \tag{8}$$

in which $\boldsymbol{\tau}_{B,l}$ and $\boldsymbol{\tau}_{B,s}$ are the bottom shear stresses on the liquid and the solid phases, respectively. The drag force of the water on the solid particles, $\mathbf{D}$, is evaluated as:

$$\mathbf{D} = \rho_l C_D \frac{\delta_{s,b}}{d} \left(\mathbf{U}_l - \mathbf{U}_s\right)\left|\mathbf{U}_l - \mathbf{U}_s\right| \tag{9}$$

where C_D is a bulk drag coefficient. The shear stress acting on the solid phase $\boldsymbol{\tau}_{B,s}$ is expressed as:

$$\frac{\boldsymbol{\tau}_{B,s}}{\rho_s} = \mu_d g \delta_{s,b} \frac{r}{r+1} \frac{\mathbf{U}_s}{\left|\mathbf{U}_s\right|} + \alpha \mathbf{U}_s \left|\mathbf{U}_s\right| \tag{10}$$

in which μ_d is the dynamic friction coefficient. Eq.(10) accounts for both frictional, expressed through Mohr-Coulomb law, and interparticle collisional (Bagnold, 1956) stresses. Following Seminara et al. (2002), the shear stress on the liquid phase is evaluated by the following relation:

$$\boldsymbol{\tau}_{B,l} = \rho_l \frac{\mathbf{U}_l}{C_{\mathrm{Ch}}^2} \left|\mathbf{U}_l\right| - \boldsymbol{\tau}_{B,s} + \rho_l g \delta_{s,b} s_B \tag{11}$$

where s_B is the bottom slope. The first term is evaluated by means of the Chezy uniform flow formula, C_{Ch} being the dimensionless Chezy coefficient.

The bottom entrainment/deposition is expressed through the following formula proposed by Pontillo et al. (2010):

$$e_B = w_s \frac{T^{3/2} - C_{s,b}}{1-p} \tag{12}$$

in which w_s denotes the sediment settling velocity and $C_{s,b}$ is the bed load concentration. The dimensionless mobility parameter T accounts for the excess of the mobilizing stresses onto the bottom surface respect to the resisting ones (van Rijn, 1984). A large number of experiments has shown that the settling velocity reduces as the particle concentration increases. The following semi-empirical formula (Richardson and Zaki, 1954) is therefore considered to evaluate the sediment settling velocity:

$$w_s = w_t \left(1 - C_{s,b}\right)^n \tag{13}$$

in which w_t is the terminal settling velocity of a single particle in an indefinite fluid. According to Baldock et al. (2004) the exponent n is about 2.5 for particles with diameter of 1 mm, while it increases up to 5 for smaller sediments.

The mobility parameter T is herein defined as:

$$T = \frac{\left|\boldsymbol{\tau}_{B,l} + \boldsymbol{\tau}_{B,s} - \boldsymbol{\tau}_c - \boldsymbol{\tau}_B\right|}{\left|\boldsymbol{\tau}_c + \boldsymbol{\tau}_B\right|} \tag{14}$$

where τ_c is the threshold shear stress for sediment motion and $\left|\boldsymbol{\tau}_B\right| = \mu_s r g \delta_{s,b}$ is the Mohr-Coulomb stress at the bottom, with μ_s the static friction coefficient. Under clear-water conditions, Eq.(12) states that the erosion rate scales with the 3/2 power of the van Rijn transport parameter, which is consistent with Van Rijn findings (Van Rijn, 1984).

The solid exchange between the bed and suspended load is modeled through a first-order kinetic law (Wu et al., 2000):

$$e_{s,b-s} = \beta\omega\left(C^*_{s,s} - C_{s,s}\right) \tag{15}$$

in which $C_{s,s}$ represents the depth-averaged suspended sediment concentration, $C^*_{s,s}$ is the corresponding capacity value. The exchange is modulated by β and ω coefficients: the former relates the depth-averaged values to the local ones; the latter expresses the adaptation of suspended load and it is usually assumed as the sediment settling velocity (i.e.: $\omega = w_s$), as it is done also herein. The expression proposed by Armanini and Di Silvio (1988) is employed to evaluate β.

The capacity value for suspended sediment concentration is estimated through the following formula proposed by Wu et al. (2000) and Wu (2007):

$$C^*_{s,s} = 0.0000262 \frac{C_{s,b}\sqrt{gdr}\,d}{\left|\mathbf{U}_l\right|\left(C_{s,b}h - \delta_{s,b}\right)}\left[\left(\frac{\theta_0}{\theta_c} - 1\right)\frac{\left|\mathbf{U}_l\right|}{w_s}\right]^{1.74} \tag{16}$$

where $\theta_0 = \tau_0/(\rho_l g d r)$ is the Shields parameter computed through the modulus of the shear stress τ_0 at the bed without considering the transport layer, and θ_c is the corresponding threshold value for the sediment transport initiation.

Model Closures

The α and C_D coefficients may be estimated from existing empirical formulas (e.g. Maude and Whitmore 1958), which however introduce other parameters. As an alternative, in the present paper both coefficients are evaluated based on the analysis of uniform flow conditions. To this aim, the model is first applied to a uniform flow characterized by a bottom slope s_B. In such a condition the two-phase conservation equations (1)-(6) reduce to the following set of relations:

$$g\left(\delta_l+\delta_{s,b}+\delta_{s,s}\right)s_B=\frac{\tau_{B,l}}{\rho_l}+\frac{D}{\rho_l} \tag{17}$$

$$g\delta_{s,b}rs_B=\frac{\tau_{B,s}}{\rho_l}-\frac{D}{\rho_l} \tag{18}$$

$$C_{s,b}=T^{3/2} \tag{19}$$

$$\beta C_{s,s}=C_{s,b} \tag{20}$$

Similarly to Parker et al. (2003), the following scaling law for the bed load volume for unit bottom area is assumed:

$$\frac{\delta_{s,b}}{d}=k_1\left(\theta_0-\theta_c\right) \tag{21}$$

with k_1 a dimensionless coefficient. Although Eq.(21) was deduced only for low Shields parameter, i.e. $\theta_0 \leq 0.1$ (Fernandez-Luque and Van Beek, 1976), recent experiments (Lajeunesse et al., 2010) confirmed its validity up to $\theta_0 \approx 0.2$. In the present analysis, Eq. (21) is therefore applied even for higher Shields number.

The peculiarities of the solid particles motion in the bed load, through saltation, rolling and sliding have been deeply investigated through experimental studies, which suggested that the sediment velocity is different from that of the carrying fluid. Several formulas have been proposed for its evaluation, witnessing the importance of its correct computation for the bed load modeling. In particular, Meland and Norrman (1966) deduced an empirical expression of the sediment average transport velocity in terms of shear velocity, roughness size and particle diameter, based on a series of experiments with glass beads rolling on a bed of homogenously sized particles. The dimensional nature of this formula limits its validity to the range of the investigated experimental conditions. Fernandez-Luque and van Beek (1976), starting from experiments carried out with a loose bed, proposed the following expression of the particles average transport velocity U_p:

$$U_p=c_a\left(u_*-0.7u_{*c}\right) \tag{22}$$

in which u_* is the shear velocity and u_{*c} is the corresponding value in the Shields critical condition; c_a is a dimensionless constant approximately equal to 11.5.

A theoretical consideration about the dynamics of the bed load sediment transport led Bridge and Dominic (1984) to deduce the following expression for the bed grain velocity:

$$U_g=c_b\left(u_*-u_{*c}\right) \tag{23}$$

with $c_b=\sqrt{\tan\mu_d}\, w_s/u_{*c}$.

Moreover, Sekine and Kikkawa (1992), presenting a deterministic-probabilistic model to investigate the nature of the bed load motion, proposed the following expression for the bed load layer averaged mean velocity of saltation:

$$\frac{U_m}{\sqrt{gdr}} = 8\frac{u_*}{w_s}\left(1-\frac{u_{*c}}{u_*}\right)^{1/2} \tag{24}$$

The effectiveness of the dimensionless parameters of Sekine and Kikkawa (1992) for describing the motion of sediment particles over transitionally-rough beds has been successively confirmed by Papanicolaou et al. (2002b) and Ramesh et al. (2011).

Seminara et al. (2002), in deriving an entrainment-based model of sediment transport that neither satisfies nor suffers from the drawbacks of the Bagnold constraint, proposed a slight modification of the Fernandez Luque and van Beek (1976) formula, which reads:

$$U_p = c_a^{'}\left(\tau-\tau_c\right)^{1/2} \tag{25}$$

with the dimensionless coefficient c'_a ranging between 8 and 9. Recently Julien and Bounvilay (2013), based on a dimensional and regression analysis carried out considering bed load particles on smooth and rough rigid plane surfaces, proposed a simple single-parameter relation, which expresses the bed load particle velocity in terms of the shear velocity and of the logarithm of the Shields parameter of the boundary roughness.

In what follows, following Seminara et al. (2002), the solid phase average velocity in the bed load layer is assumed to be:

$$\frac{U_s}{\sqrt{gdr}} = k_2\left(\theta_0-\theta_c\right)^{1/2} \tag{26}$$

with k_2 an experimental dimensionless coefficient. By postulating the validity of Eqs. (21) and (26), the following expression of the bed load solid discharge is deduced:

$$\frac{U_s\delta_{s,b}}{d\sqrt{gdr}} = k_1k_2\left(\frac{\tau_0-\tau_c}{\rho_l gdr}\right)^{3/2} = k_1k_2\left(\theta_0-\theta_c\right)^{3/2} \tag{27}$$

Eq. (27) has the same structure of the well-known Meyer-Peter and Müller (1948) formula, which is exactly reproduced provided that the k_1k_2 product is set equal to the Meyer-Peter and Müller coefficient (K_{MPM}). K_{MPM} ranges from about 4, as indicated in the re-analysis of original Meyer-Peter and Müller's dataset described in Wong and Parker (2006), to 12, used in the numerical simulations reported in El Kadi Abderrezzak and Paquier (2011). The original and most used value of 8 (Meyer-Peter and Müller, 1948) is adopted in what follows. Assuming the classical value K_{MPM} = 8, the two empirical parameters k_1 and k_2 are fixed by considering the bounds deriving by the consistency of the model, as shown in the following.

The water velocity may be computed through the Chezy's law:

$$\frac{U_l}{\sqrt{gdr}} = C_{Ch}\theta_0^{1/2} \tag{28}$$

Finally, it is postulated that the shear stress acting on the liquid phase may be represented as follows:

$$\tau_{B,l} = \tau_c + c_1\left(\tau_0 - \tau_c\right) \tag{29}$$

with c_1 a non-negative parameter smaller than unity, i.e. $0 \le c_1 \le 1$. In fact, the case c_1=0 corresponds to the Bagnold's hypothesis, i.e. the shear between fluid and bottom reduces to the critical value (Bagnold, 1956). On the other hand, the condition c_1=1 implies that the shear stress acting on the liquid phase equals the corresponding value in absence of sediment transport, i.e. no momentum is transferred to the solid phase. However - as it will be shown later - a more restrictive upper bound may be specified for it. While clear indications may be found in the literature for estimating the C_{Ch} and K_{MPM} coefficients in their well-defined variability ranges, the dimensionless non-negative coefficient c_1 represents a free model parameter. In the Results section, classical literature values are assumed for C_{Ch} and K_{MPM}, while the c_1 coefficient is allowed to vary, in order to investigate its influence on the model predictions.

Substituting the relations (21), (26), (28) and (29) into Eq.(17), the following expression of the drag coefficient may be easily obtained:

$$C_D = \frac{1-c_1}{k_1}\frac{\rho_l gdr}{\left[C_{Ch}\tau_0^{1/2} - k_2\left(\tau_0 - \tau_c\right)^{1/2}\right]^2} \tag{30}$$

The substitution of (21) and (26) into the momentum equation of the solid phase in the bed load layer, Eq. (18), gives the following expression for α:

$$\alpha = \frac{\left(1-c_1\right) - k_1\left(\mu_d - s_B\right)}{\left(r+1\right)k_2^2} \tag{31}$$

Expressions (30) and (31), strictly valid only in uniform flow, are herein employed also in non-uniform conditions considering the local and instantaneous values of s_B and τ_0, for a fixed value of c_1. As far as the c_1 value is concerned, inspection of Eq. (31) enlightens that the positivity of the α coefficient imposes the following upper bound:

$$c_1 \le 1 - k_1\left(\mu_d - s_B\right) \tag{32}$$

The considered closures suggest a way to select the value for the k_1 coefficient, which has been experimentally found to vary between 0.66 (Seminara et al., 2002) e 2.51 (Lajeunesse et al., 2010). Indeed, rewriting the transport stage parameter T as:

$$T = \frac{(\theta_0 - \theta_c)(1 - k_1\mu_s)}{\theta_c + k_1\mu_s(\theta_0 - \theta_c)} \tag{33}$$

and the concentration $C_{s,b}$ as:

$$C_{s,b} = \frac{\delta_{s,b}}{K_s d} \tag{34}$$

with K_s the ratio of the bed load layer thickness to sediment diameter, the bottom entrainment/deposition condition (19) leads to the following expression for K_s:

$$K_s = \frac{k_1}{(1 - k_1\mu_s)^{3/2}} \frac{\left[\theta_c + k_1\mu_s(\theta_0 - \theta_c)\right]^{3/2}}{(\theta_0 - \theta_c)^{1/2}} \tag{35}$$

Moreover, accounting for Eq.(21), (35) may be equivalently rewritten in terms of the bed load volume for unit bottom area as follows:

$$K_s = \frac{k_1^{3/2}}{(1 - k_1\mu_s)^{3/2}} \frac{\left[\theta_c + \mu_s\,\delta_{s,b}/d\right]^{3/2}}{(\delta_{s,b}/d)^{1/2}} \tag{36}$$

Eqs. (35) or (36) indicates that the positiveness of K_s implies the following condition on k_1:

$$k_1 < \frac{1}{\mu_s} \tag{37}$$

Furthermore, for sufficiently large values of the shear stress, i.e. $(\theta_0 - \theta_c) >> \theta_c$, as those corresponding to sheet-flow regime, Eq. (35) can be approximated as:

$$K_s^{SF} \cong \frac{k_1^{5/2}\mu_s^{3/2}}{(1 - k_1\mu_s)^{3/2}}(\theta_0 - \theta_c) \tag{38}$$

and therefore the bed load concentration asymptotically approaches the value:

$$C_{s,b}^{SF} = \frac{(1 - k_1\mu_s)^{3/2}}{k_1^{3/2}\mu_s^{3/2}} \tag{39}$$

Since the asymptotic concentration (39) cannot exceed the sediment concentration in the erodible bottom, an additional condition for the k_1 value has to be respected:

$$k_1 \geq \frac{1}{\mu_s\left[1 + (1 - p)^{2/3}\right]} \tag{40}$$

In what follows the value of k_1 is evaluated as the average between the lower Eq.(37) and upper Eq.(40) bounds:

$$k_1 = \frac{1}{2\mu_s}\frac{2+(1-p)^{2/3}}{1+(1-p)^{2/3}} \tag{41}$$

It is easy to verify that for common values of the porosity (p) and of the static friction coefficient (μ_s), Eq. (41) provides values for the k_1 coefficient within the range of empirical values mentioned above. Furthermore, assuming the validity of the Meyer-Peter and Müller formula, the k_2 coefficient is determined as:

$$k_2 = \frac{K_{MPM}}{k_1} \tag{42}$$

In Figure 1, the consistency of the above set of closures is verified by comparing the prediction of the dimensionless saltation height provided by Eq. (35), with available experimental (Lee and Hsu, 1994; Nino et al., 1994; Nino and Garcia, 1998; Lee et al., 2000) and numerical (Wiberg and Smith, 1985) results. Since unfortunately the considered references do not specify the values of porosity and of the static friction coefficient, Eqs. (35) and (41) have been applied considering two reasonable pairs of (μ_s, p), namely (0.5, 0.6) and (1.0, 0.4). On the other hand, accordingly with the values provided for the dimensionless threshold shear stress in the reference data, θ_c has been assumed equal to 0.03 (Figure 1a) in the comparison with data of Lee and Hsu (1994) and Wiberg and Smith (1985), and equal to 0.06 in the comparison with data of Lee et al. (2000), Nino and Garcia (1998) and Nino et al. (1994), (Figure 1b).

Figure 1 shows that Eqs. (35) and (41) provide relatively accurate predictions of the bed load layer thickness up to values of the Shields parameter order of unity. The fairly good agreement justifies the use of the relation (21) for the sediment volume for unit bottom area in combination with the entrainment formulation proposed by Pontillo et al. (2010) up to $\theta_0 \approx 1$.

Model properties and numerical method

In order to show the hyperbolic character of the presented flow model, system (1)-(6) is rewritten in quasi-linear form. Accounting for (34) and (36) and without considering the source terms, it reads:

$$\mathbf{C}\frac{\partial \mathbf{W}}{\partial t} + \mathbf{A}\frac{\partial \mathbf{W}}{\partial x} + \mathbf{B}\frac{\partial \mathbf{W}}{\partial y} = 0 \tag{43}$$

in which, denoting with U and V the x and y components of velocity vector for both phases, the unknowns' vector $\mathbf{W}$ is:

$$\mathbf{W} = \begin{bmatrix} \delta_l \\ U_l \\ V_l \\ \delta_{s,b} \\ U_s \\ V_s \\ z_B \\ \delta_{s,s} \end{bmatrix} \tag{44}$$

and the **C**, **A**, **B**, matrices may be easily deduced from Eqs. (1)-(6), through standard algebra.

Following Courant and Hilbert (1961), the mathematical character of system (43) is investigated by looking for the eigenvalues of the matrix

$$\mathbf{M} = \mathbf{C}^{-1}\left(\mathbf{A}n_x + \mathbf{B}n_y\right) \tag{45}$$

with n_x and n_y the director cosines of an arbitrary direction in the (x, y) plane of the unitary vector $\boldsymbol{n}$. The eigenvalues read:

$$\lambda_1 = 0 \quad \lambda_{2,3} = \mathbf{U}_l \cdot \mathbf{n} \quad \lambda_4 = \mathbf{U}_s \cdot \mathbf{n}$$

$$\lambda_{5,6} = \mathbf{U}_l \cdot \mathbf{n} \pm \sqrt{gh}\sqrt{\frac{\delta_l + \delta_{s,s}}{\delta_l}} \; \lambda_{7,8} = \mathbf{U}_s \cdot \mathbf{n} \pm \sqrt{\frac{gdr}{2(r+1)}}\sqrt{K_s + \frac{dK_s}{d\delta_{s,b}}\delta_{s,b}} \tag{46}$$

in which the derivative of the dimensionless bed load layer thickness with respect to $\delta_{s,b}$ has the following expression:

$$\frac{dK_s}{d\delta_{s,b}} = \frac{1}{2\delta_{s,b}}\left(\frac{k_1}{1-k_1}\right)^{3/2}\sqrt{\frac{d}{\delta_{s,b}}\theta_c + \mu_s}\left(2\mu_s\frac{\delta_{s,b}}{d} - \theta_c\right) \tag{47}$$

Accounting for (47) eigenvalues $\lambda_{7,8}$ may be equivalently rewritten as follows:

$$\lambda_{7,8} = \mathbf{U}_s \cdot \mathbf{n} \pm \frac{1}{2}\sqrt{\frac{gdr}{r+1}}\sqrt{\left(\frac{k_1}{1-k_1}\right)^{3/2}\left(4\mu_s\frac{\delta_{s,b}}{d} + \theta_c\right)\sqrt{\frac{d}{\delta_{s,b}}\theta_c + \mu_s}} \tag{48}$$

From (46) and (48) it follows that, independently of the **n** unitary vector, the matrix **M** possesses only real eigenvalues. Therefore, the present two-phase model is always hyperbolic, and the characteristics theory allows to define the correct number of conditions on each boundary of the computational domain.

The model represented by Eqs. (1)-(6) may be equivalently rewritten in a compact form as follows:

$$\frac{\partial \mathbf{U}_c}{\partial t} + \frac{\partial \mathbf{F}\left(\mathbf{U}_c\right)}{\partial x} + \frac{\partial \mathbf{G}\left(\mathbf{U}_c\right)}{\partial y} + \mathbf{N} + \mathbf{S}_c = 0 \tag{49}$$

in which:

$$\mathbf{U}_c = \begin{pmatrix} \delta_l \\ \delta_{s,b} \\ \delta_{s,s} \\ U_l\delta_l \\ V_l\delta_l \\ U_s\delta_{s,b} \\ V_s\delta_{s,b} \\ z_B \end{pmatrix}; \quad \mathbf{N} = \begin{pmatrix} 0 \\ 0 \\ 0 \\ g\left(\delta_l + \delta_{s,b} + \delta_{s,s}\right)\dfrac{\partial z_B}{\partial x} \\ g\left(\delta_l + \delta_{s,b} + \delta_{s,s}\right)\dfrac{\partial z_B}{\partial y} \\ g\dfrac{r}{r+1}\delta_{s,b}\dfrac{\partial z_B}{\partial x} \\ \mathrm{g}\dfrac{r}{r+1}\delta_{s,b}\dfrac{\partial z_B}{\partial y} \\ 0 \end{pmatrix}; \quad \mathbf{S}_c = \begin{pmatrix} pe_B \\ (1-p)e_B - e_{s,b-s} \\ e_{s,b-s} \\ S_{l,x} \\ S_{l,y} \\ S_{s,x} \\ S_{s,y} \\ e_B \end{pmatrix} \tag{50}$$

and:

$$\mathbf{F} = \begin{pmatrix} \delta_l U_l \\ \delta_{s,b}U_s \\ \delta_{s,s}U_l \\ \delta_l U_l^2 + g\dfrac{\left(\delta_l + \delta_{s,b} + \delta_{s,s}\right)^2}{2} \\ \delta_l U_l V_l \\ \delta_{s,b}U_s^2 + g\dfrac{r}{r+1}\dfrac{\delta_{s,b}{}^2}{2C_{s,b}} \\ \delta_{s,b}U_s V_s \\ 0 \end{pmatrix}; \quad \mathbf{G} = \begin{pmatrix} \delta_l V_l \\ \delta_{s,b}V_s \\ \delta_{s,s}V_l \\ \delta_l U_l V_l \\ \delta_l V_l^2 + g\dfrac{\left(\delta_l + \delta_{s,b} + \delta_{s,s}\right)^2}{2} \\ \delta_{s,b}U_s V_s \\ \delta_{s,b}V_s^2 + g\dfrac{r}{r+1}\dfrac{\delta_{s,b}{}^2}{2C_{s,b}} \\ 0 \end{pmatrix} \tag{51}$$

It is worth of noting that vector **N** represents the non-conservative terms in the partial differential system, arising from the bed slope source term.

The system (49) can be solved with any of the numerical schemes commonly employed for hyperbolic PDEs. The Finite Volume solver FIVFLOOD (Leopardi et al., 2002, Greco et al., 2012a) has been adapted to solve the PDEs of the two-phase model, along with an appropriate treatment of the bed slope source term **N** (Valiani and Begnudelli, 2006; Greco et al., 2008a). To this aim, with reference to a structured rectangular mesh Eq. (49) is written in the following semi-discrete conservative form:

$$\frac{d\overline{\mathbf{U}_c}}{dt} = -\frac{1}{A_0}\left[\sum_{k=1}^{4}\left(\mathbf{H}_k \cdot l_k \mathbf{n}_k\right) - \overline{\mathbf{S}_c}\right] \tag{52}$$

In Eq.(52), the overbar denotes the averaging over the computational cell of area A_0, l_k is the length of the k-th side of the cell, $\mathbf{n}_k$ is the normal vector and $\mathbf{H}_k$ is the average value of the flux on the same side, defined as:

$$\mathbf{H}_k = \mathbf{F}' n_x + \mathbf{G}' n_y \tag{53}$$

being $\mathbf{F}'$ and $\mathbf{G}'$ the vectors of the numerical fluxes, modified as follows to include the slope terms:

$$\mathbf{F}' = \begin{pmatrix} \delta_l U_l \\ \delta_{s,b} U_s \\ \delta_{s,s} U_l \\ \delta_l U_l^2 + g \dfrac{\left(\delta_l + \delta_{s,b} + \delta_{s,s}\right)}{2} \left[\left(\delta_l + \delta_{s,b} + \delta_{s,s}\right) + z_B - \tilde{z}\right] \\ \delta_l U_l V_l \\ \delta_{s,b} U_s^2 + g \dfrac{r}{r+1} \dfrac{\delta_{s,b}}{2C_{s,b}} \left[\delta_{s,b} + z_B - \tilde{z}\right] \\ \delta_{s,b} U_s V_s \\ 0 \end{pmatrix}$$

$$\mathbf{G}' = \begin{pmatrix} \delta_l V_l \\ \delta_{s,b} V_s \\ \delta_{s,s} V_l \\ \delta_l U_l V_l \\ \delta_l V_l^2 + g \dfrac{\left(\delta_l + \delta_{s,b} + \delta_{s,s}\right)}{2} \left[\left(\delta_l + \delta_{s,b} + \delta_{s,s}\right) + z_B - \tilde{z}\right] \\ \delta_{s,b} U_s V_s \\ \delta_{s,b} V_s^2 + g \dfrac{r}{r+1} \dfrac{\delta_{s,b}}{2C_{s,b}} \left[\delta_{s,b} + z_B - \tilde{z}\right] \\ 0 \end{pmatrix} \tag{54}$$

$\tilde{z}$ is the bed elevation at the side of the cell opposite the one on which flux has to be evaluated; the terms in the square bracket are considered null if negative (Greco et al., 2008a).

Time integration of Eq. (52) is performed with a predictor-corrector (McCormack) scheme:

$$\mathbf{U}_c^{*} = \mathbf{U}_c^{t} - \frac{\Delta t}{A_0} \left[\sum_{k=1}^{4} \left(\mathbf{H}_k^{t} \cdot l_k \mathbf{n}_k \right) - \bar{\mathbf{S}}^{t} \right]$$

$$\mathbf{U}_c^{**} = \mathbf{U}_c^{t} - \frac{\Delta t}{A_0} \left[\sum_{k=1}^{4} \left(\mathbf{H}_k^{*} \cdot l_k \mathbf{n}_k \right) - \bar{\mathbf{S}}^{*} \right] \tag{55}$$

$$\mathbf{U}_c^{t+\Delta t} = \frac{\mathbf{U}_c^* + \mathbf{U}_c^{**}}{2}$$

The numerical fluxes at the interfaces are computed by a three-point parabolic interpolation of the conserved variables values. In the predictor stage, two cells on a side of the interface and one on the opposite side are considered, vice versa in the corrector stage. The numerical stability of the proposed method is guaranteed provided that the Courant–Friedrichs–Lewy condition is satisfied for the largest eigenvalue (Eqs.46).

TEST CASES AND RESULTS

In the next two sub-sections the proposed model is tested against two laboratory experiments: a one-dimensional dam-break, over a dry erodible bed (Capart and Young, 1998), and a two-dimensional dam-break, over both dry and wet bed (Soares-Frazão et al., 2012). Finally, in the last section of this paragraph, the present model is compared to four existing non-equilibrium models.

One dimensional dam-break

The first test case is the fast geomorphic transient experimentally investigated by Capart and Young (1998). The experiments were carried out at National Taiwan University and they consist of small-scale laboratory dam-break of initial water depth h_0 = 10 cm over an erodible bed in a prismatic rectangular channel. Notably, a very light sediment was employed (density ρ_s = 1048 kg m^{-3}) with d = 6.1 mm. Scouring propagates both upstream and downstream of the dam, where intense erosion occurs. Apart from the near-field evolution soon after the dam removal, the flood wave exhibits a rather regular shape characterized by a steep sediment-laden bore, at the front of the wave, and an enduring weak hydraulic jump at the centre of the wave.

As indicated by the experimenters, the bottom porosity p has been fixed equal to 0.6, while the sediment free-fall velocity w_t in Eq. (13) is assumed equal to 0.067 m/s. The settling velocity w_s is computed through Eq.(13) at each point and time accordingly to the actual concentration value and with the n value fixed equal to 2.5. The values of the static and dynamic friction coefficients are μ_s = 0.52 and μ_d = 0.32, respectively. The dimensionless Chezy coefficient has been evaluated by Griffiths' formula (Griffiths, 1981) for a value of the h/d ratio of about 12. The threshold Shields number was fixed at the classical value of θ_c=0.047 and the Meyer-Peter and Müller coefficient (K_{MPM}) has been assumed equal to 8. The k_1 and k_2 coefficients have been evaluated through Eq.(41) and Eq.(42), respectively, and their values are k_1=1.05 and k_2=7.62. Finally, the upper bound value of the free parameter $c_{1,}$ deduced by Eq.(32) is 0.44.

Simulations have been carried out with a grid size Δx = 0.010 m and Δt = 1/4096 s. The computational domain was sufficiently long to exclude any influence of the boundary conditions. Three different values of the c_1 parameter, namely c_1=0, c_1=0.2 and c_1=0.4, have been considered. In Figure 2 two snapshots of the experimental results from Fraccarollo and Capart (2002), corresponding to t = 0.4 s and t = 0.5 s after dam removal, are compared with the computed results. The numerical results show a very limited sensitivity to the c_1 value and moreover they indicate that the model predictions closely agree with the main features of the process, i.e. the celerity of the downstream tail, the free surface profile upstream and downstream the dam, and the scour of the bottom. The shape of the scour strongly resembles the experimental one, with a steep adverse slope just downstream the original dam location (x=0), followed by a nearly horizontal scoured bed. A general slight underestimation of the maximum scour occurring just upstream the bore is however observed at t = 0.4 s. The observed weak hydraulic jump is also qualitatively reproduced in the simulations, with a bore appearing more upstream than in the experiments and with a sharper front.

As far as the sediment transport reproduction is concerned, Figure 3a depicts in the space-time plane the suspended sediment discharge values $q_{s,s}=\delta_{s,s}U_l$ divided by the total solid discharge $q_{s,tot}=\delta_{s,s}U_l + \delta_{s,b}U_s$, while Figure 3b reports the space-time evolution of the ratio $K_s d/h$. Even if in a large portion of the plane the suspended transport represents a small percentage, about 2%, of the total solid discharge, the map shows that there are some areas in which it increases up to 20%. The suspended solid discharge represents an appreciable contribution to the solid discharge only in a limited portion of the (x, t) plane, while it is absent in most of the region downstream to the original dam (i.e. x > 0), although in this region the Rouse number is less than one (results not shown herein). Such a result may be explained accounting for that, downstream the original dam position, the bed load thickness saturates the full flow depth (Figure 3b) and therefore the solid discharge is entirely conveyed as bed load.

Two dimensional dam-break

An example of a two-dimensional fast geomorphic transient involving a wide range of the Shields parameter values is provided by the experiments carried out within the NSF-Pire project (Soares-Frazão et al., 2012).

The tests concern dam-break waves expanding over a flat mobile bed, in a 3.6 m wide, 36 m long flume, whose geometry is reported in Figure 4. The breached dam is represented by two impervious blocks and a 1.0 m wide gate located between the blocks. The sudden rise of the gate induces a flood wave expanding along both longitudinal and transversal directions. An initial 85-mm thick layer of coarse sand was put down upon the fixed bed, from 1 m upstream to 9 m downstream the gate. Sediments were constituted of an uniformly graded sand with d=1.61 10^{-3} m with relative density r = 1.63, with a bottom porosity p = 0.42. The sediment free-fall velocity w_t is 0.18 m/s. Also in this test case the settling velocity w_s has been computed through Eq.(13) with n = 2.5 and considering the actual concentration value. The following values of friction coefficients have been assumed μ_s = 0.73 and μ_d = 0.63. The value of the k_1 coefficient through Eq.(41) is k_1=1.09. The threshold Shields parameter and the Meyer-Peter and Müller coefficients have been fixed equal to θ_c=0.047 and K_{MPM}=8, as in the previous test, so that k_2=7.34. The dimensionless Chezy coefficient has been similarly evaluated using the Griffiths' formula. Here the ratio h/d is about 200. The upper bound of the c_1 parameter is 0.29.

Two configurations were experimentally investigated: (1) an initial water level of 47 cm in the upstream reservoir and no water downstream (dry-bed test); (2) an initial water level of 51 cm in the upstream reservoir and a water level of 15 cm downstream (wet-bed test). The time evolution of the water level was measured at eight gauges by means of ultrasonic probes (Figure 4), whose location is indicated in Tables 1 and 2 for dry and wet bed test, respectively. The final topography was measured by a bottom profiler with 5 cm resolution along y. Further details about the experimental procedure may be found in the paper by Soares-Frazão et al. (2012).

Both the dry- and wet-bed experiments have been simulated by means of a non-uniform mesh of about 35000 cells, with variable size in x and y directions. The smallest cells, used to discretise the erodible floodplain, have size Δx=Δy =$2.5 \cdot 10^{-2}$ m. The adopted timestep was Δt= 1/2048 s. Freefall has been considered at the outlet section of the flume, whereas impervious boundaries have been considered for the flume sidewalls.

With reference to Test Case 1 (dry-bed), Figure 5 compares measured and computed time series of free-surface elevation at the gauge points, obtained with three different values of the c_1 parameter, namely 0, 0.1 and 0.2. Measures from symmetrical gauge-points are grouped on the same plot.

An estimate of the experiment reproducibility has been provided by Soares-Frazão et al. (2012) resulting in mean observed standard deviation between σ_{mean}= 0.006 ÷ 0.016 m with maximum values being between σ_{max} =0.018 ÷ 0.032 m, depending on the considered gauge. It is noticed that in all the gauges the arrival time of the surge caused by the dam failure is well captured, along with the general trend of the free-surface elevation decay after the surge transition.

The experimental and simulated final bottom topographies for three values of the y coordinate (y=0.2 m, y= 0.7 m and y=1.45 m) are compared in Figure 6, still considering the same three different c_1 values of Figure 5. A slight but systematic under-prediction of the deposition is observed in the simulated profile. This performance appears satisfactory if the scattering between the results of different repeated experimental runs is accounted for. Indeed, Soares-Frazão et al. (2012) estimated mean and maximum standard deviation of σ_{mean}=0.008 m and σ_{max}=0.029 m, respectively, with the latter value referring to the most intensely scoured zone. Moreover, the results depicted in both Figures 5 and 6 confirm the limited influence of the c_1 parameter on the results quality.

Figure 7 reports the vector plot of both water and sediment velocities at different times (t = 2 s, t = 5 s, t = 20 s), showing the differences between the velocity fields of the two phases. In particular, the different alignment of the velocities vectors of the two phases is evident for t = 5 s, after that the flood wave impacted the sidewall and it was reflected toward the channel axis. The fluid flow is more responsive than the sediment to the impact of the wave. As far as the far-field t = 20 s snapshot is considered, the sediment transport has ceased in the recirculation zone past the rigid blocks. Moreover, the symmetry of the velocity vectors respect to the longitudinal axis confirms the ability of the adopted numerical scheme to predict symmetric results. With reference to the same instants, the wide range of the Shields parameter of this flow is witnessed in Figure 8.

Finally, Figure 9 represents the instantaneous values of $C_{s,b}$ for the same time of Figure 7. At all times, a steep transversal gradient of the concentration is observed in the narrow channel between the blocks. For t = 2 s, the bulb-like flood-wave exhibits a nearly constant concentration in its body and a gradual decrease close to the wave tip region, where the solid phase is transferred towards the suspension. However, maximum observed $C_{s,s}$ values are smaller by more than one order of magnitude than the $C_{s,b}$ ones (not reported). The results of both Figures 8 and 9 also show a symmetric behaviour respect to the longitudinal axis.

With reference to Test Case 2 (wet-bed), Figures 10 and 11 report the time series of the free-surface elevation at the different gauge points and of the final topography for the three longitudinal sections y = 0.2, 0.7 and 1.45 m, respectively. The sensitivity respect to the c_1 parameter is also represented. The results show that the present model is able to reproduce satisfactorily even in this test the wave propagation process (Figure 10), independently of the $c_1$value. Moreover, the computed bed profile (Figure 11) is characterized by bedforms in the scour hole with a comparable length than in the experiments, whereas the remaining of the profile is less wavy compared than the experimental one.

The vector plot of both water and sediment velocities at different instants (t =2 s, t =5 s, t =20 s) are represented in Figure 12. As far as the direction of the liquid and solid velocity is concerned, the presence of the water downstream the dam tends to dampen the differences. On the other hand, the initial quiescent water downstream the dam obstacles the momentum diffusion, which leads to a significantly different shear stress distribution with respect to the dry-bed test-case. Indeed, while the range of the shear stress values encountered by the flow is comparable with that of the previous test-case, the spatial distribution is characterized by a more pronounced shear stress concentration in the region downstream the corner, as shown in Figure 13.

Along with the different shear stress distribution, the wet-bed test-case differs significantly from the dry-bed one also for the bed load concentration distribution. To enlighten such an aspect, the $C_{s,b}$ distribution is represented in Figure 14 with reference to the same instants considered for the previous case. At the first snapshot (t = 2 s), in fact, spatial gradients are more pronounced than in the dry-bed test-case. At t=5 s, the $C_{s,b}$ distribution is characterized by concentrations progressively reducing in the positive x direction. The non-uniform distribution evolves in time towards a more homogeneous one. In the near-field, however, the capability of the present model to account for variable-concentration seems fundamental for the bed load sediment routing.

Comparison with literature models

In this section results of present model are compared against the ones obtained with four different models discussed in the literature review.

The comparison concerns the main underlying assumptions of the different models, the evaluation of their specific parameters, the computational complexity (herein intended as the number of equations to be solved), along with the agreement with the experimental tests considered in the previous sections.

As detailed in the Model closures section, the present model essentially contains three dimensionless parameters, i.e. C_{Ch}, K_{MPM} and c_1. The parameters $\mathrm{C_{Ch}}$ and K_{MPM} may be evaluated based on extensive literature indications, while for c_1 lower and upper bounds can be estimated. As far as the computational complexity is concerned, the one-dimensional (resp. two-dimensional) form of the proposed model needs the solution of five (resp. seven) differential equations expressing conservation principles of mass and momentum. Additionally, the bed evolution equation (Eq. 6) has to be solved, which is however computationally less expensive than the other ones.

As far as the one dimensional test-case is concerned, the single-phase model of Wu and Wang (2007) and the two-phase one of Greco et al. (2012a) have been considered for comparison. The one-dimensional model by Wu and Wang (2007) is a single-phase mixture model, which considers both the suspended and bed load and accounts for variable bed load concentration. It is slightly less computationally expensive than the presented model, since it requires the solution of four differential equations, plus the bed evolution one. The inertia of the bed load sediment is considered through an empirical spatial lag between the actual bed load solid transport rate and the capacity value. As a consequence, in addition to the Manning coefficient, two empirical parameters defining the non-equilibrium adaptation length of total load sediment transport have to be defined. Moreover, a correction factor for the transport stage number in the Van Rijn (1984) formula (k_{t}) is introduced. It has been shown by the Authors that, while the results' sensitivity to the adaptation length value was limited, the correction factor k_{t} significantly affected the predicted erosion magnitude.

The two-phase model of Greco et al. (2012a) is constituted by four conservation laws plus the bed deformation equation. The suspended sediment motion is not accounted for and the sediment concentration in the bed load is assumed to be constant. The concrete model application needs the estimation of the Chezy coefficient and of the bed load concentration. The latter has been assumed to be equal to the bed concentration (Greco et al., 2012a).

Figure 15 compares the results for the one dimensional test of the proposed model and of the two considered literature ones. Figure 15 indicates an evident improvement of the present model with respect to the one by Greco et al. (2012a). In particular, the latter model fails to reproduce the observed weak hydraulic jump, with a gradual variation of the free surface and a very different position of the downstream water front. A significant underestimation of the bed scour is also noted. Present results support the consideration formulated by Li et al. (2013), that the assumption of a constant bed load concentration may fail during highly unsteady flows. Conversely, the present model performs similarly to the mixture model by Wu and Wang (2007), both in terms of bottom elevation and free surface profile (Figure 15). Although the mixture model may appear more attractive for the lower computational complexity, it is worthwhile to point out that the agreement in the bed erosion significantly depends on the calibrated value of the correction factor k_t.

For the two-dimensional test-cases, the comparison involves the single phase model of Canelas et al. (2013) and the two-layer one of Swartenbroekx et al. (2013). The mixture two-dimensional model of Canelas et al. (2013) exhibits a much smaller computational complexity than the present one, being constituted by four conservation type laws plus the bed evolution one. Similarly to the Wu and Wang (2007) model, a spatial lag between the actual bed load discharge and the equilibrium value is introduced to mimic the effects of the bed load inertia in the layer. The spatial lag is computed through an ad hoc formula which includes three additional calibration parameters fixed through a heuristic adjustment process. The computational complexity of the two-layer model of Swartenbroekx et al. (2013) is slightly smaller than the one of the present model. Indeed, it is composed by six conservation equations plus the bed evolution one. Similarly to the two-phase model of Greco et al. (2012), it does not account for the suspended load and the sediment concentration in the bed load is assumed constant. The sediment inertia in the bed load layer is fully described through the balance equation for the mixture momentum in the transport layer. The shear stresses between the layers are expressed through two constant friction factors, which have been determined through calibration against experimental results.

Figure 16 (resp. 18) compares the results of the present model for the two dimensional Test Case 1 (resp. Case 2) in terms of free-surface elevation with the ones of Canelas et al. (2013) and Swartenbroekx et al. (2013). Figure 17 (resp. Figure 19) is the counterpart of Figure 16 (resp. 18) in terms of final topography. Both free-surface elevation history (Figures 16 and 18) and final bottom topography (Figures 17 and 19) are reproduced with an accuracy comparable to that of the model by Swartenbroekx et al. (2013) and with a slight improvement with respect to the mixture model of Canelas et al. (2013), despite the proper calibration of the three additional parameters. However, all models exhibit a slight but systematic under-prediction of the experimentally observed deposition.

CONCLUSIONS

A two-phase depth-averaged model able to deal with both bed load and suspended sediment transport has been proposed. The mathematical model, based on mass and momentum conservation equations for liquid and sediment phases, accounts for variable concentration both in the bed load and in the suspended load region. The entrainment/deposition of sediments from the bed towards the bed load layer is evaluated by a formula based on a modified van Rijn mobility parameter, while for the exchange between bed and suspended load a first-order exchange law is considered. The adopted set of closure relations is shown to comply, under uniform conditions of flow, with several empirical scaling laws for sediment transport and to allow for relatively accurate evaluation of the bed load layer thickness up to values of the Shields parameter order of unity. Two of the three dimensionless parameters of the model, the Chezy and the Meyer-Peter and Müller formula coefficients, may be evaluated based on extensive literature indications. The third one, c_1, is allowed to vary in a range limited by theoretically deduced lower and upper bounds.

It has been proved that the proposed model is hyperbolic and the analytical expression of the eigenvalues has been provided. A numerical method based on a finite-volume approach has been employed for the simulation of three experiments concerning three different dam-breaks, showing a good agreement between simulated and experimental results. The results show that accounting for the variability concentration in the two phase formulation leads to a neat improvement of the model performance. Finally, for all test, it has been demonstrated that the value of the free parameter c_1 has only a marginal influence on the results' quality. A further confirmation of this conclusion could be obtained through future application of the model to a wider class of morphodynamic transients.

REFERENCES

Ancey C., Andreini N., and Epely-Chauvin G., 2012. Viscoplastic dambreak waves: Review of simple computational approaches and comparison with experiments. *Advances in Water Resources*, 48, 79–91.

Armanini A., and Di Silvio G., 1988. A one-dimensional model for the transport of a sediment mixture in non-equilibrium conditions. *Journal of Hydraulic Research*, 26(3), 275–292.

Armanini A., 2013. Granular flows driven by gravity. *Journal of Hydraulic Research*, 51(2), 111–120.

Baldock T.E., Tomkins M.R., Nielsen P., and Hughes M.G., 2004. Settling velocity of sediments at high concentrations. *Coastal Engineering*, 51, 91–100.

Bagnold R.A., 1956. The flow of cohesionless grains in fluids. *Philosophic Transactions of the Royal Society*, *A* 240, 235–297.

Bridge J.S., and Dominic D.F., 1984. Bed load grain velocities and sediment transport rates. *Water Resources Research*, 20(4), 476–490.

Brooks G.R., and Lawrence D.E., 1999. The drainage of the Lake Ha! Ha! reservoir and downstream impacts along Ha! Ha! River, Saguenay area, Quebec, Canada. *Geomorphology*, 28, 141–168.

Byrd, T.C., and Furbish D.J., 2000. Magnitude of deviatoric terms in vertically averaged flow equations, *Earth Surf. Processes Landforms*, 25(3), 319– 328.

Canelas R., Murillo J., and Ferreira R.M., 2013. Two-dimensional depth-averaged modelling of dam-break flows over mobile beds. *Journal of Hydraulic Research*, 51(4), 392–407.

Cao Z., and Carling P.A., 2002. Mathematical modelling of alluvial rivers: reality and myth. Part 1: general overview. *Maritime Engineering*, 154(3), 207–219.

Cao Z., Day R., and Egashira S., 2002. Coupled and Decoupled Numerical Modeling of Flow and Morphological Evolution in Alluvial Rivers. *Journal of Hydraulic Engineering – ASCE*, 128(3), 306–321.

Capart H., and Young D.L., 1998. Formation of a jump by the dambreak wave over a granular bed. *Journal of Fluid Mechanics*, 372, 165–187.

Capart H., and Young D., 2002. Two-layer shallow water computations of torrential geomorphic flows. *Proc. River Flow 2002*, 1003–1012.

Chen S.C., and Peng, S.H., 2006. Two-dimensional numerical model of two-layer shallow water equations for confluence simulation. *Advances in Water Resources*, 29(11), 1608–1617.

Cheng N.-S., 2006. Influence of shear stress fluctuation on bed particle mobility. *Physics of Fluids*,18, 096602,1–7.

Courant R., and Hilbert D., 1961. *Methods of mathematical physics*, Vol. 2. Interscience, New York.

Defina A., and Bixio A.C., 2005. Mean flow and turbulence in vegetated open channel flow, *Water Resources Research*, 41(7), W07006, 1-12.

Dewals B., Rulot F., Erpicum S., Archambeau P. and Pirotton M., 2011. Advanced Topics in Sediment Transport Modelling: Non-alluvial Beds and Hyperconcentrated Flows, Sediment Transport, Dr. Silvia Susana Ginsberg (Ed.), ISBN: 978-953-307-189-3, InTech, DOI: 10.5772/15025. Available from: http://www.intechopen.com/books/sediment-transport/advanced-topics-in-sediment-transport-modelling-non-alluvial-beds-and-hyperconcentrated-flows

Di Cristo C., Iervolino M., and Vacca A., 2006. Linear stability analysis of a 1-D model with dynamical description of a bed load transport. *Journal of Hydraulic Research*, 44(4), 480–487.

Di Cristo C., Iervolino M., and Vacca A., 2014a. Applicability of Kinematic, Diffusion and Quasi-Steady Dynamic Wave Models to Shallow Mud Flows. *Journal of Hydrologic Engineering - ASCE*, 19(5), 956-965 DOI:10.1061/(ASCE)HE.1943-5584.0000881.

Di Cristo C., Iervolino M., and Vacca A., 2014b. Simplified Wave Models Applicability to Shallow Mud Flows Modeled as Power-Law Fluids. *Journal of Mountain Sciences*, doi: 10.1007/s11629-014-3065-6.

Di Cristo C., Evangelista S., Leopardi A., Greco M., and Iervolino M., 2014c. Numerical simulation of a dam-break with a wide range of Shields parameter. Proc. River Flow 2014,1, 1680-1687.

Di Cristo C., Iervolino M., and Vacca A., 2014d. Diffusive approximation for unsteady mud flows with backwater effect. *Advances in Water Resources*, DOI: 10.1016/j.advwatres.2014.10.002.

Duran O., Andreotti B. and Claudin P., 2012. Numerical simulation of turbulent sediment transport, from bed load to saltation. *Physics of Fluids*, 24, 103306, 1–23.

El Kadi Abderrezzak K., and Paquier A., 2011. Applicability of Sediment Transport Capacity Formulas to Dam-Break Flows over Movable Beds, *Journal of Hydraulic Engineering - ASCE*, 137(2), 209–221.

Evangelista S., Altinakar M.S., Di Cristo C., and Leopardi A. 2013. Simulation of dam-break waves on movable beds using a multi-stage centred scheme. *International Journal of Sediment Research*, 28(3), 269–284.

Fernandez-Luque R., and Van Beek R., 1976. Erosion and transport of bed-load sediment. *Journal of Hydraulic Research*, 14(2), 127–144.

Furbish D.J., Haff P.K., Roseberry J.C., and Schmeeckle M.W., 2012. A probabilistic description of the bed load sediment flux: 1. Theory. *J. Geophys. Res.*, 117(F3), F03031, DOI: 10.1029/2012JF002352.

Fraccarollo L., and Capart H., 2002. Riemann wave description of erosional dam-break flows. *Journal of Fluid Mechanics*, 461, 183–228.

Garegnani G., Rosatti G., and Bonaventura L., 2011. Free surface flows over mobile bed: mathematical analysis and numerical modeling of coupled and decoupled approaches. *Communications in Applied and Industrial Mathematics*, 2(1), 1–22.

Graf W.H., 1998. *Fluvial Hydraulics: Flow and transport processes in channels of simple geometry.* John Wiley and Sons, England.

Greco M., Iervolino M., and Leopardi A., 2008a. Discussion on “Divergence Form for Bed Slope Source Term in Shallow Water Equations. *Journal of Hydraulic Engineering - ASCE*, 134(5), 676–678.

Greco M., Iervolino M., and Vacca A., 2008b, Discussion on “Boundary conditions in a two-layer geomorphological model: application to a hydraulic jump over a mobile bed.” by Savary C. and Zech Y. (2007). *Journal of Hydraulic Research*, 46 (6), 856–858.

Greco M., Iervolino M., Leopardi A., and Vacca A., 2012a. A Two-Phase Model for Fast Geomorphic Shallow Flows, *International Journal of Sediment Research*, 27(4), 409–425.

Greco M., Iervolino M., Vacca A., and Leopardi, A., 2012b. Two-phase modelling of total sediment load in fast geomorphic transients. *Proc. River Flow 2012*, 1, 643–648.

Griffiths G.A., 1981. Flow resistance in coarse gravel bed rivers. *Journal of the Hydraulic Division - ASCE*, 107(HY7), 899–916.

Julien P.Y., and Bounvilay B., 2013. Velocity of Rolling Bed Load Particles. *Journal of Hydraulic Engineering - ASCE*, 139(2), 177–186.

Keylock C.J., Hardy R.J., Parsons D.R., Ferguson R.I., Lane S.N., and Richards K.S., 2005. The theoretical foundations and potential for large-eddy simulation (LES) in fluvial geomorphic and sedimentological research. *Earth-Science Reviews*, 71 (2005) 271–304.

Lamb M.P., Dietrich W.E., and Venditti J.G., 2008. Is the critical Shields stress for incipient sediment motion dependent on channel-bed slope? *Journal of Geophysical Research*, 113, F02008, 1–23.

Lajeunesse E., Malverti L., and Charru F., 2010. Bed load transport in turbulent flow at the grain scale: Experiments and modelling. *Journal of Geophysical Research F: Earth Surface*, 115 (4), art. no. F04001.

Lee H.Y., and Hsu I. S., 1994. Investigation of saltating particle motion. *Journal of Hydraulic Engineering - ASCE*, 120(7), 831–845.

Lee H.Y., Chen Y.H., You J.Y., and Lin Y.T., 2000. Investigations of continuous bed load saltating process. *Journal of Hydraulic Engineering - ASCE*, 126(9), 691–700.

Leopardi A., Oliveri E., and Greco M., 2002. Two-dimensional modeling of floods to map risk prone areas. *Journal of Water Resources Planning and Management - ASCE*, 128(3), 168–178.

Li. J., Cao, Z., Pender G., and Liu Q., 2013. A double layer-averaged model for dam-break flows over mobile bed. *Journal of Hydraulic Research*, 51(5), 518–534.

Lopez F., and Garcia M.H., 1996. Turbulence structure in cobble-bed open-channel flow, in *Civil Engineering Studies*, University of Illinois, Urbana, Illinois.

Marsooli R., and Wu W., 2015. Three-Dimensional Numerical Modeling of Dam-Break Flows with Sediment Transport over Movable Beds. *Journal of Hydraulic Engineering - ASCE*, 141(1), DOI: 10.1061/(ASCE)HY.1943-7900.0000947.

Maude A.D., and Whitmore R.L., 1958. A generalized theory of sedimentation. *British Journal of Applied*, 9, 477–482.

Meland N., and Norrman J.O., 1966. Transport velocities of single particles in bed load motion. *Geografiska Annaler*, 48A(4), 165–182.

Meyer-Peter E., and Müller R., 1948. Formulas for bed-load transport. *Proc. of Intern. Assoc. Hydr. Res., 2nd Meeting*, Stockholm.

Nino Y., Garcia M., and Ayala L., 1994. Gravel saltation 1. Experiments. *Water Resources Research*, 30(6), 1907–1914.

Nino Y., and Garcia M., 1998. Experiments on saltation of sand in water. *Journal of Hydraulic Engineering - ASCE*, 124(10), 1014–1025.

Nikora V., and Goring D., 2000. Flow turbulence over fixed and weakly mobile gravel beds. *Journal of Hydraulic Engineering - ASCE*., 126(9), 679– 690.

Papanicolaou A. N., Diplas P., Evaggelopoulos N., and Fotopoulos S., 2002a. Stochastic Incipient Motion Criterion for Spheres under Various Bed Packing Conditions. *Journal of Hydraulic Engineering- ASCE*, 128(4), 269–380.

Papanicolaou A.N., Knapp, D., Strom K., 2002b. Bedload predictions by using the concept of particle velocity: applications. *Proc. ASCE/EWRI and IAHR Int. conf. on hydraulic measurements and experimental methods*, Estes Park, Colorado, United States,1–10.

Parker G., Seminara G., and Solari L., 2003. Bed load at low Shields stress on arbitrarily sloping beds: alternative entrainment formulation. *Water Resources Research*, 39(7), 1183–1194, DOI: 10.1029/ 2001WR001253.

Pelanti M., Bouchut F., and Mangeney A., 2008. A Roe-Type scheme for two-phase shallow granular flows over variable topography. *Math. Model. Numer. Anal.*, 42, 851–885.

Pitman E.B., and Le L., 2005. A two-fluid model for avalanche and debris flows, *Philos. Trans. R. Soc. A*, 363, 1573–1602.

Pontillo M., Schmocker L., Greco M., and Hager W.H., 2010. 1D numerical evaluation of dike erosion due to overtopping. *Journal of Hydraulic Research*, 48(5), 573-582.

Pudasaini S.P., Wang Y., and Hutter K., 2005. Modelling debris flows down general channels, *Nat. Hazards Earth Syst. Sci*., 5, 799–819.

Pudasaini S.P., 2012. A general two-phase debris flow model. *Journal of Geophysical Research*, 117, F03010, doi:10.1029/2011JF002186.

Ramesh B., Kothyari U.C., and Murugesan K., 2011. Near-bed particle motion over transitionally-rough bed. *Journal of Hydraulic Research*, 49(6), 757–765.

Richardson J.F., and Zaki W.N., 1954. Sedimentation and fluidisation: part 1, *Trans. Inst. Chem. Eng*. 32, 35– 53.

Rosatti G., and Begnudelli L., 2013. A closure-independent Generalized Roe solver for free-surface, two-phase flows over mobile bed. *Journal of Computational Physics*, 255, 362–383.

Sabbagh-Yazdi S., and Jamshidi M., 2013. Depth-Averaged Hydrodynamic Model for Gradual Breaching of Embankment Dams Attributable to Overtopping Considering Suspended Sediment Transport. *Journal of Hydraulic Engineering - ASCE*, 139(6), 580–592.

Savary C., and Zech Y., 2007. Boundary conditions in a two-layer geomorphological model: Application to a hydraulic jump over a mobile bed. *Journal of Hydraulic Research*, 45(3), 316–332.

Savary C., and Zech Y., 2008. Closure on “Boundary conditions in a two-layer geomorphological model: Application to a hydraulic jump over a mobile bed.” by Savary C. and Zech Y.. *Journal of Hydraulic Research*, 46 (6), 858–860.

Seminara G., Solari L., and Parker G., 2002. Bedload on arbitrary sloping beds. Part 1: Failure of the Bagnold hypothesis. *Water Resources Research*, 38(11), 1249–1271.

Sekine M., and Kikkawa H., 1992. Mechanics of saltating grains. II. *Journal of Hydraulic Engineering - ASCE*, 118(4), 513–535.

Simpson G., and Castelltort S., 2006. Coupled model of surface water flow, sediment transport and morphological evolution. *Computers & Geosciences*, 32, 1600–1614.

Singh A.K., Kothyari U.C., and Ranga Raju K.G., 2004. Rapidly varying transient flows in alluvial rivers. *Journal of Hydraulic Research*, 42(5), 473–486.

Soares-Frazão S., Canelas R., Cao Z., Cea L., Chaudhry H.M., Die Moran A., El Kadi K., Ferreira R., Fraga Cadórniga I., Gonzalez-Ramirez N., Greco M., Huang W., Imran J., Le Coz J., Marsooli R., Paquier A., Pender G., Pontillo M., Puertas J., Spinewine B., Swartenbroekx C., Tsubaki R., Villaret C., Wu W., Yue Z., and Zech Y., 2012. Dam-break flows over mobile beds: experiments and benchmark tests for numerical models. *Journal of Hydraulic Research*, 50(4), 364–375.

Soldati A., and Marchioli C., 2012. Sediment transport in steady turbulent boundary layers: potentials, limitations, and perspectives for Lagrangian tracking in DNS and LES. *Advances in Water Resources*, 48, 18–30.

Spinewine B., and Zech Y., 2007. Small-scale laboratory dam-break waves on movable beds. *Journal of Hydraulic Research*, 45(extra issue), 73–86.

Sturm T.W., 2013. Hydraulic Engineering: A Rising Wave of Progress. *Journal of Hydraulic Engineering - ASCE*, 139(2), 111–113.

Swartenbroekx C., Zech Y., and Soares-Frazão S., 2013. Two-dimensional two-layer shallow water model for dam break flows with significant bed load transport. *International Journal for Numerical Methods in Fluids*, 73(5), 477–508.

Valiani A., and Begnudelli L., 2006, Divergence form for bed slope source term in shallow water equations. *Journal of Hydraulic Engineering*-ASCE, 132(7), 652–665.

Van Rijn L.C., 1984. Sediment pick-up functions. *Journal of Hydraulic Engineering - ASCE*, 110(10), 1494–1502.

Wang S.S.Y., and Wu W.M., 2005. Computational simulation of river sedimentation and morphology – a review of the state of the art. *International Journal of Sediment Research*, 20(1), 7–29.

Wiberg P.L., and Smith J.D., 1985. A theoretical model for saltating grains in water. *Journal of Geophysical Research*, 91(c4), 7341–7354.

Wohl E.E., and Thompson D.M., 2000. Velocity characteristics along a small step-pool channel. *Earth Surf. Processes Landforms*, 25(4), 353–367.

Wong, M., and Parker, G., 2006. Reanalysis and Correction of Bed-Load Relation of Meyer-Peter and Müller Using Their Own Database, *Journal of Hydraulic Engineering - ASCE*, 132(11), 1159–1168.

Wong M., Parker G., De Vries P., Brown T.M., and Burges S.J., 2007. Experiments on dispersion of tracer stones under lower-regime plane-bed equilibrium bed load transport. *Water Resources Research*, 43(3), W03440, 1–23.

Wu W., Wang S.S.-Y., and Jia Y., 2000. Nonuniform Sediment Transport in Alluvial Rivers. *Journal of Hydraulic Research*, 38(6), 427–434.

Wu W., 2007. *Computational River Dynamics*. Routeledge. Taylor & Francis Group.

Wu W., and Wang S.S.-Y., 2007. One dimensional modeling of dam-break flow over movable beds, *Journal of Hydraulic Engineering - ASCE*, 133(1),48–58.

Wu F.C., and Chou Y.J., 2003. Rolling and lifting probabilities for sediment entrainment. *Journal of Hydraulic Engineering-ASCE*, 129(2), 110–119.

Xia J., Lin B., Falconer R.A., and Wang G., 2010. Modelling dam-break flows over mobile beds using a 2D coupled approach. *Advances in Water Resources*, 33(2), 171–183.

Table 1. Gauges locations for test 1dry-bed test

Gauge n°	x (m)	y (m)
1	0.64	-0.5
2	0.64	-0.165
3	0.64	0.165
4	0.64	0.5
5	1.94	-0.99
6	1.94	-0.33
7	1.94	0.33
8	1.94	0.99

Table 2. Gauges locations for test 1wet-bed test

Gauge n°	x (m)	y (m)
1	0.64	-0.5
2	0.64	-0.165
3	0.64	0.165
4	0.64	0.5
5	2.34	-0.99
6	2.34	-0.33
7	2.34	0.33
8	2.34	0.99

Figure
Click here to download high resolution image

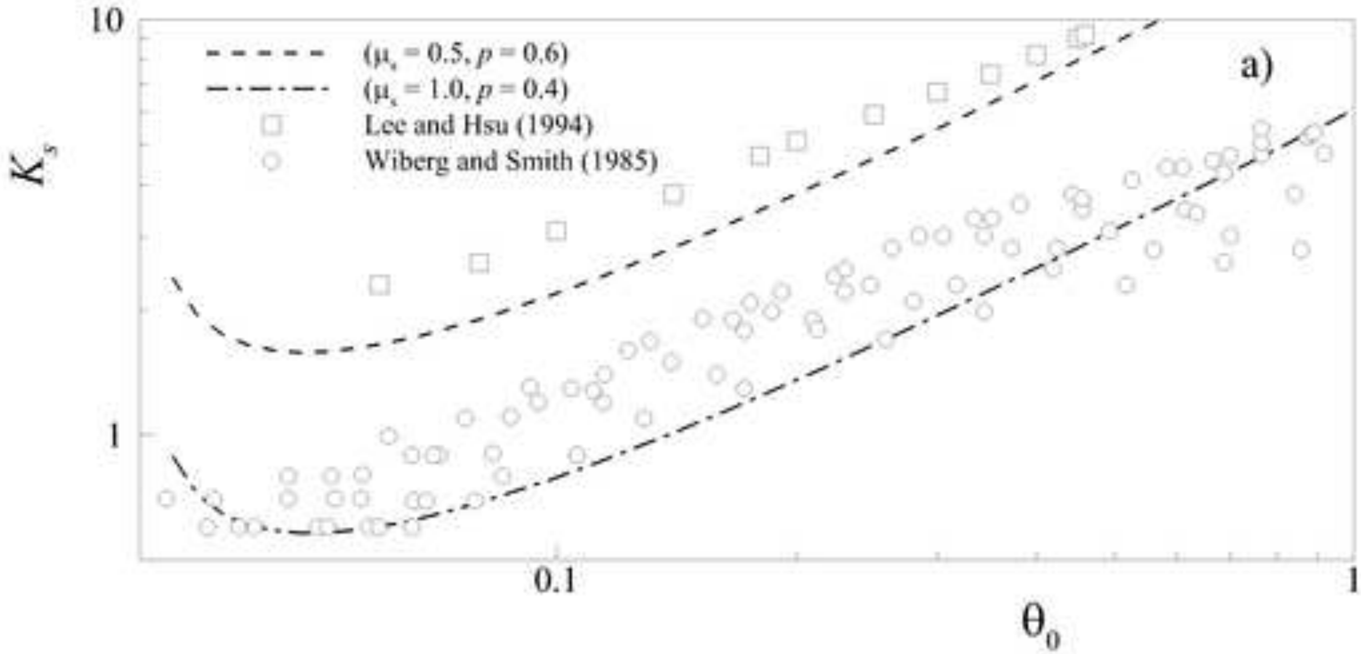

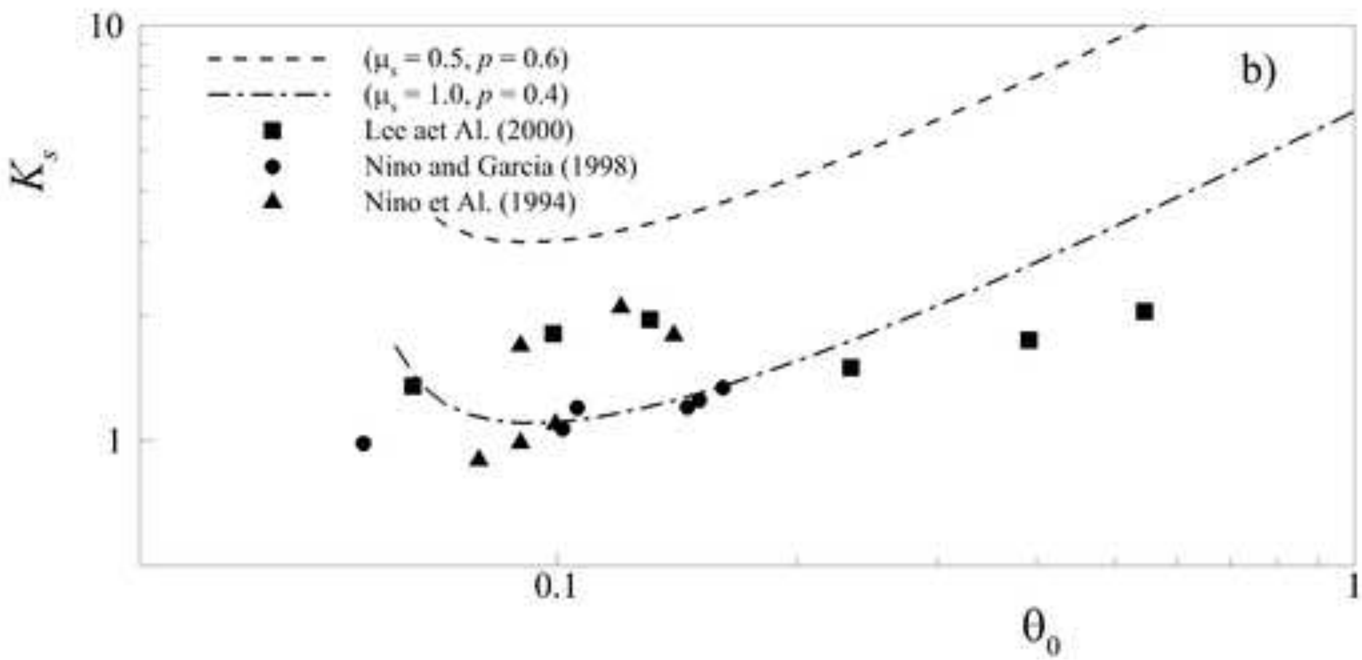

Figure
Click here to download high resolution image

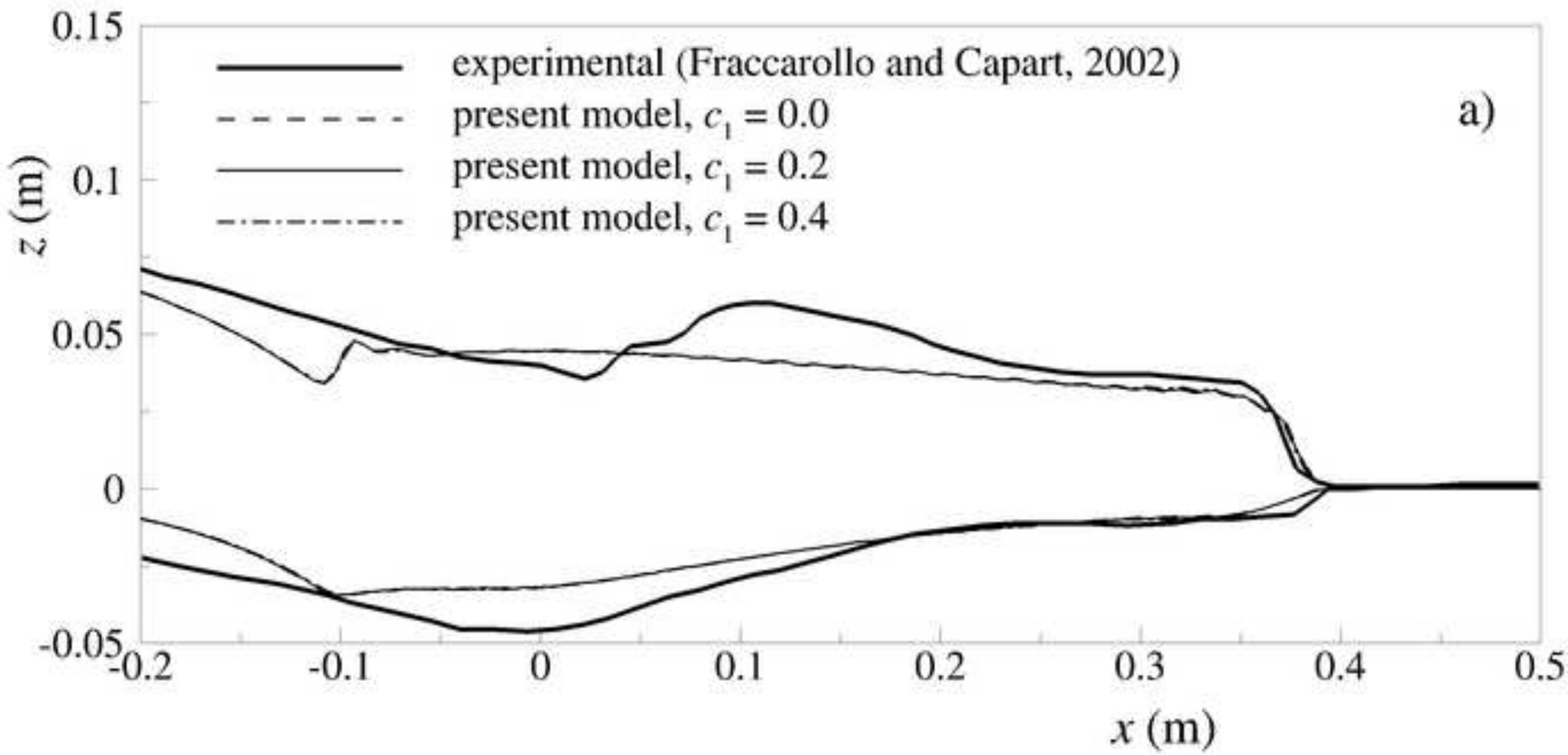

Figure
Click here to download high resolution image

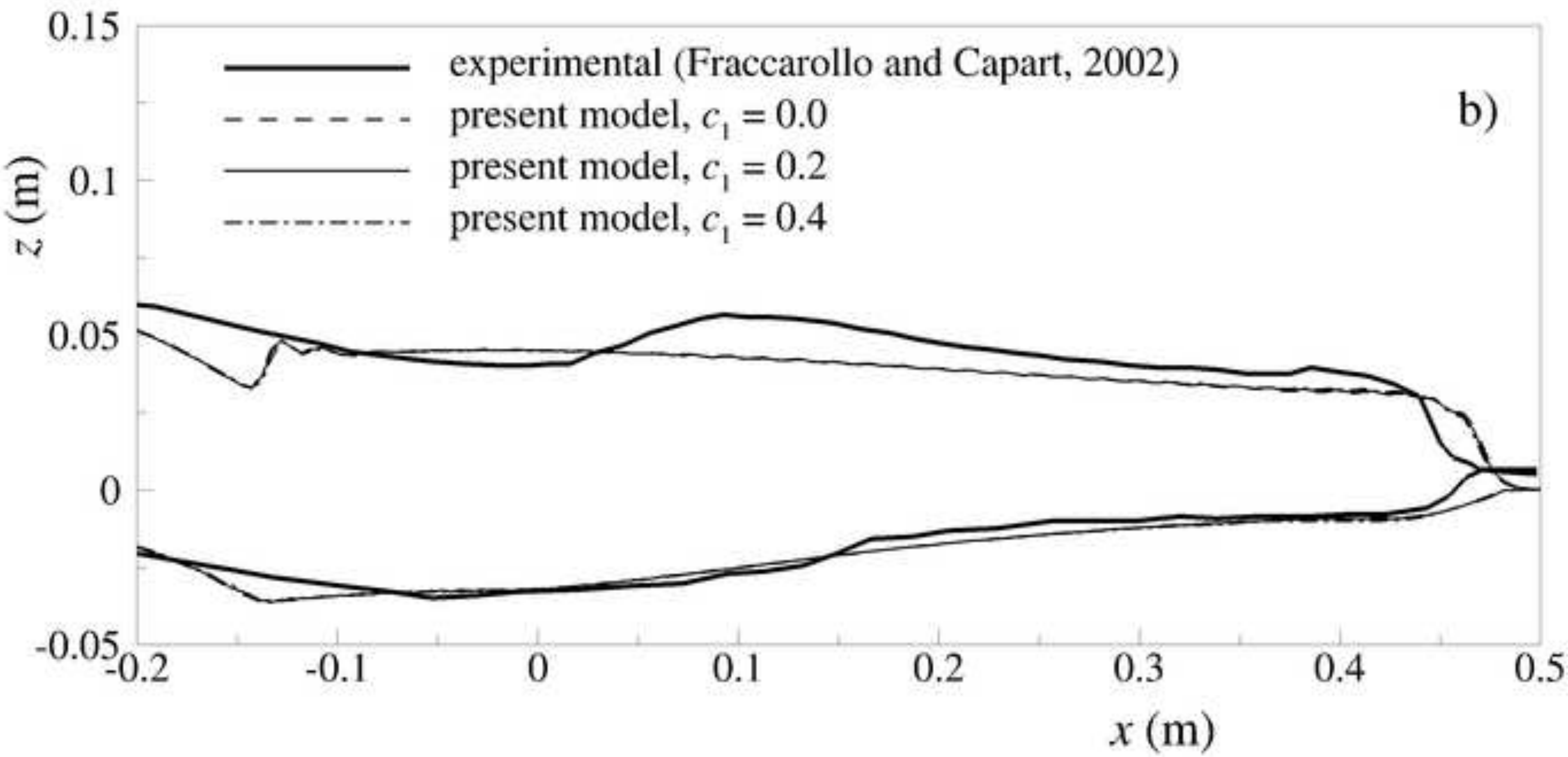

Figure
Click here to download high resolution image

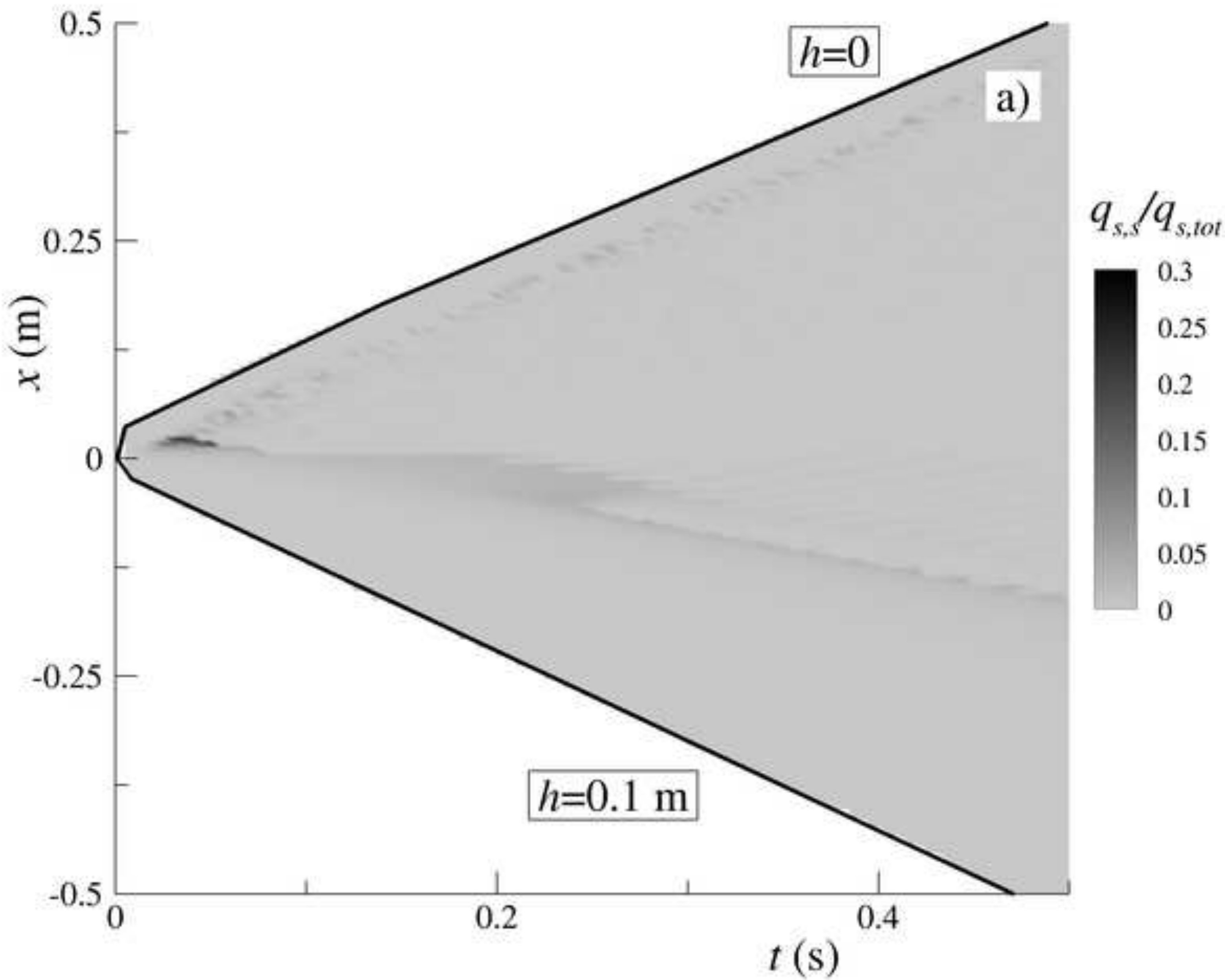

Figure
Click here to download high resolution image

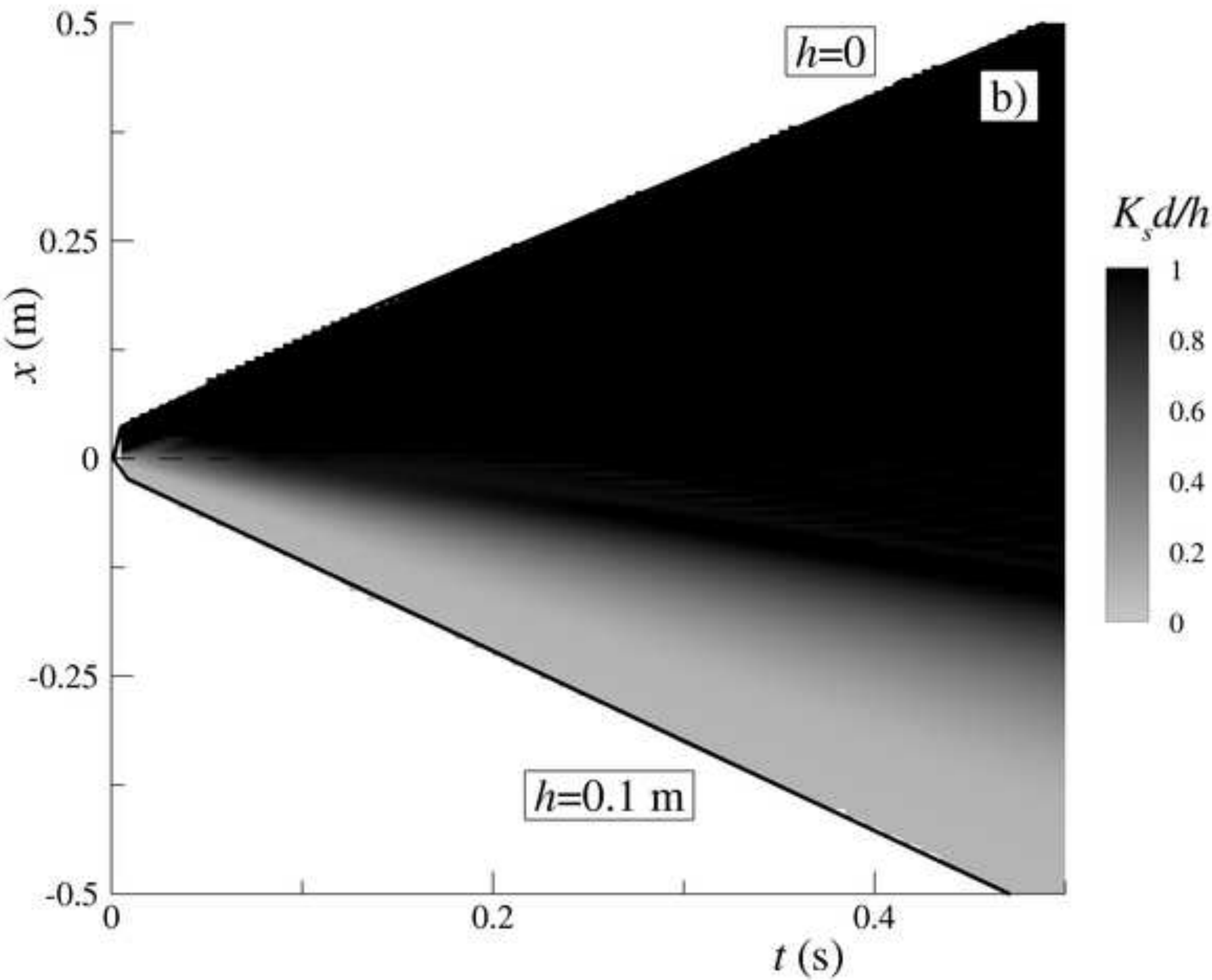

Figure
Click here to download high resolution image

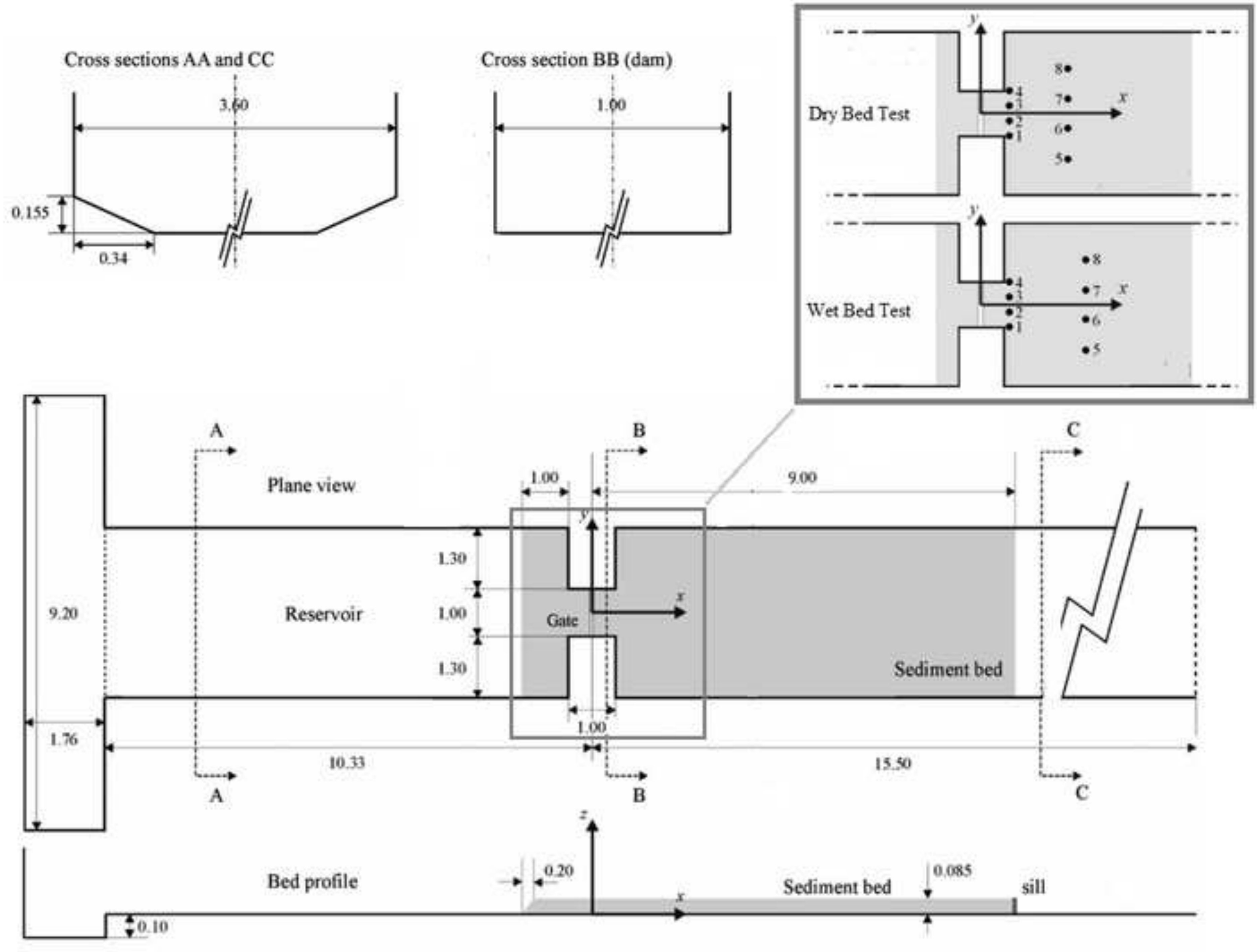

Figure
Click here to download high resolution image

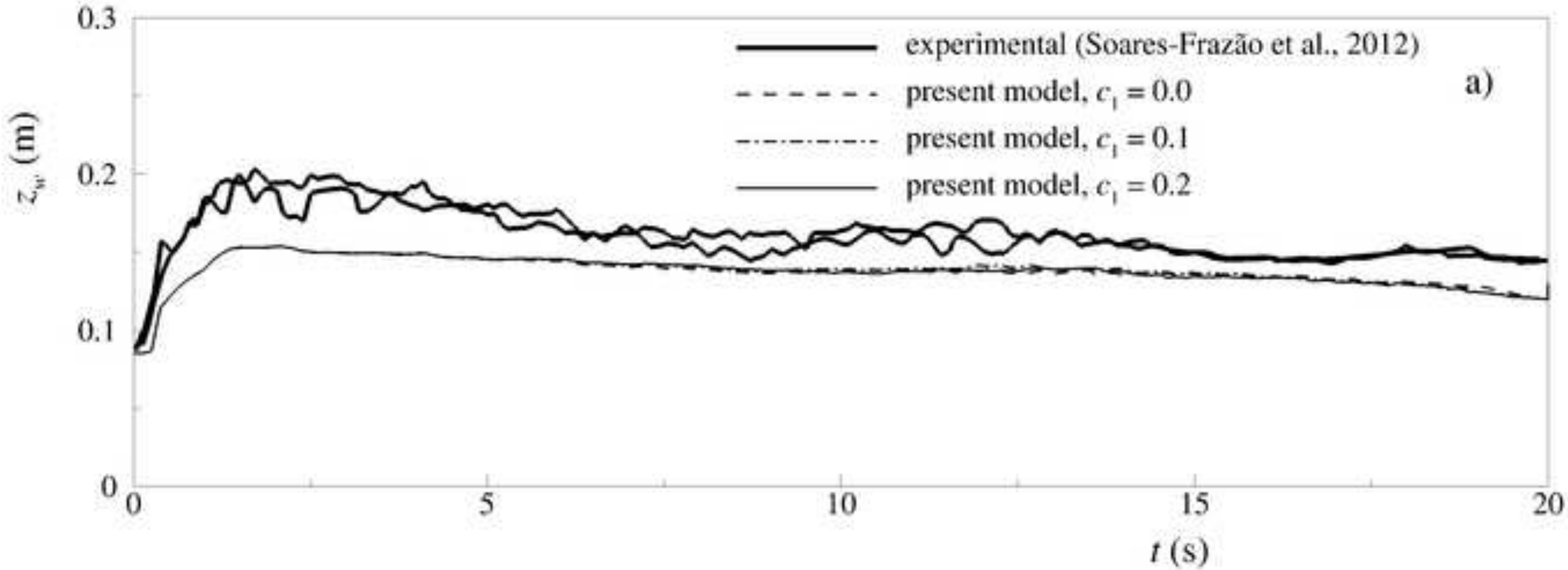

Figure
Click here to download high resolution image

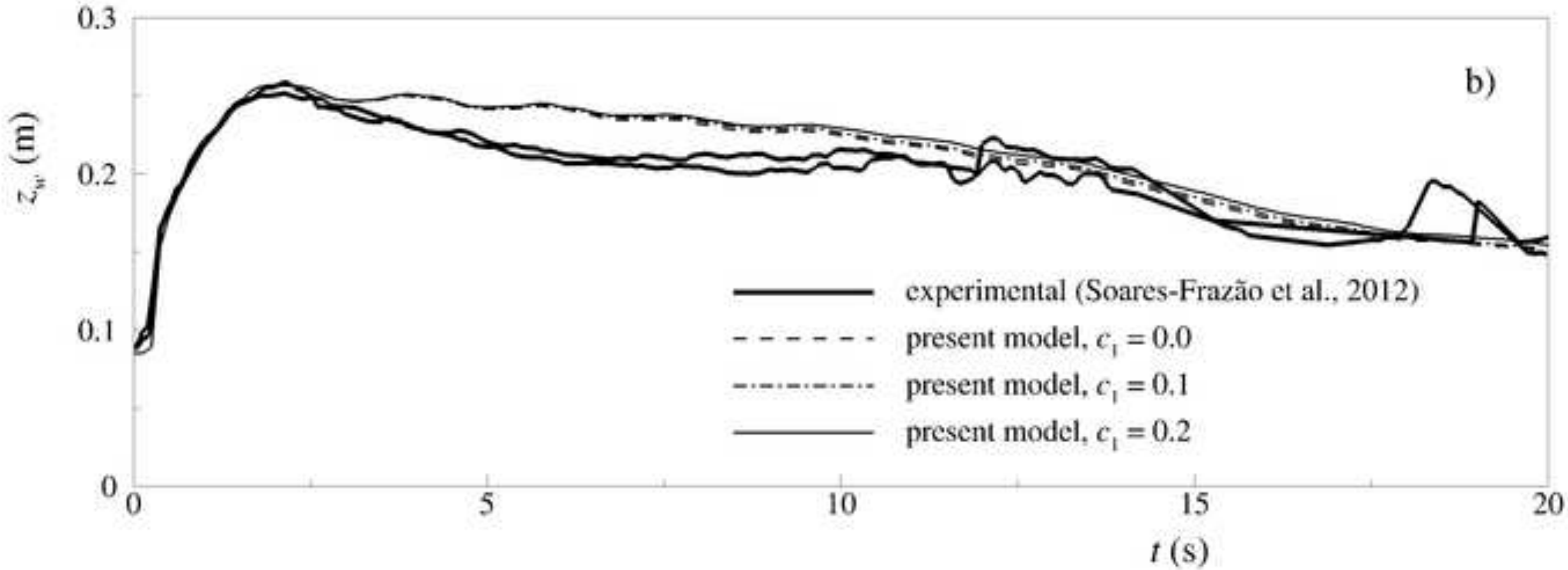

Figure
Click here to download high resolution image

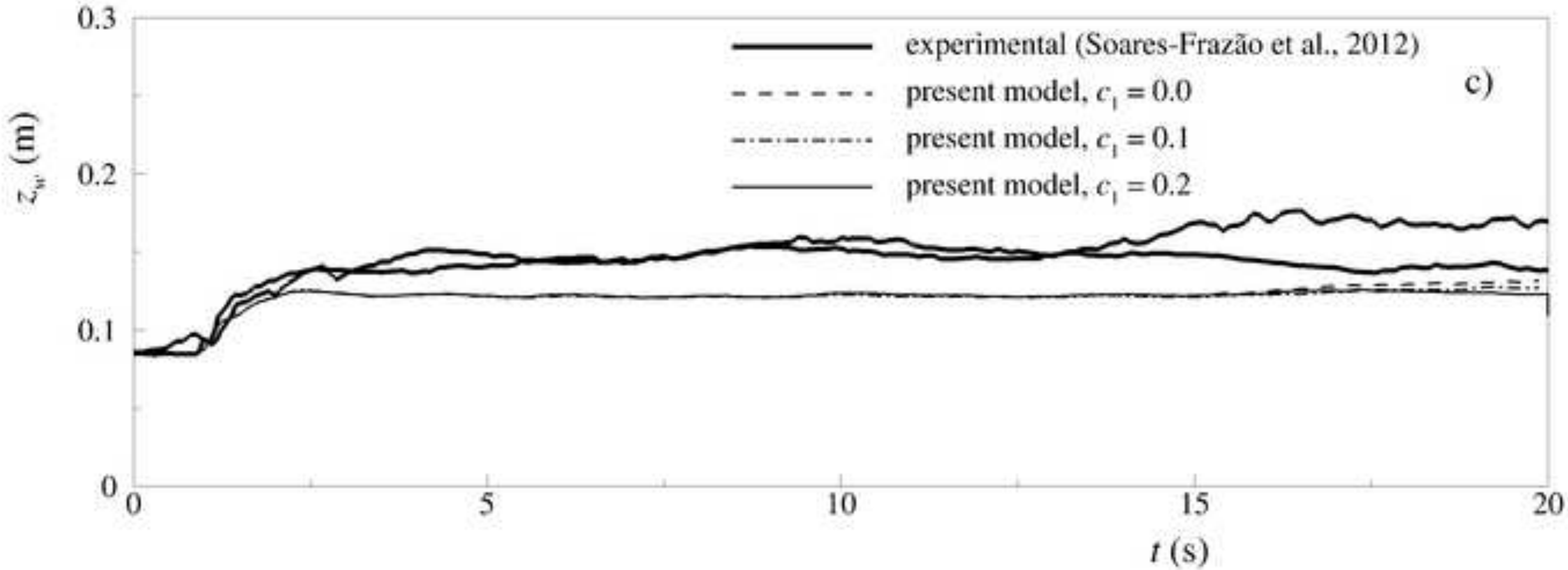

Figure
Click here to download high resolution image

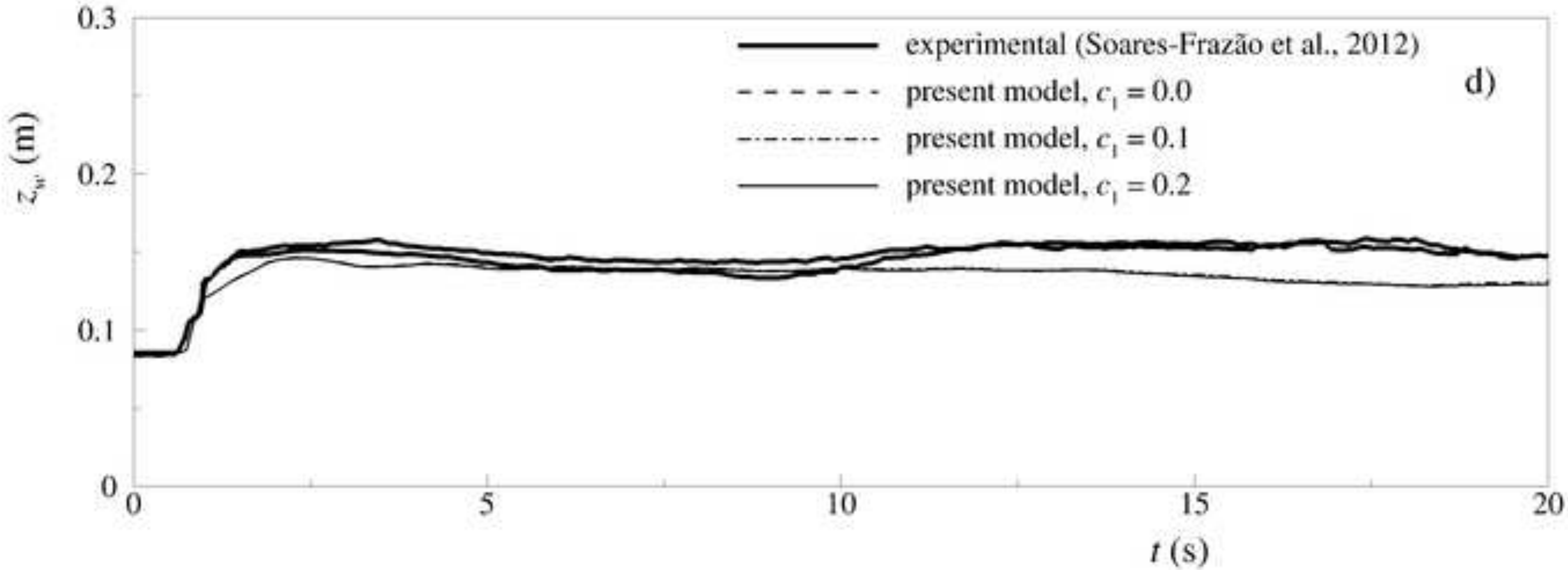

Figure
Click here to download high resolution image

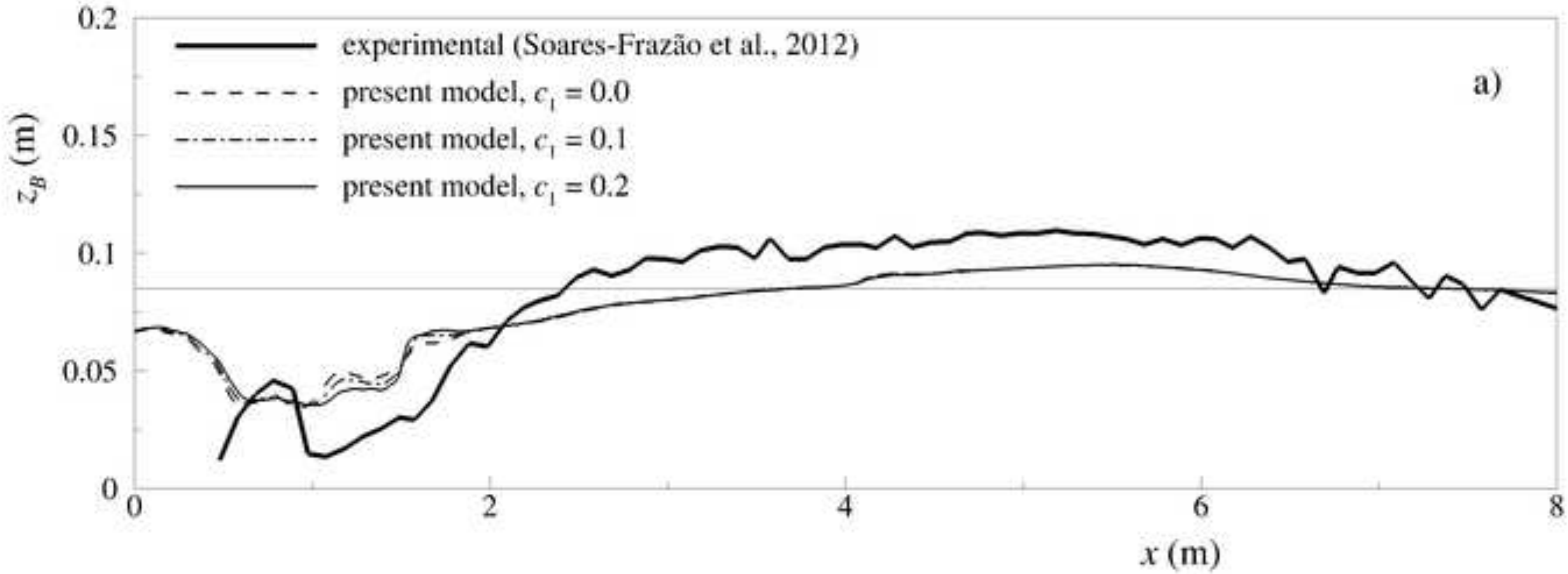

Figure
Click here to download high resolution image

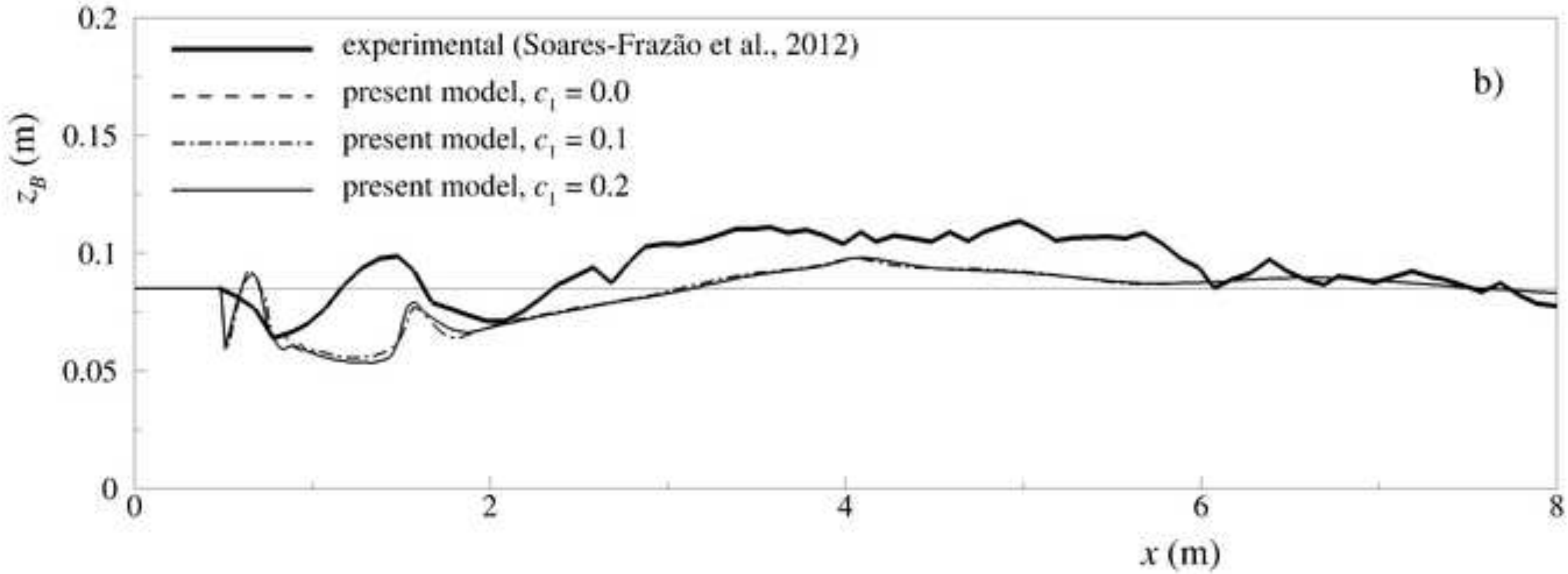

Figure
Click here to download high resolution image

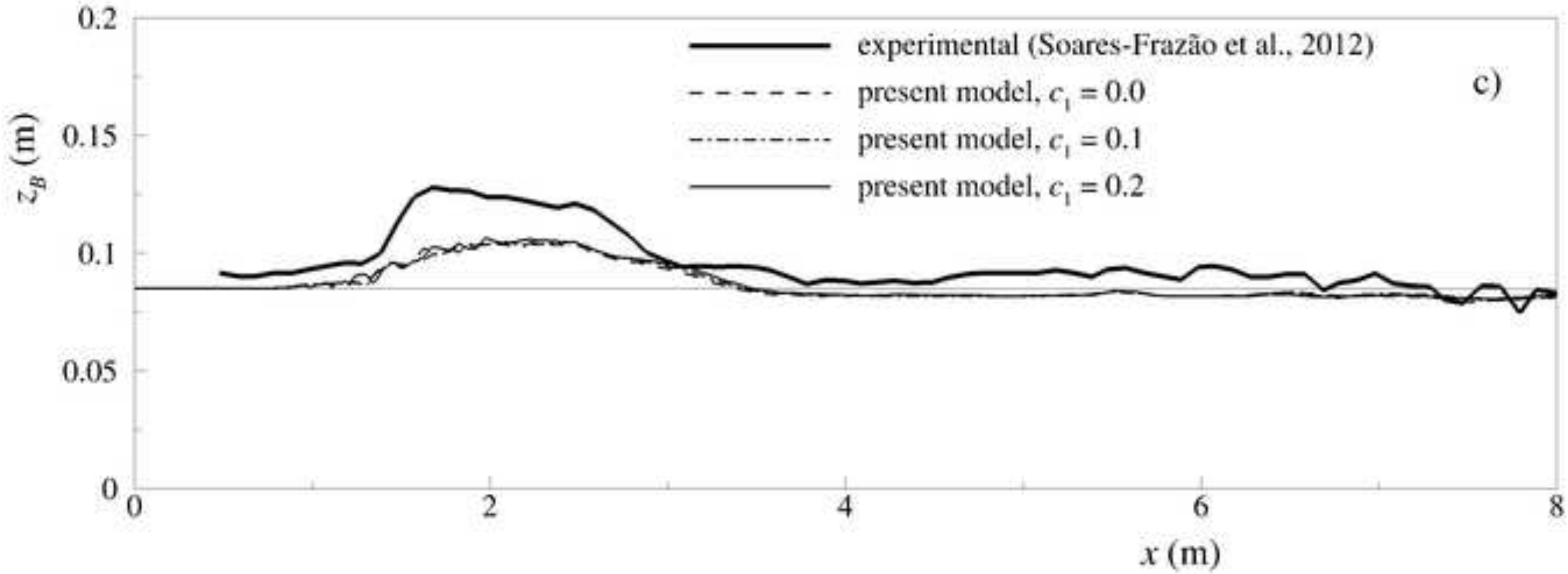

Figure
Click here to download high resolution image

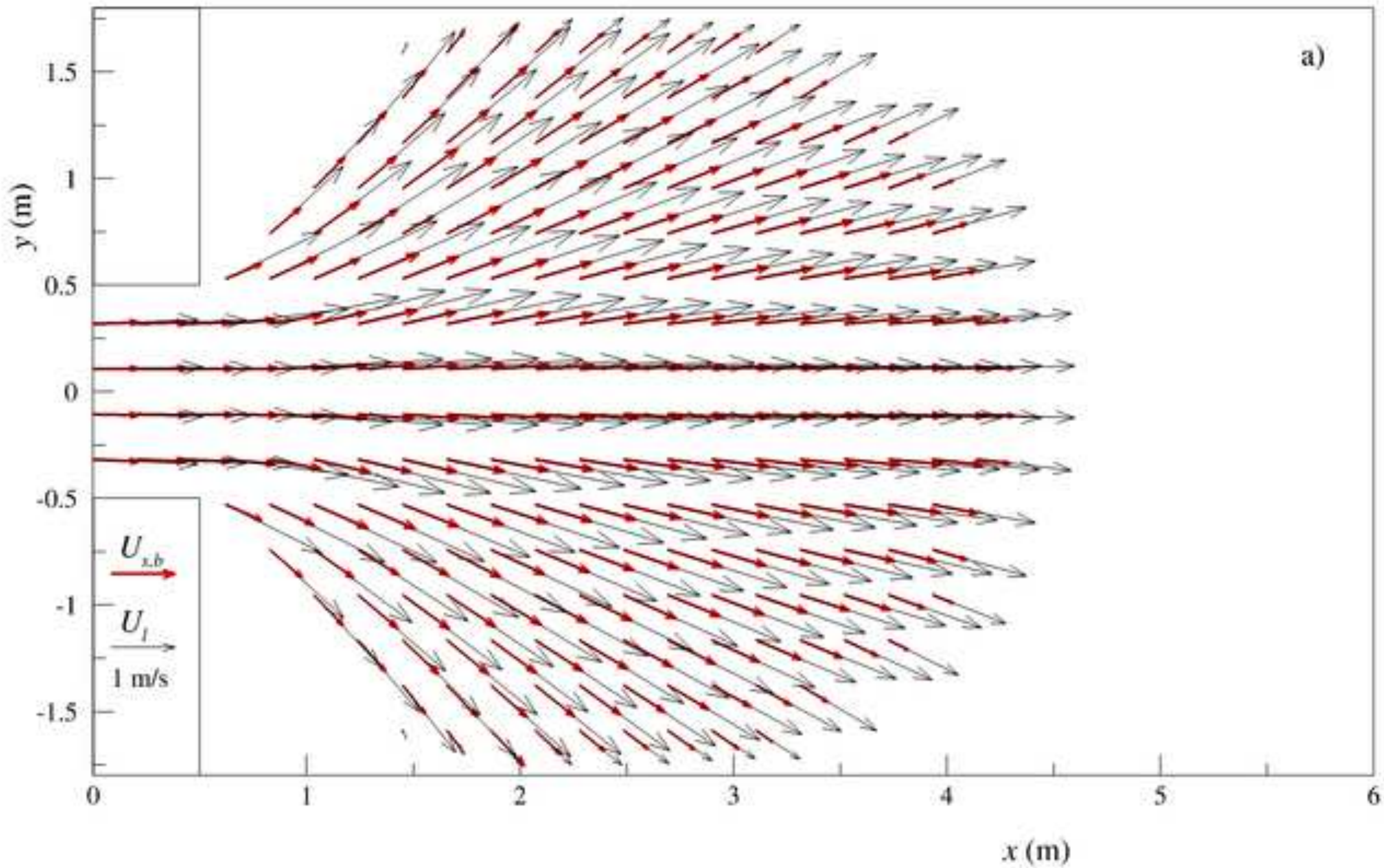

Figure
Click here to download high resolution image

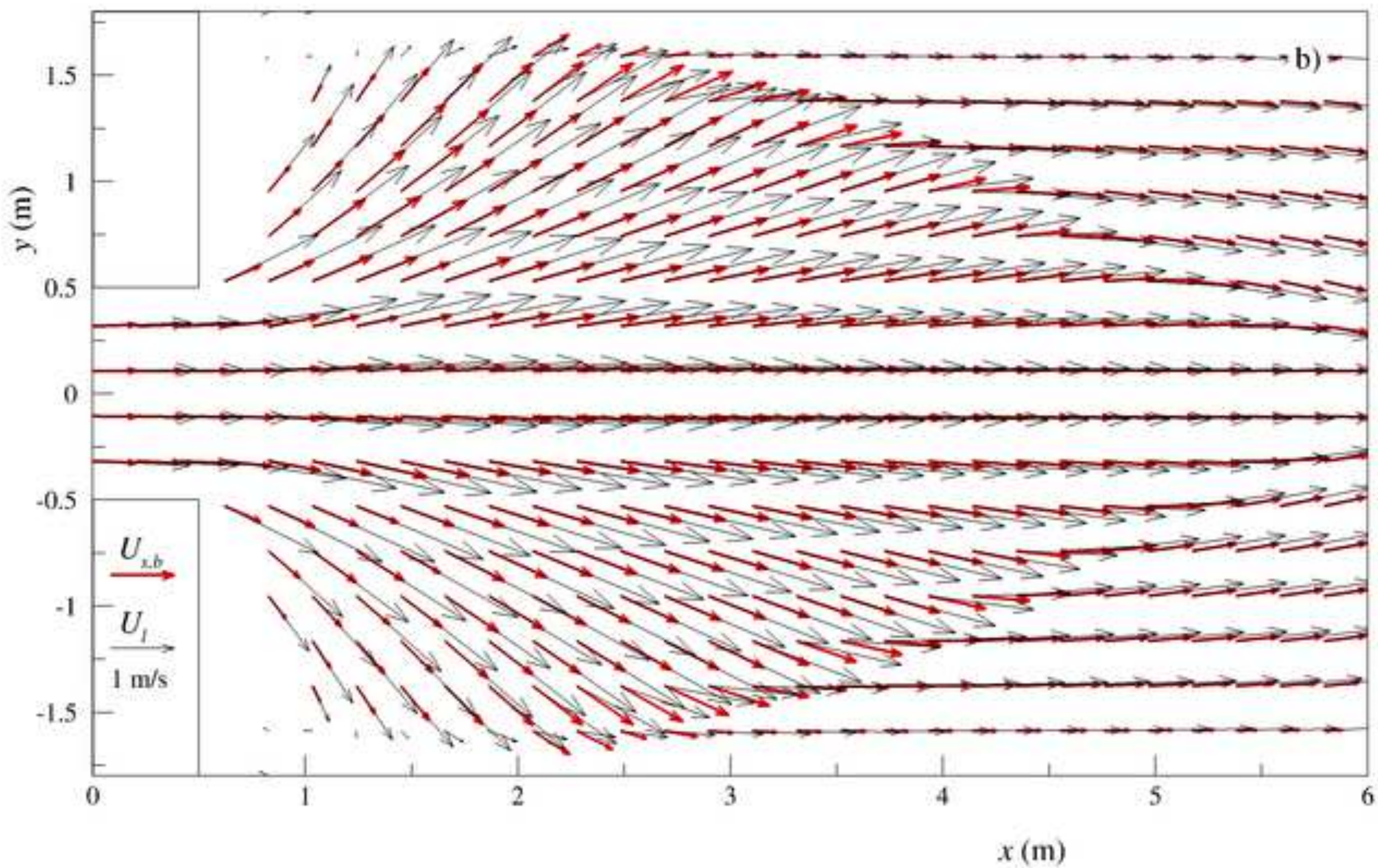

Figure
Click here to download high resolution image

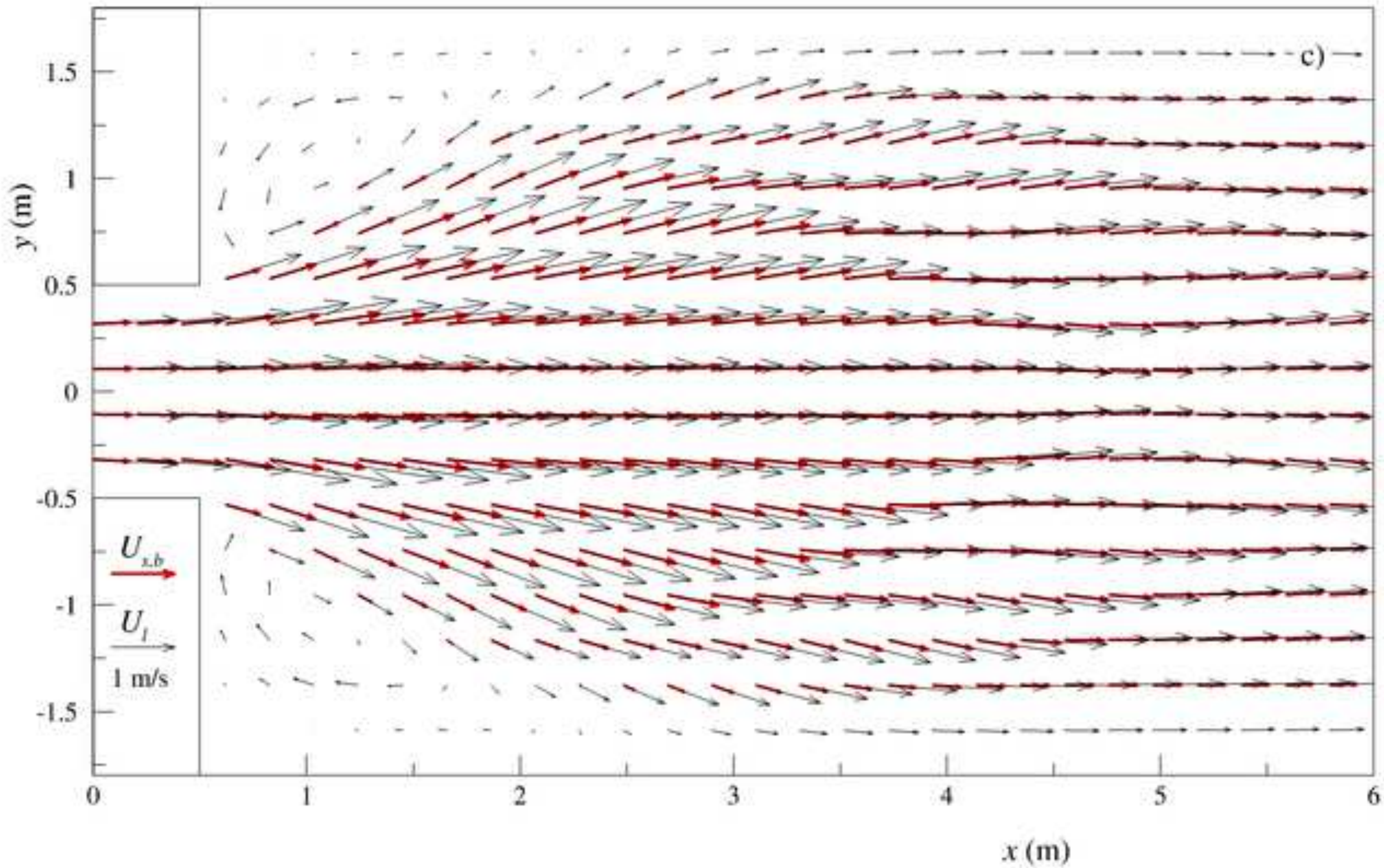

Figure
Click here to download high resolution image

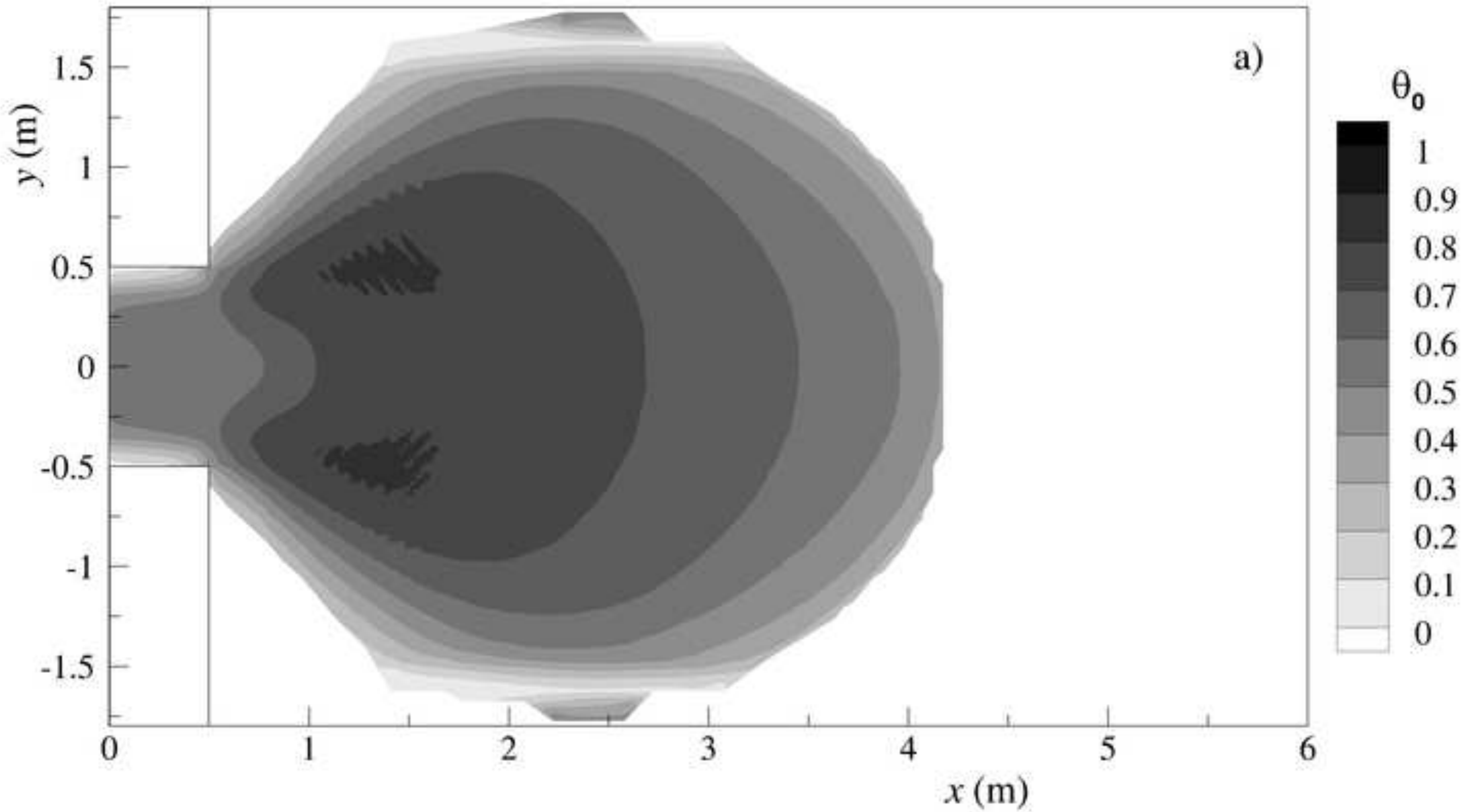

Figure
Click here to download high resolution image

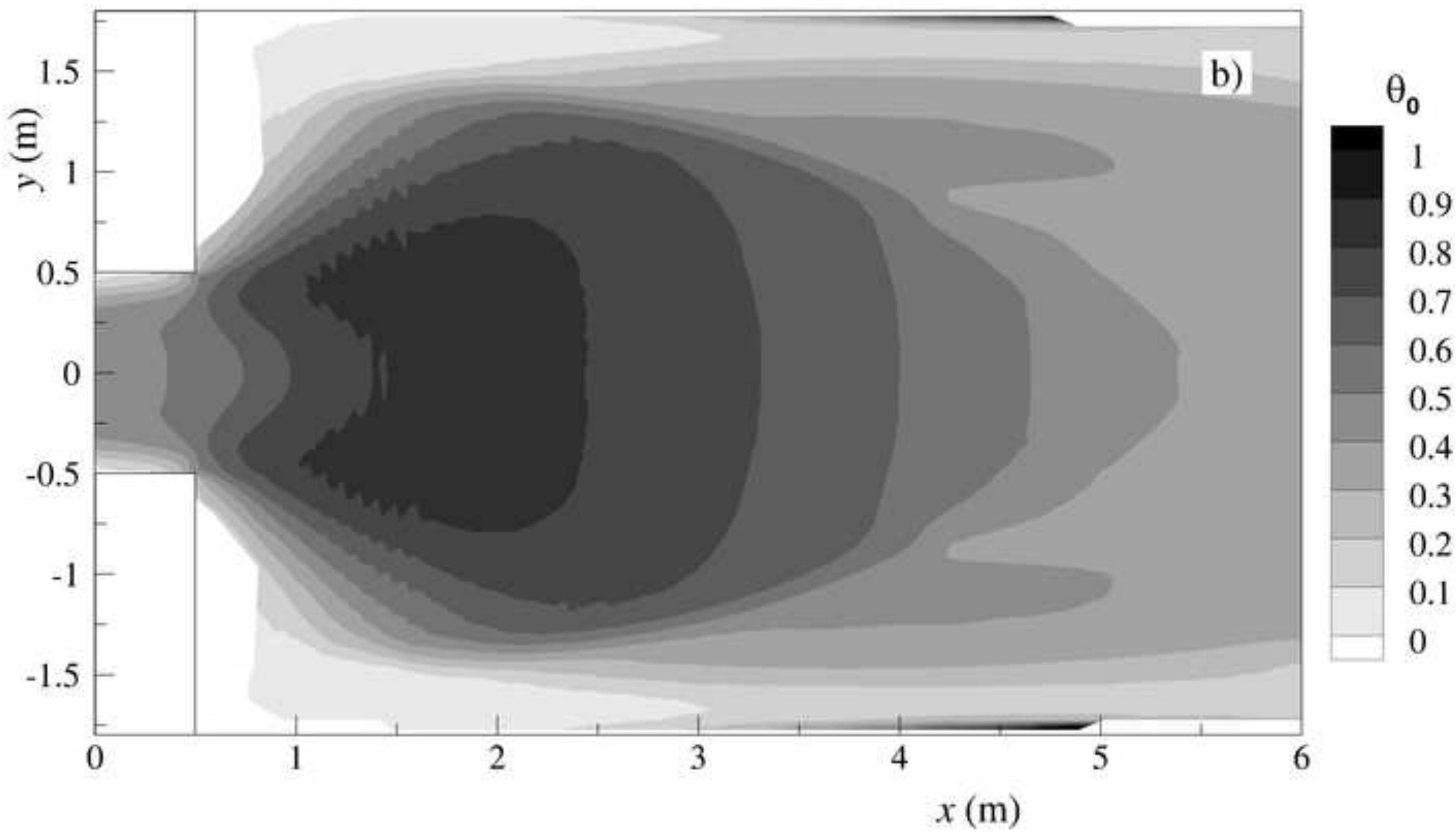

Figure
Click here to download high resolution image

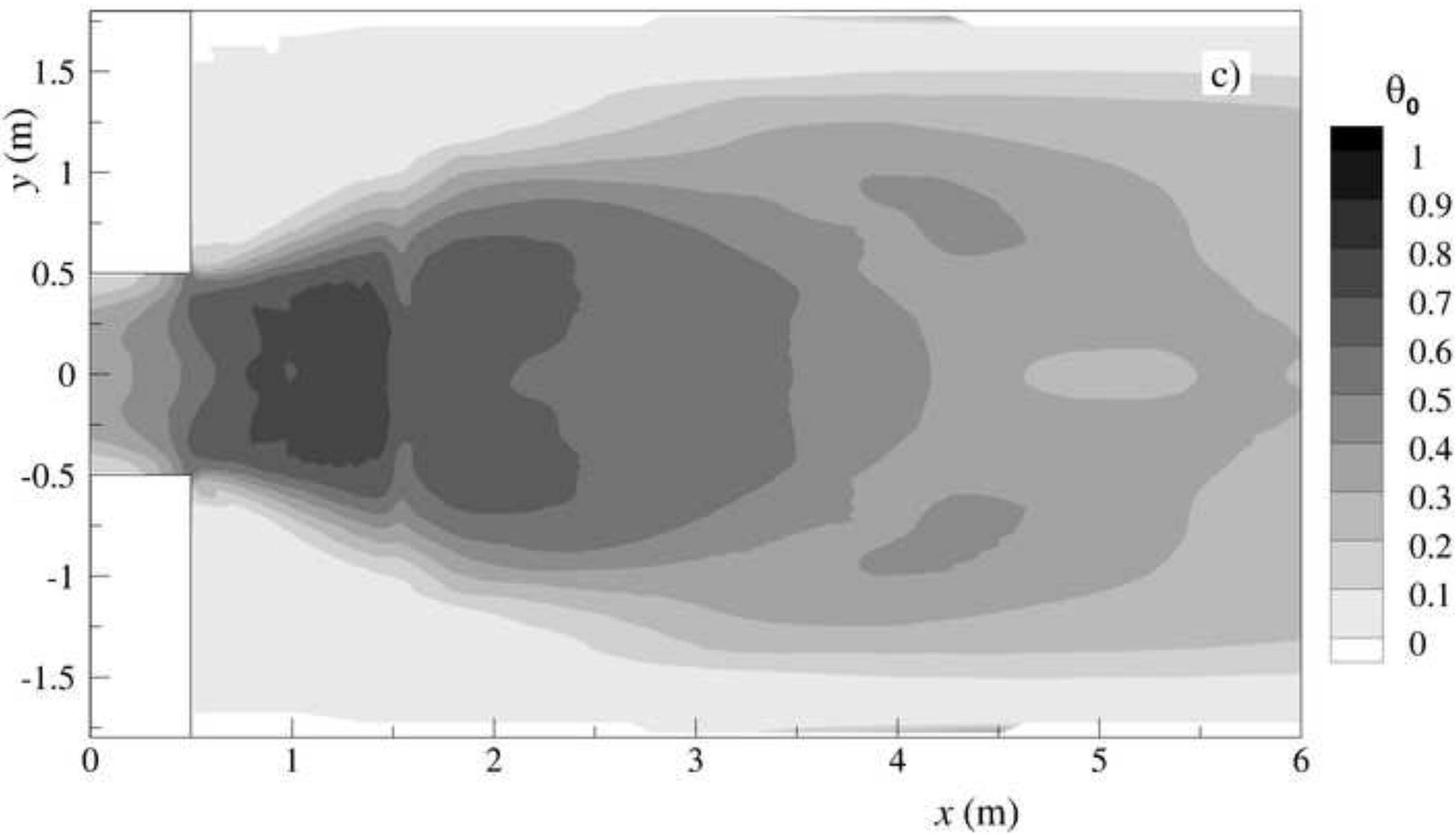

Figure
Click here to download high resolution image

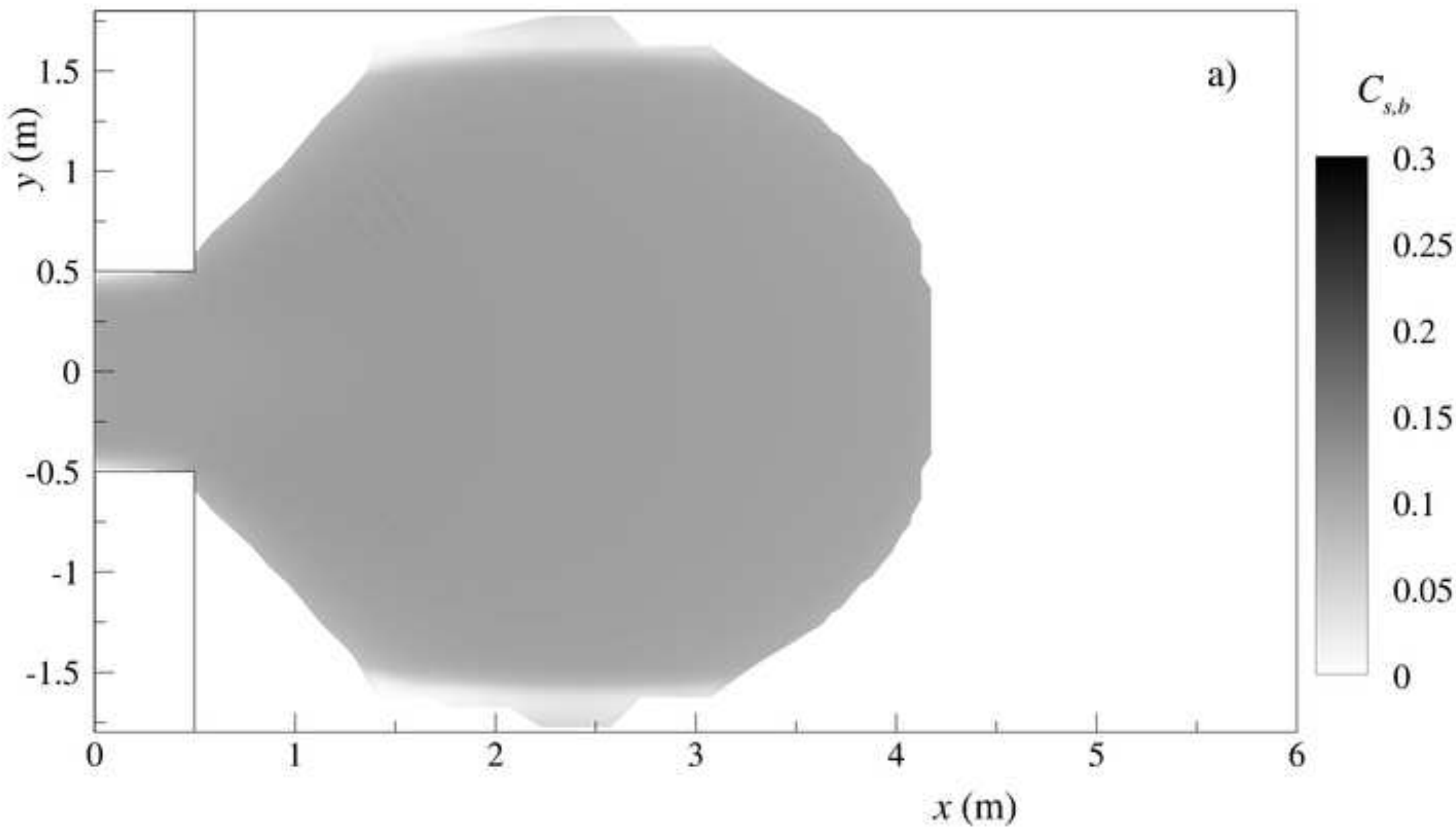

Figure

Click here to download high resolution image

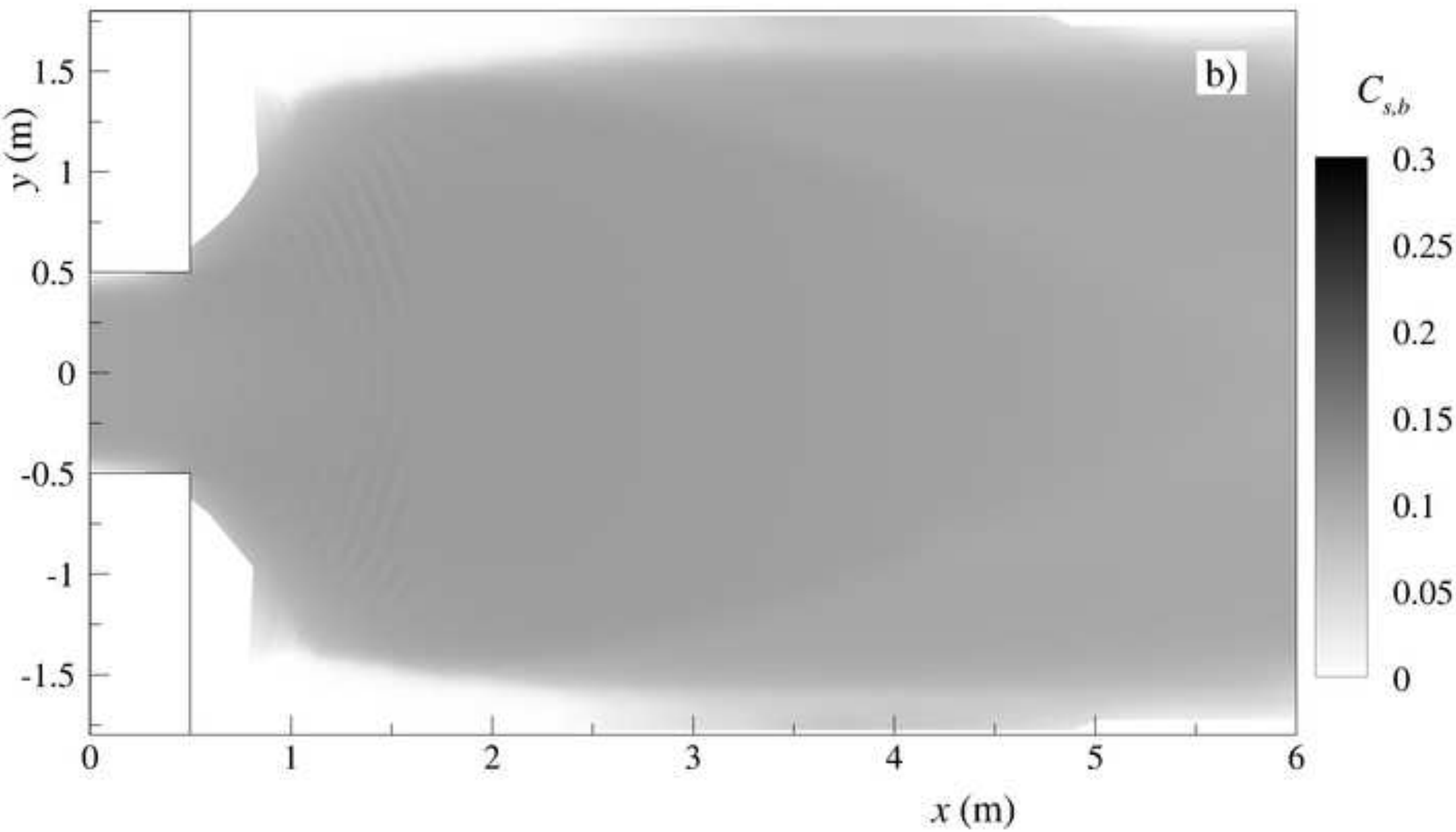

Figure
Click here to download high resolution image

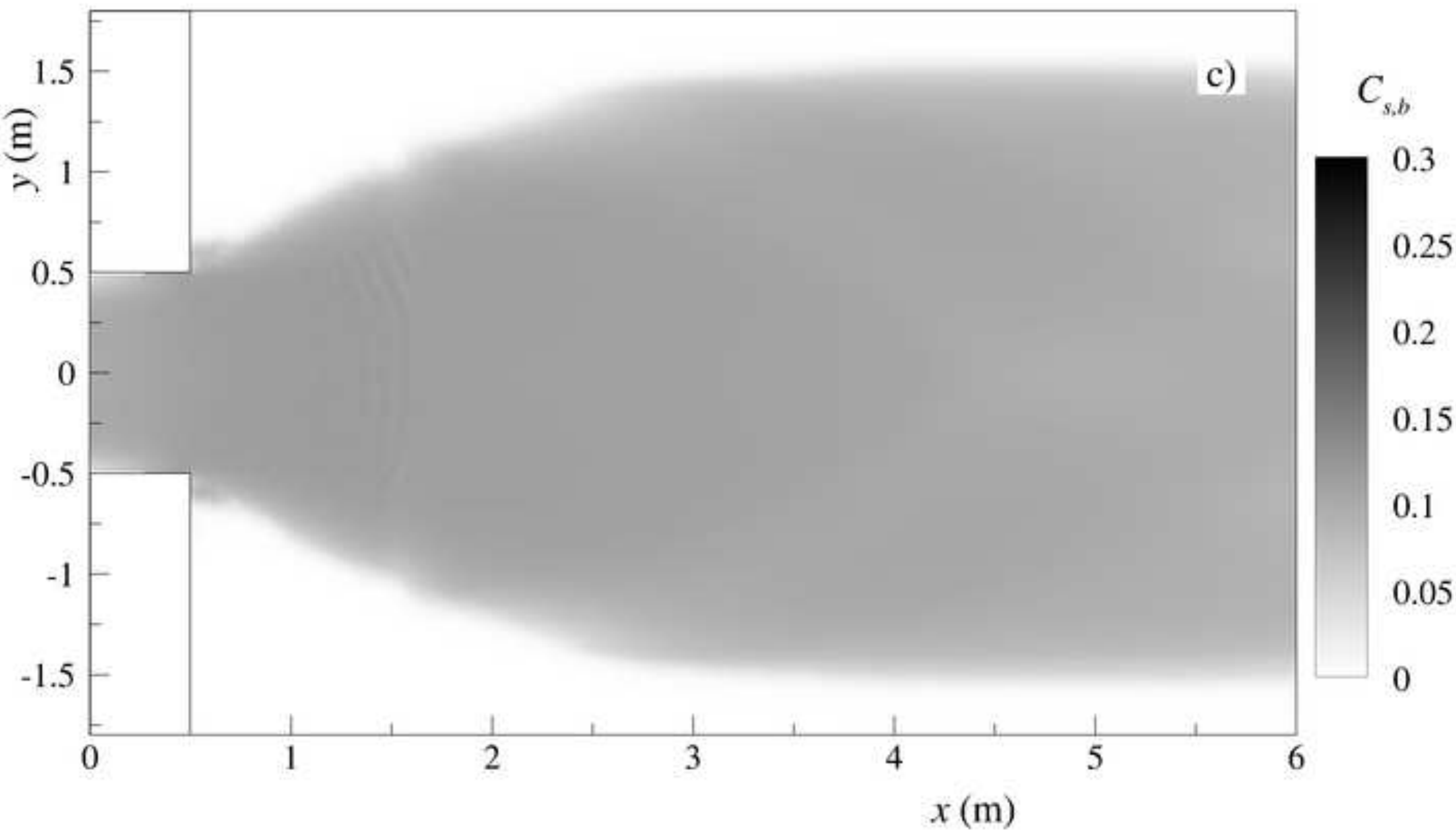

Figure

Click here to download high resolution image

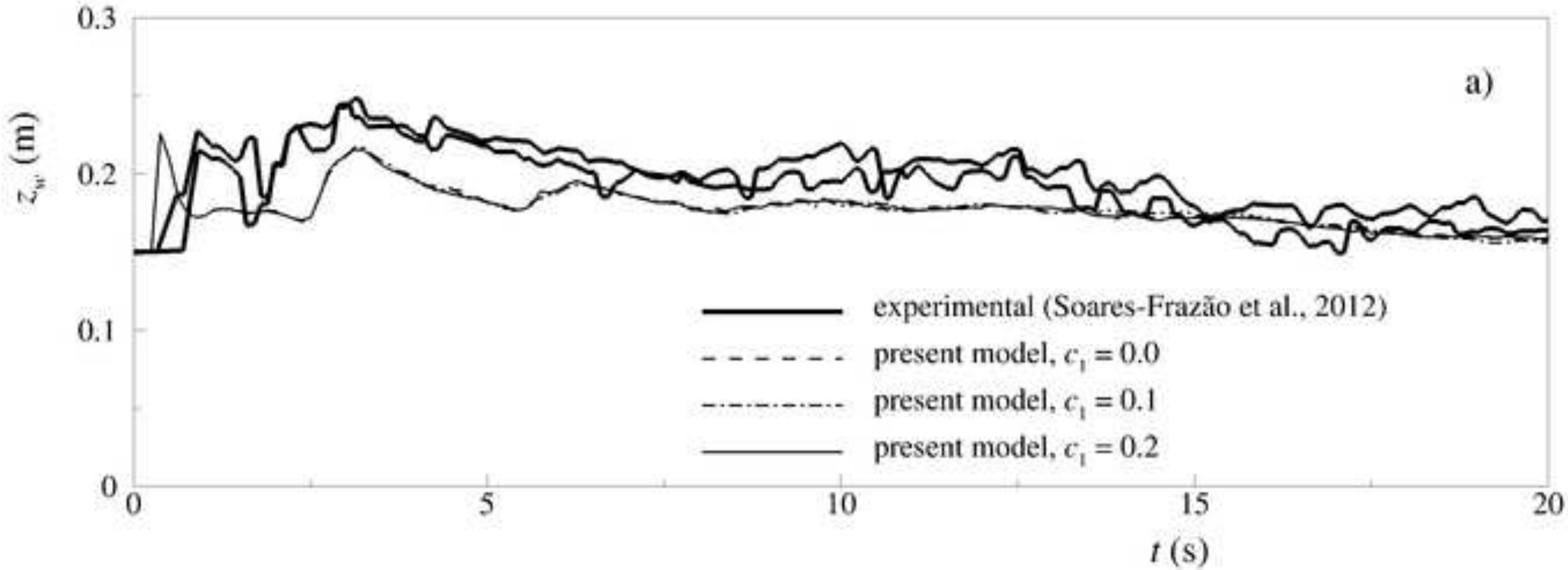

Figure
Click here to download high resolution image

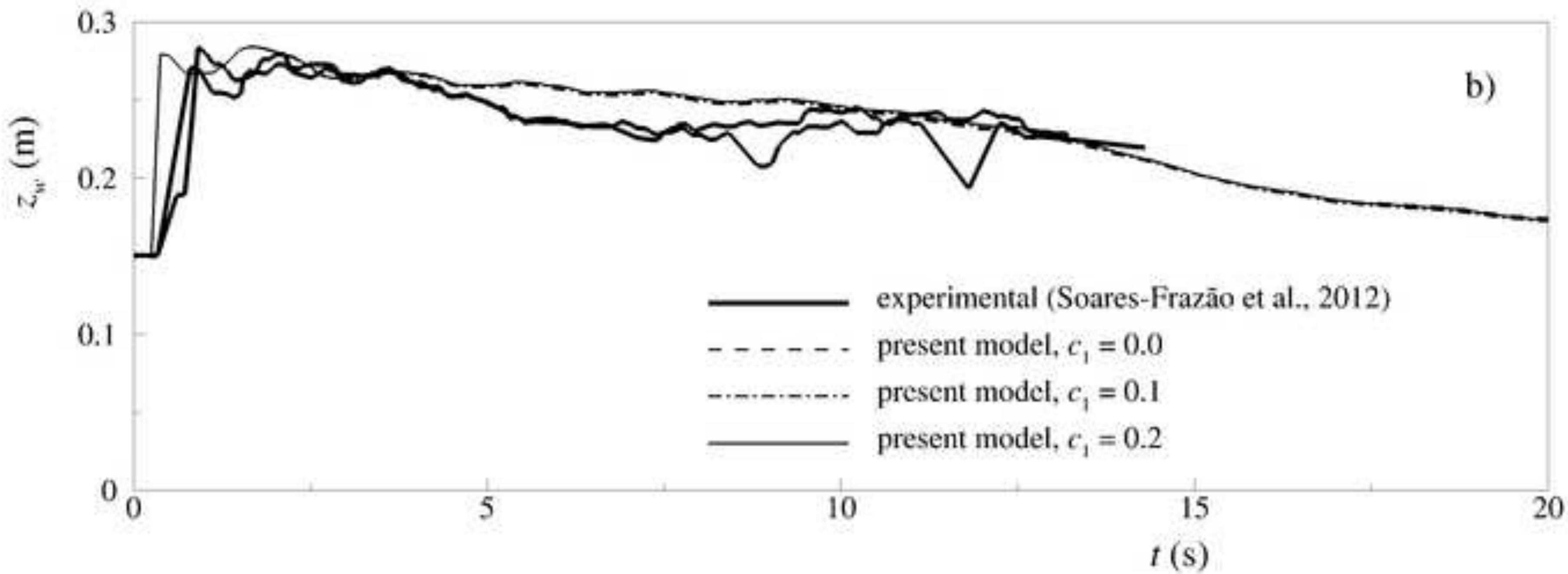

Figure
Click here to download high resolution image

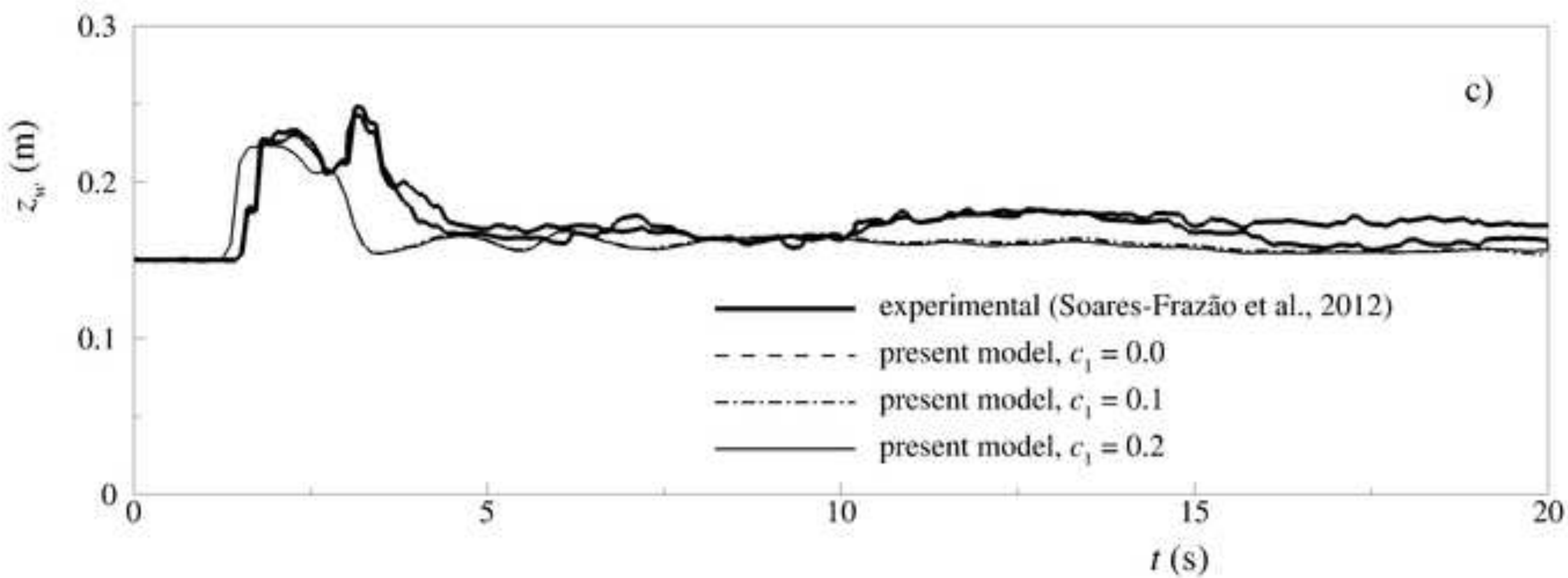

Figure
Click here to download high resolution image

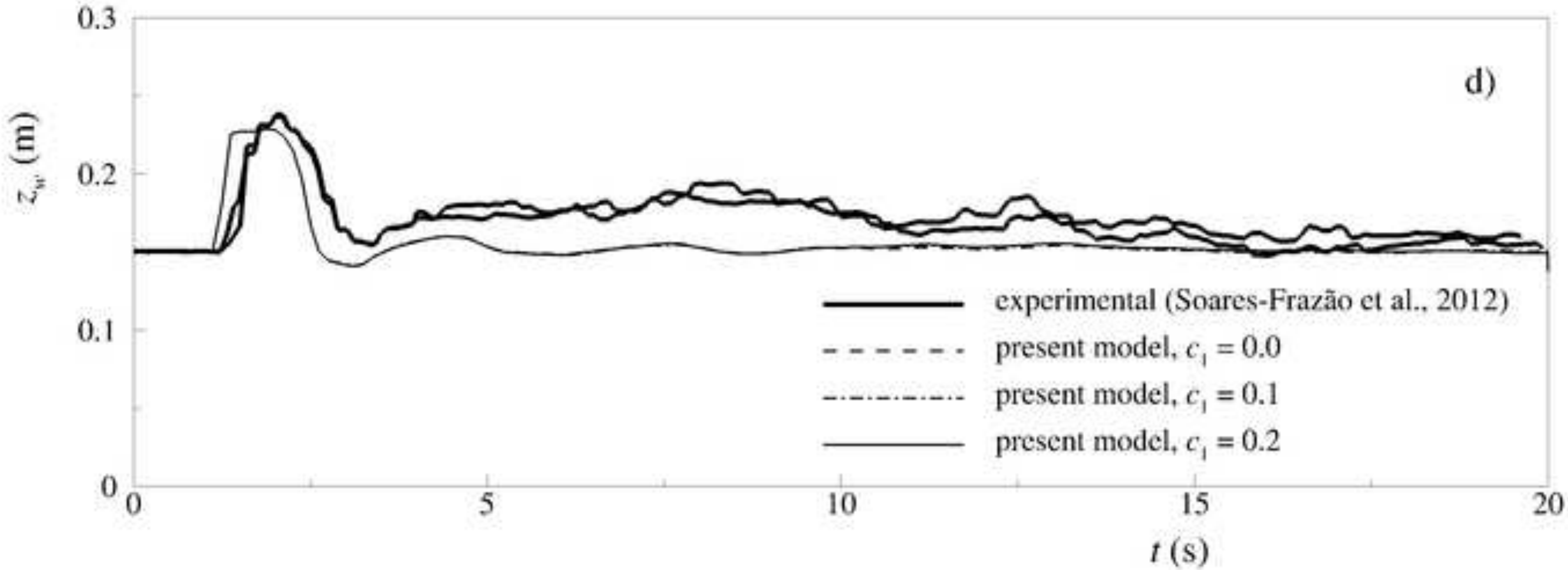

Figure
Click here to download high resolution image

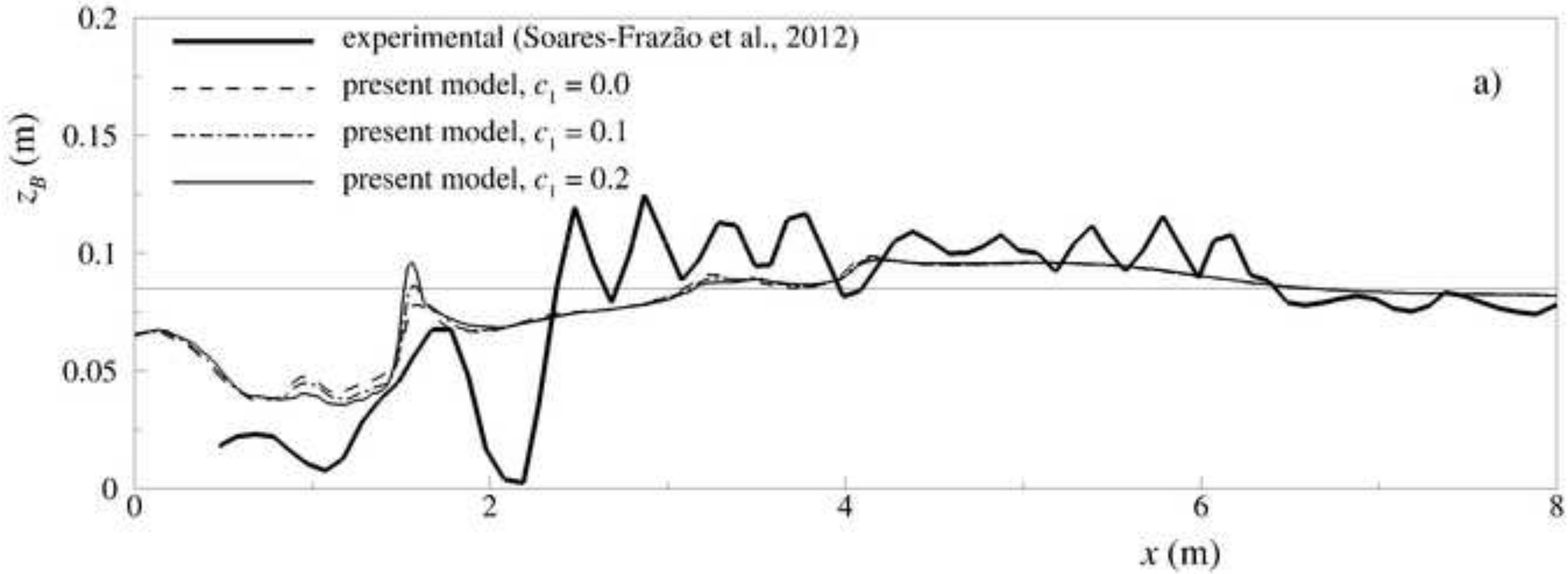

Figure
Click here to download high resolution image

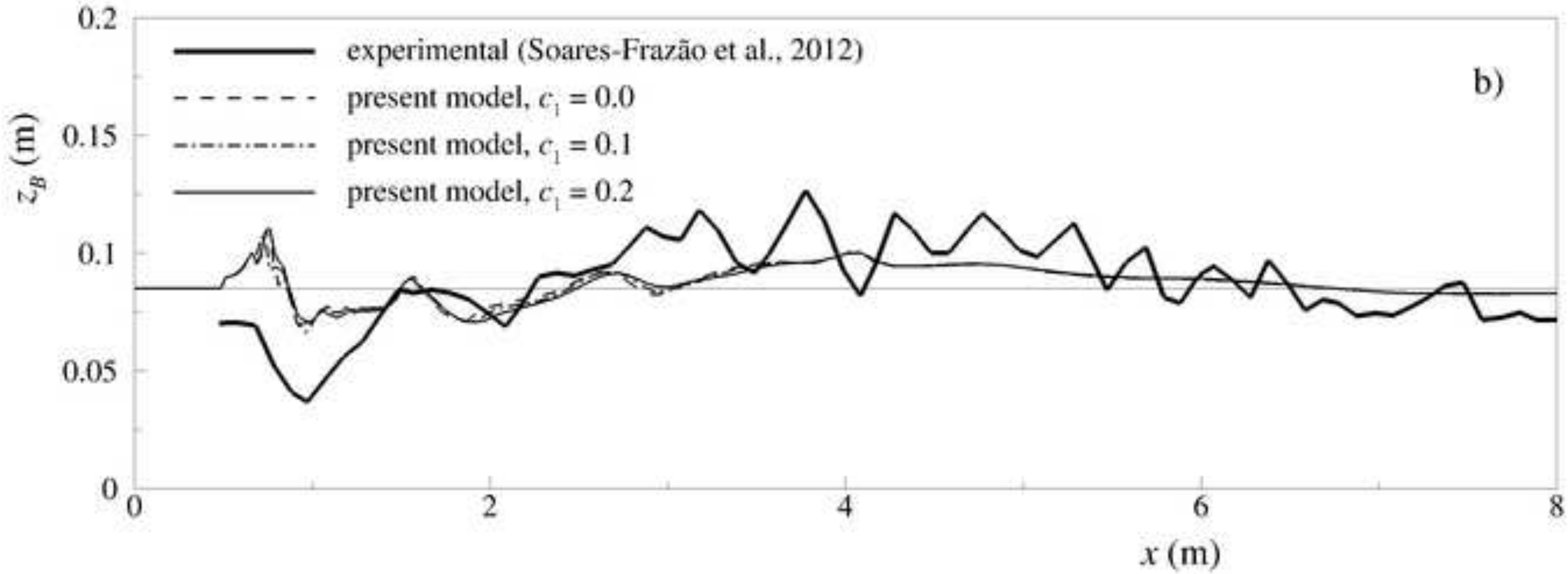

Figure
Click here to download high resolution image

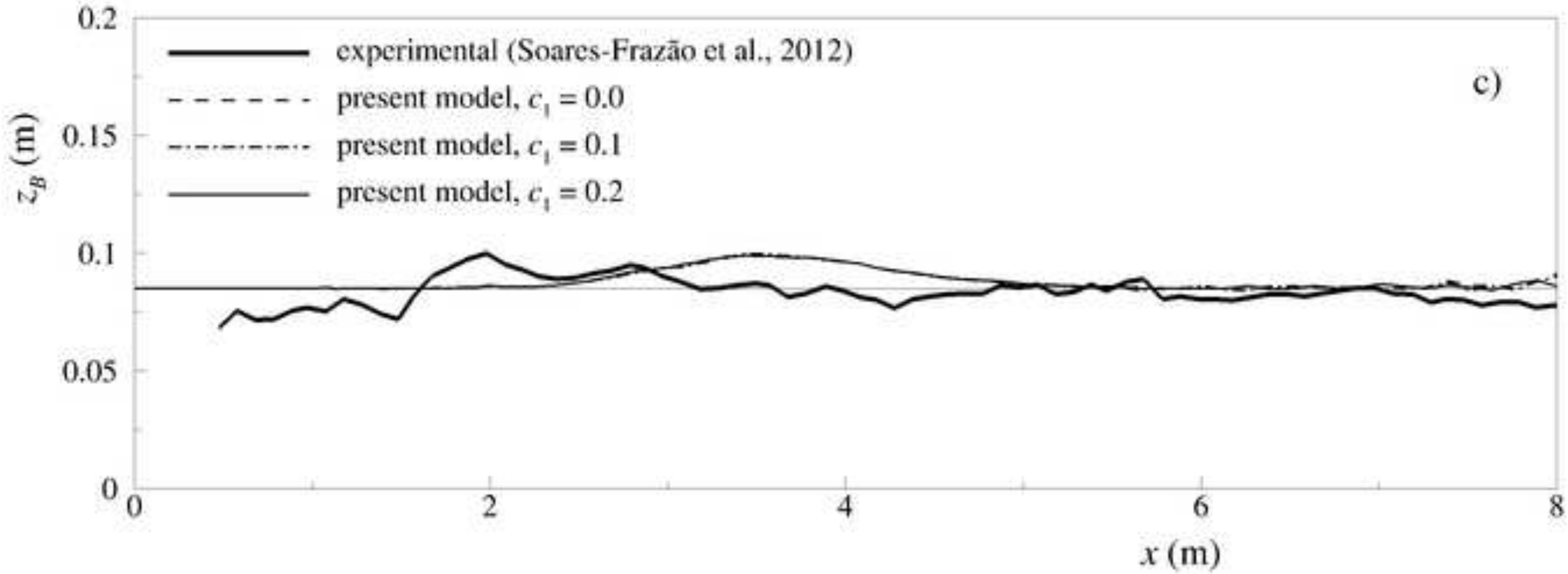

Figure

Click here to download high resolution image

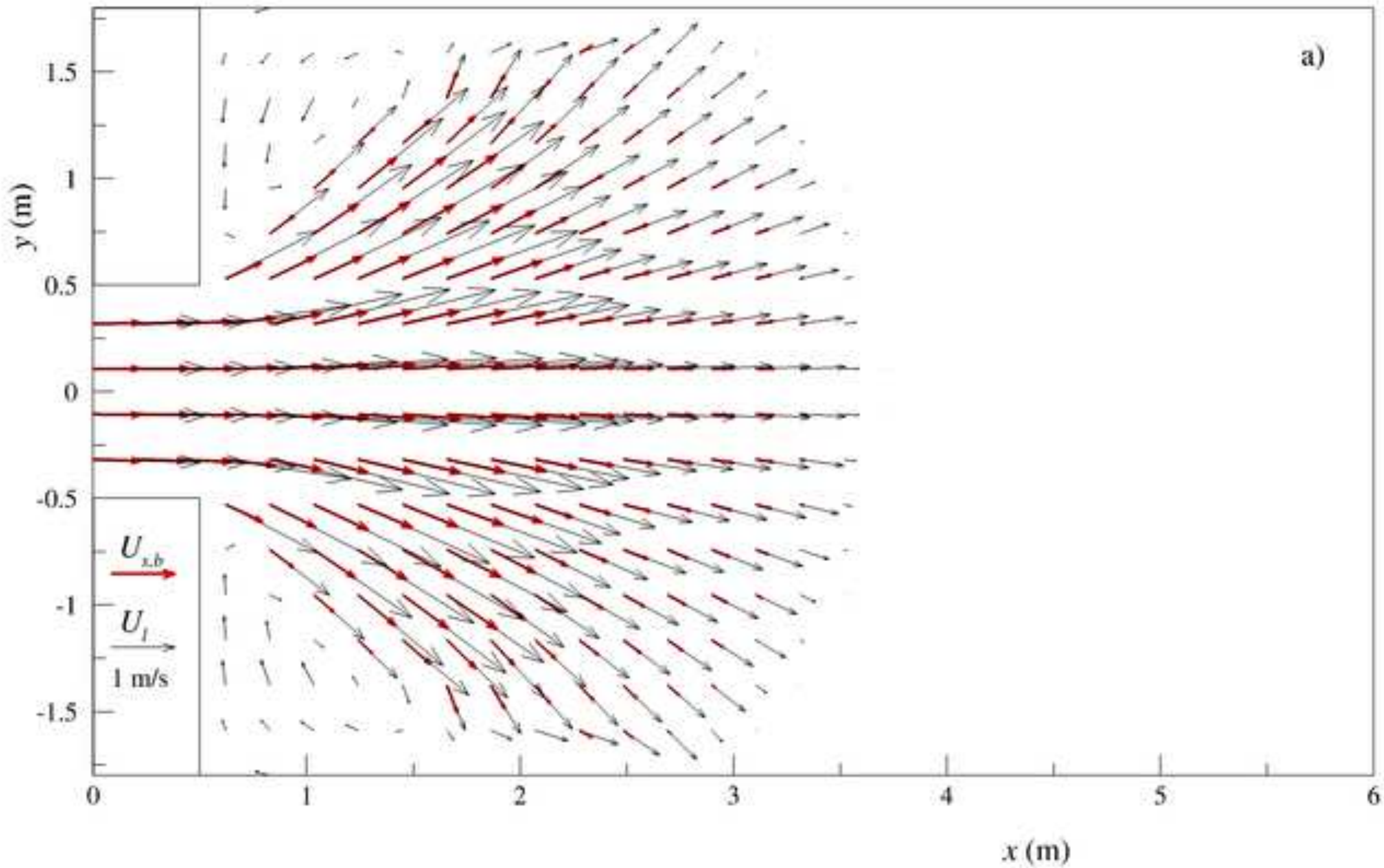

Figure
Click here to download high resolution image

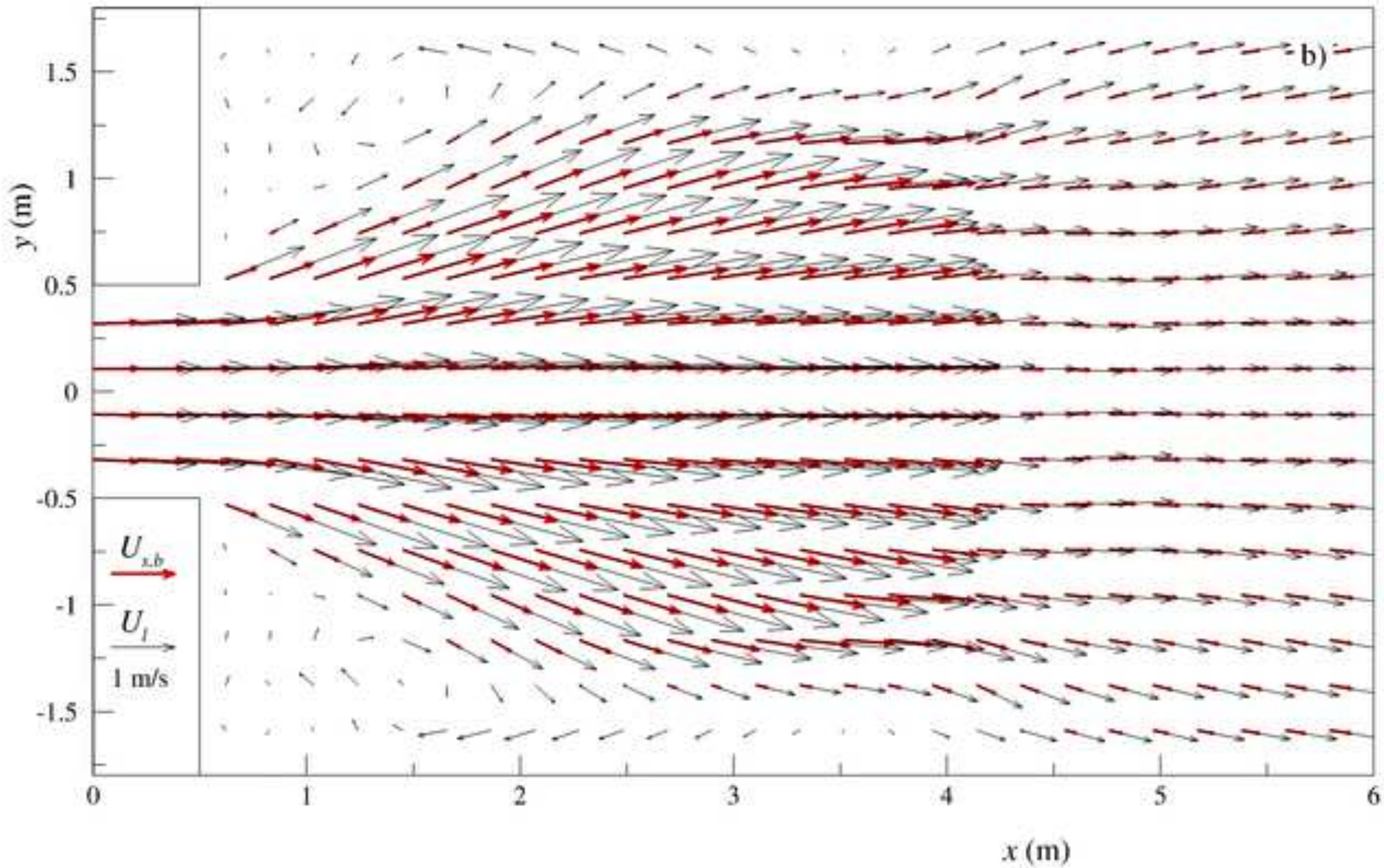

Figure
Click here to download high resolution image

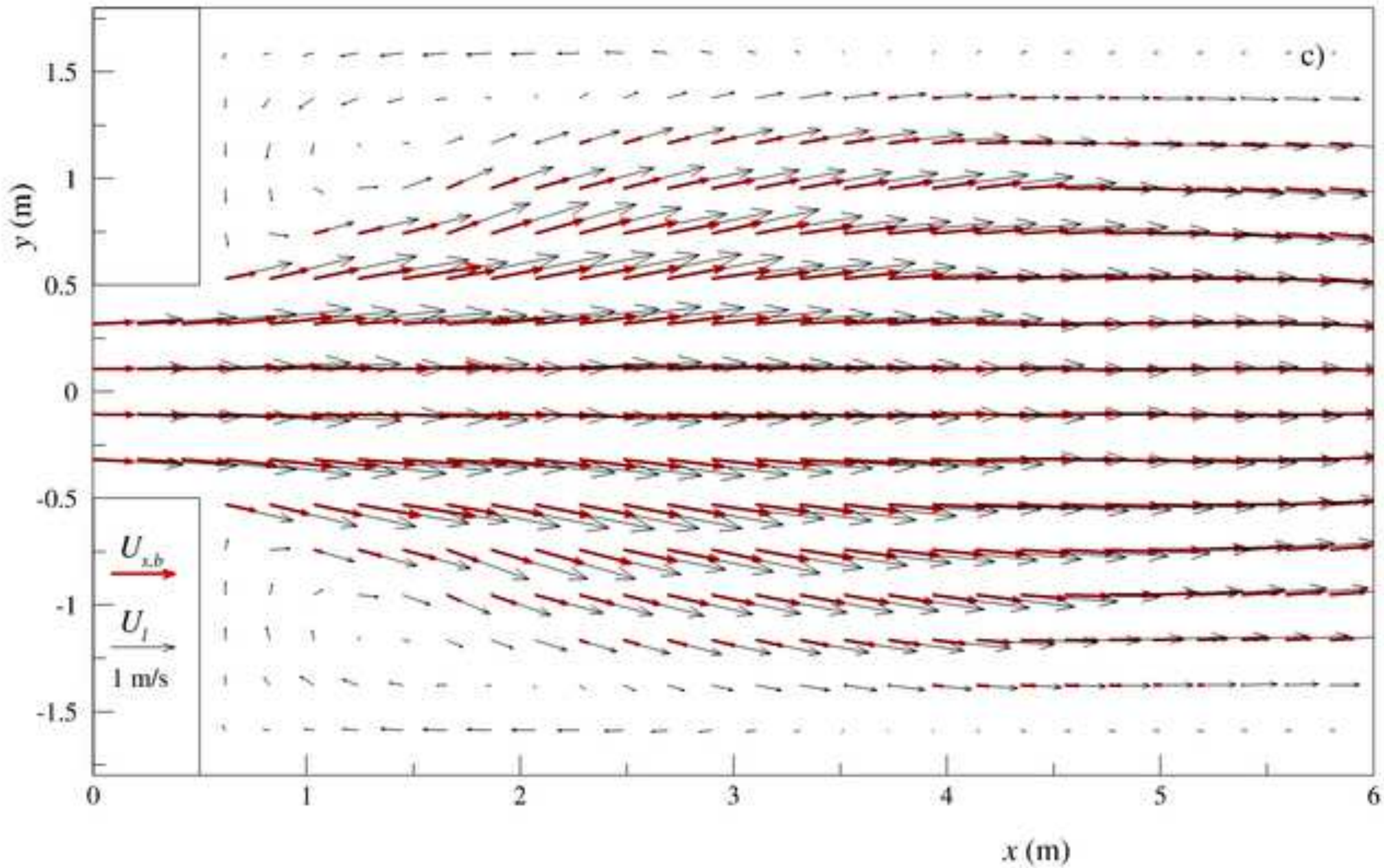

Figure
Click here to download high resolution image

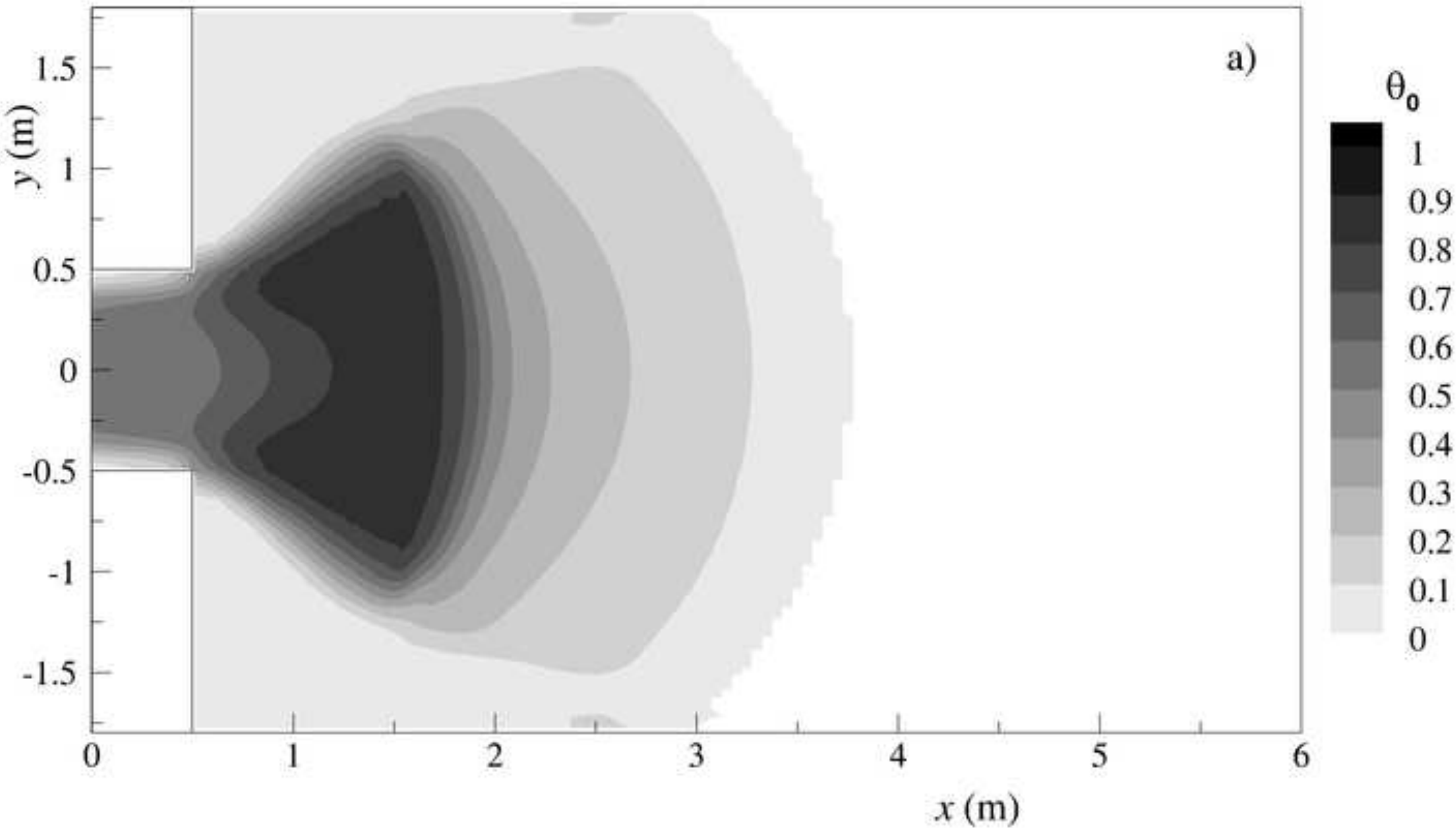

Figure
Click here to download high resolution image

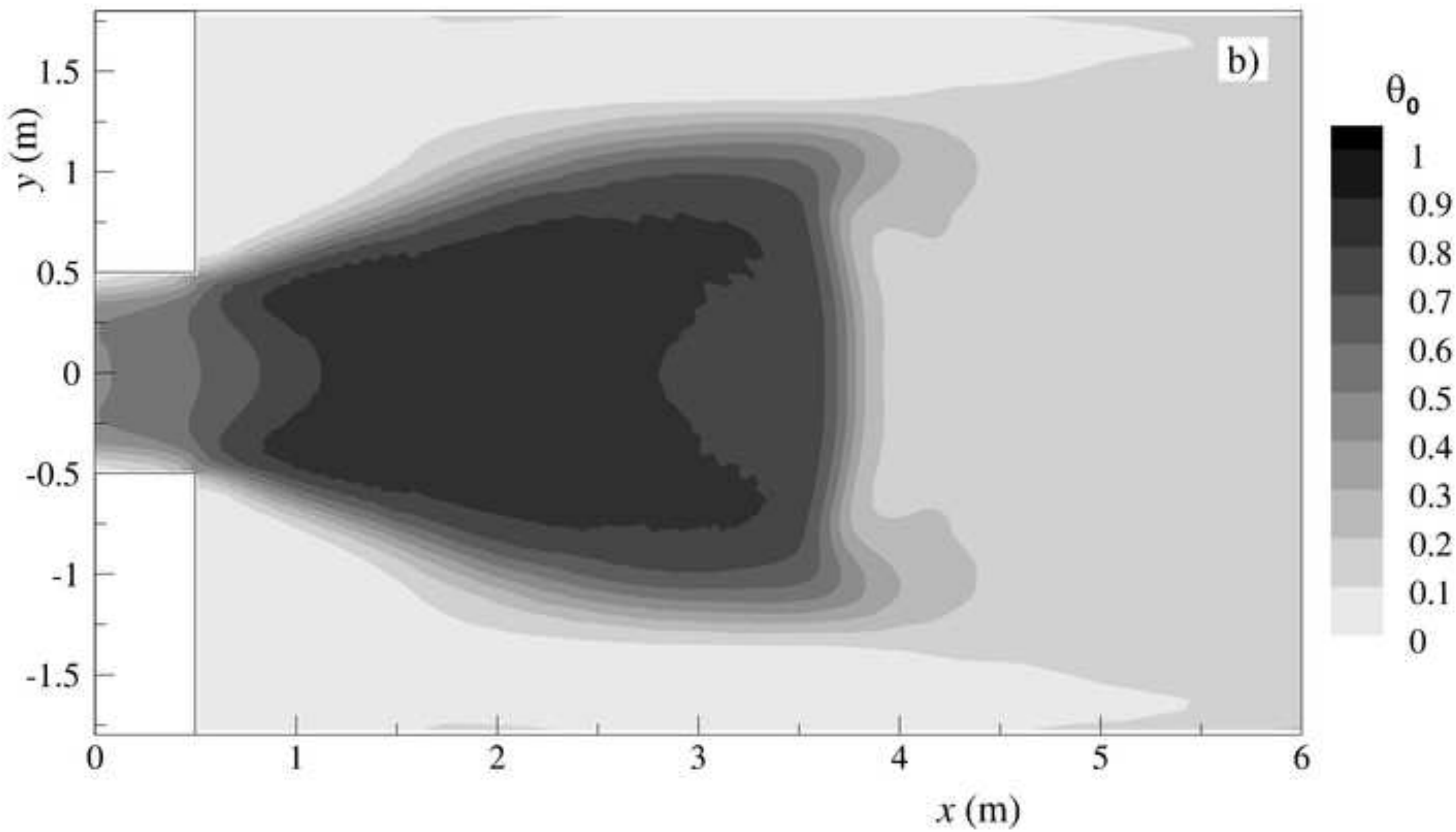

Figure
Click here to download high resolution image

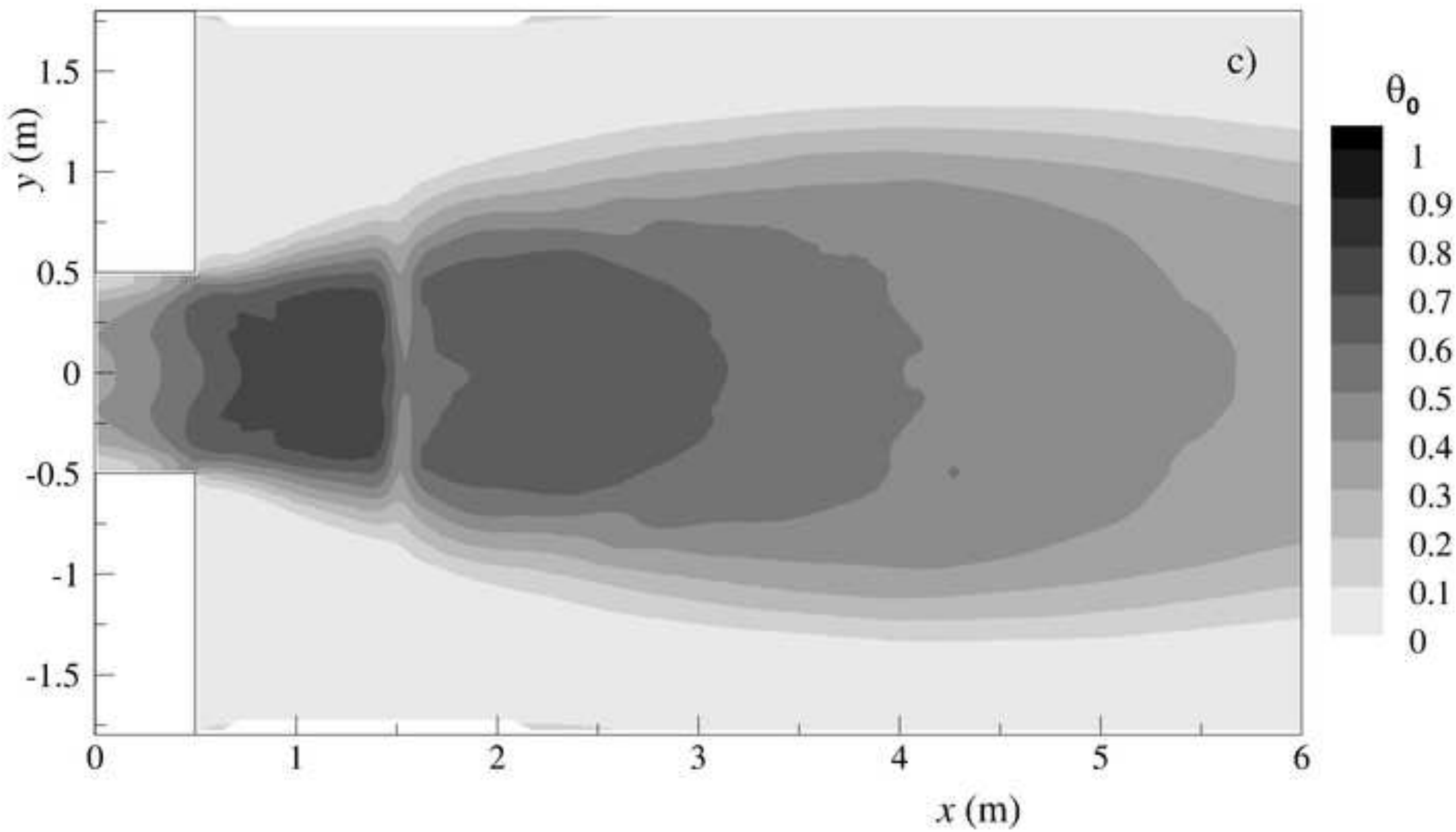

Figure
Click here to download high resolution image

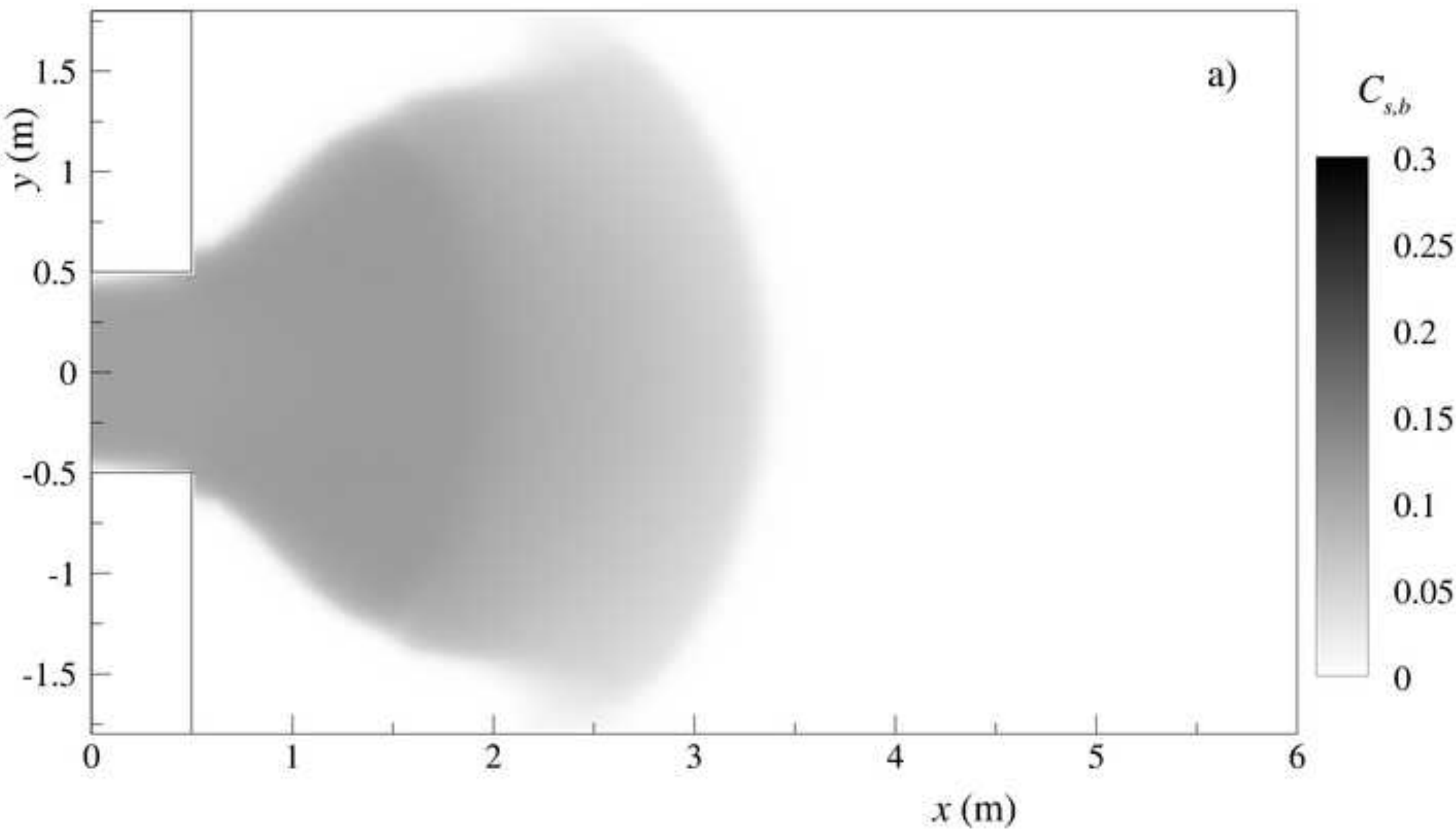

Figure
Click here to download high resolution image

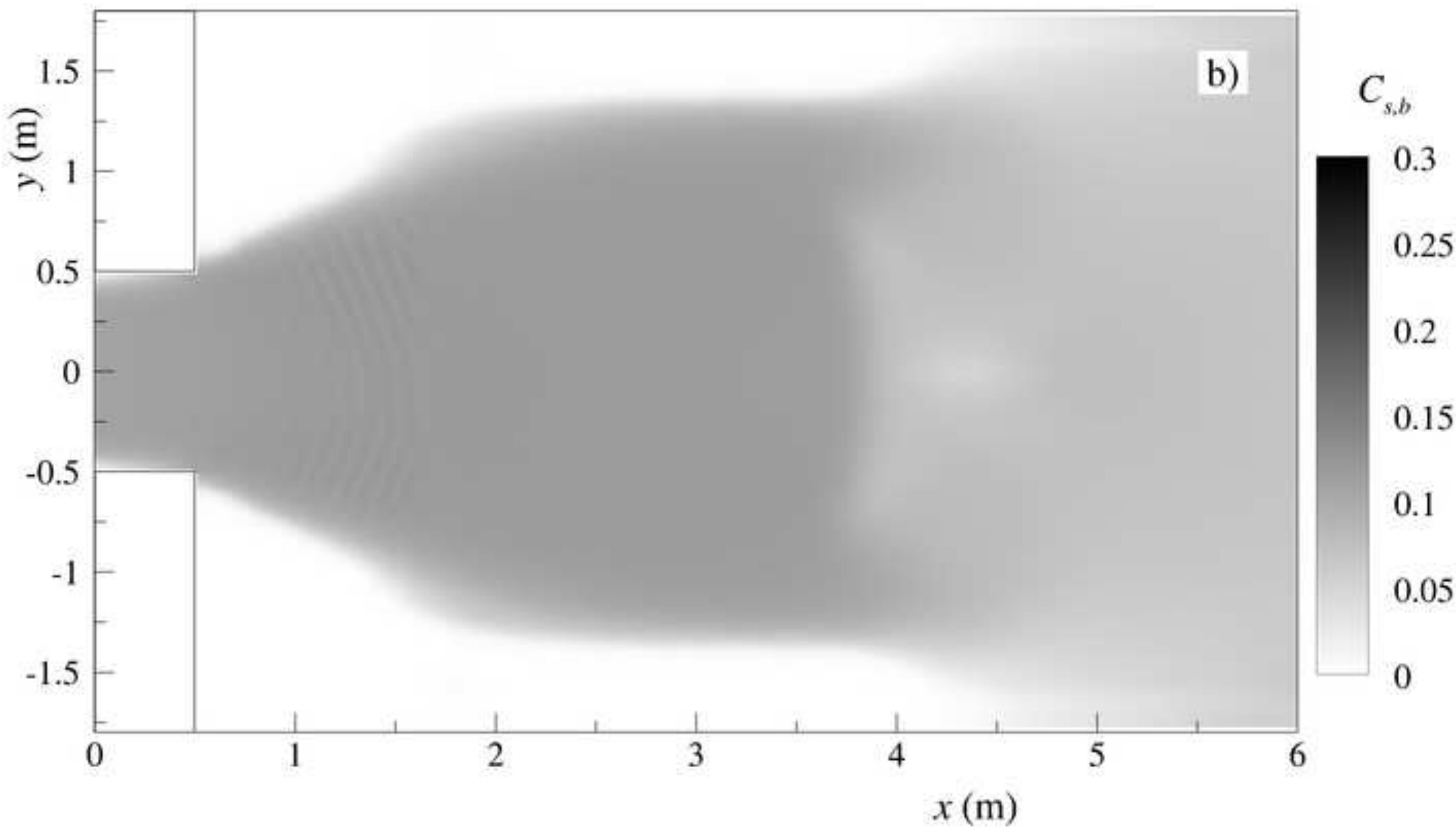

Figure
Click here to download high resolution image

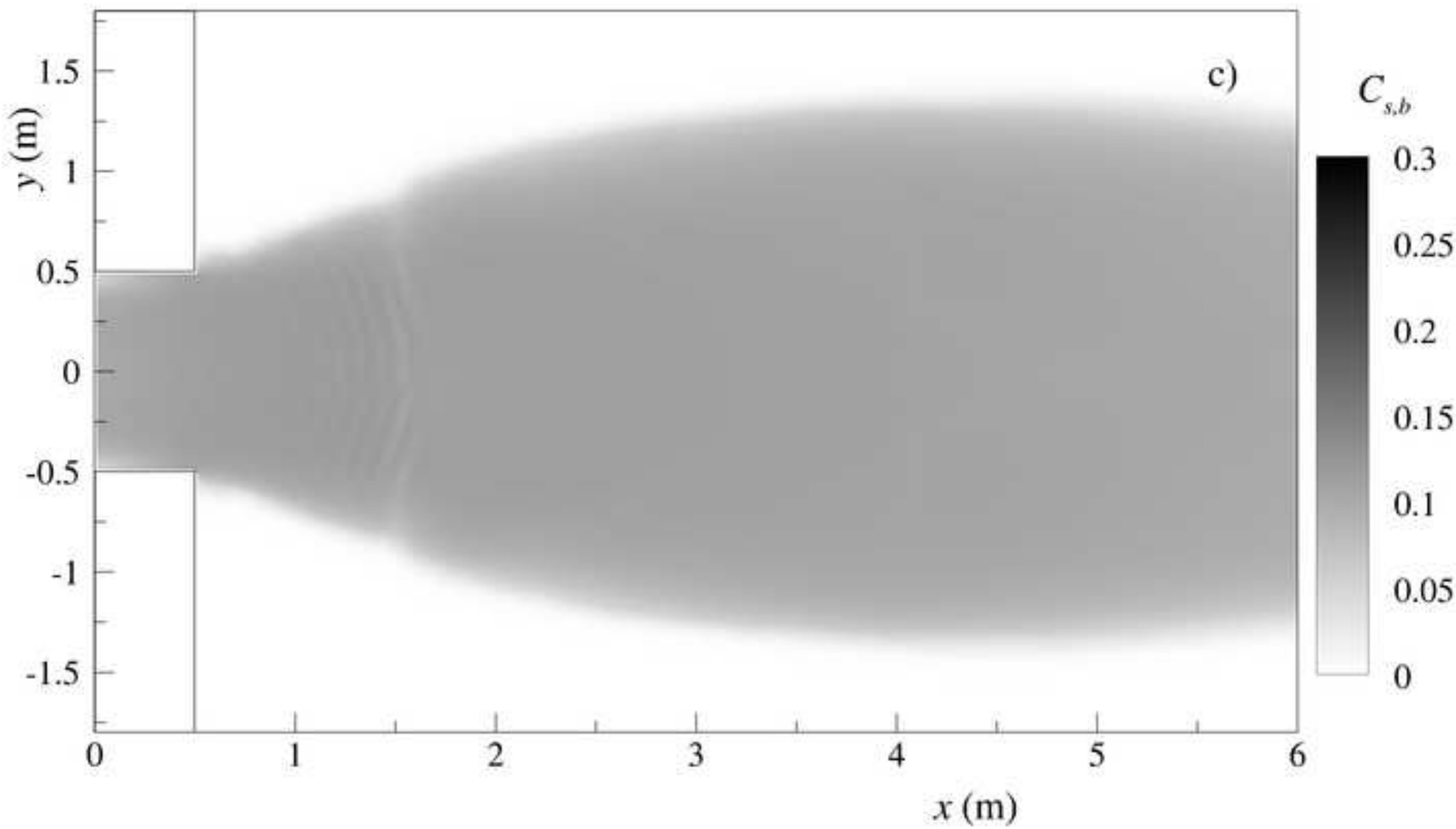

Figure
Click here to download high resolution image

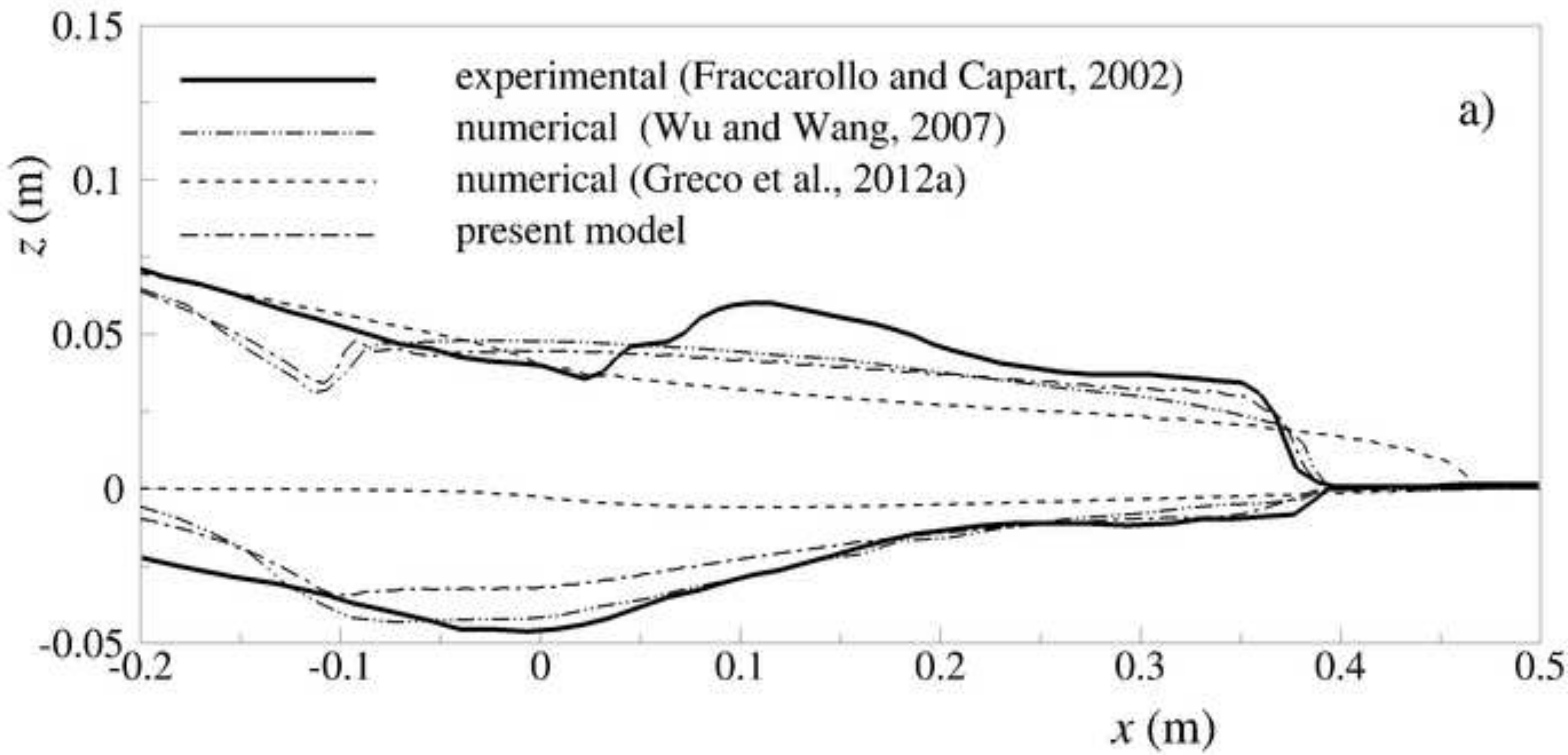

Figure
Click here to download high resolution image

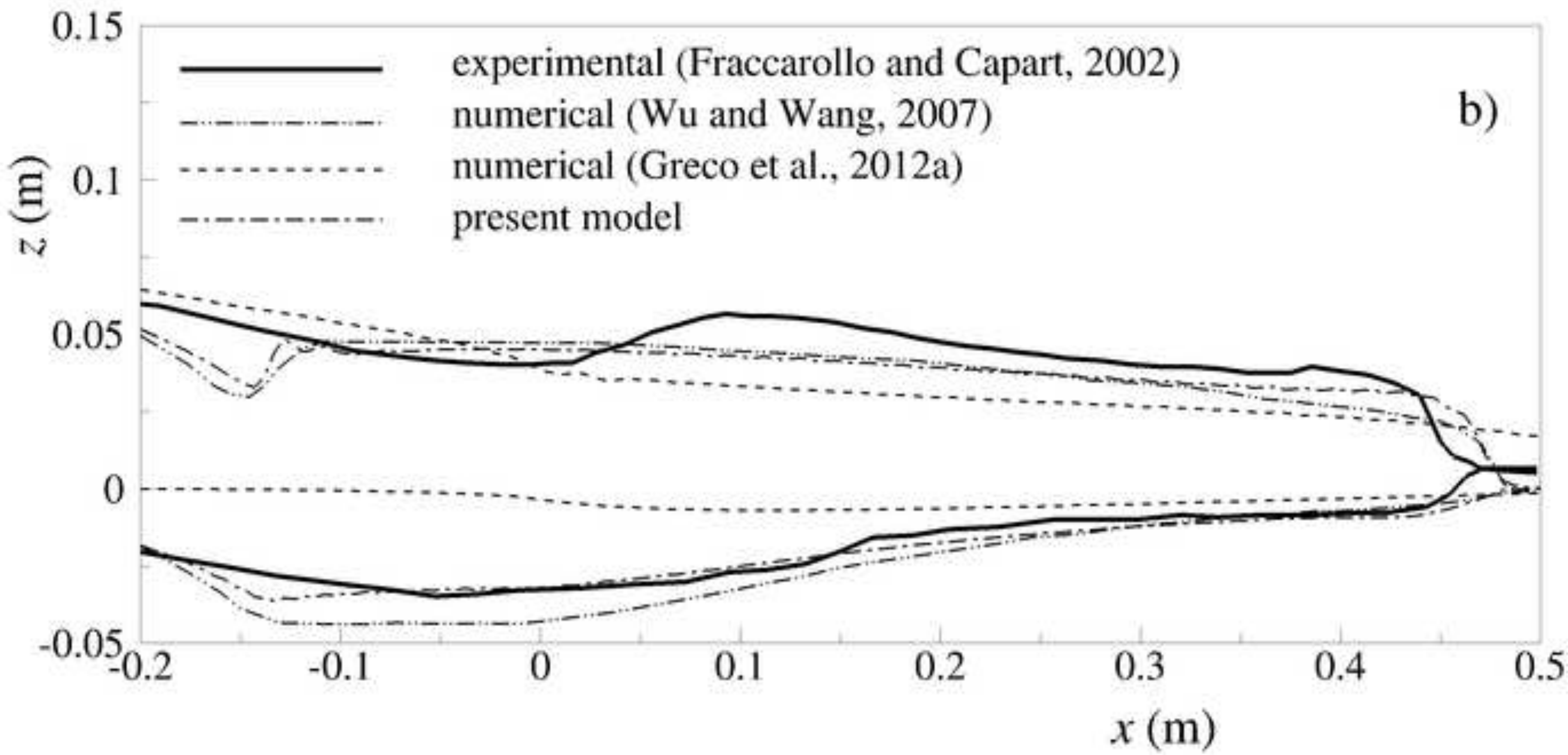

Figure
Click here to download high resolution image

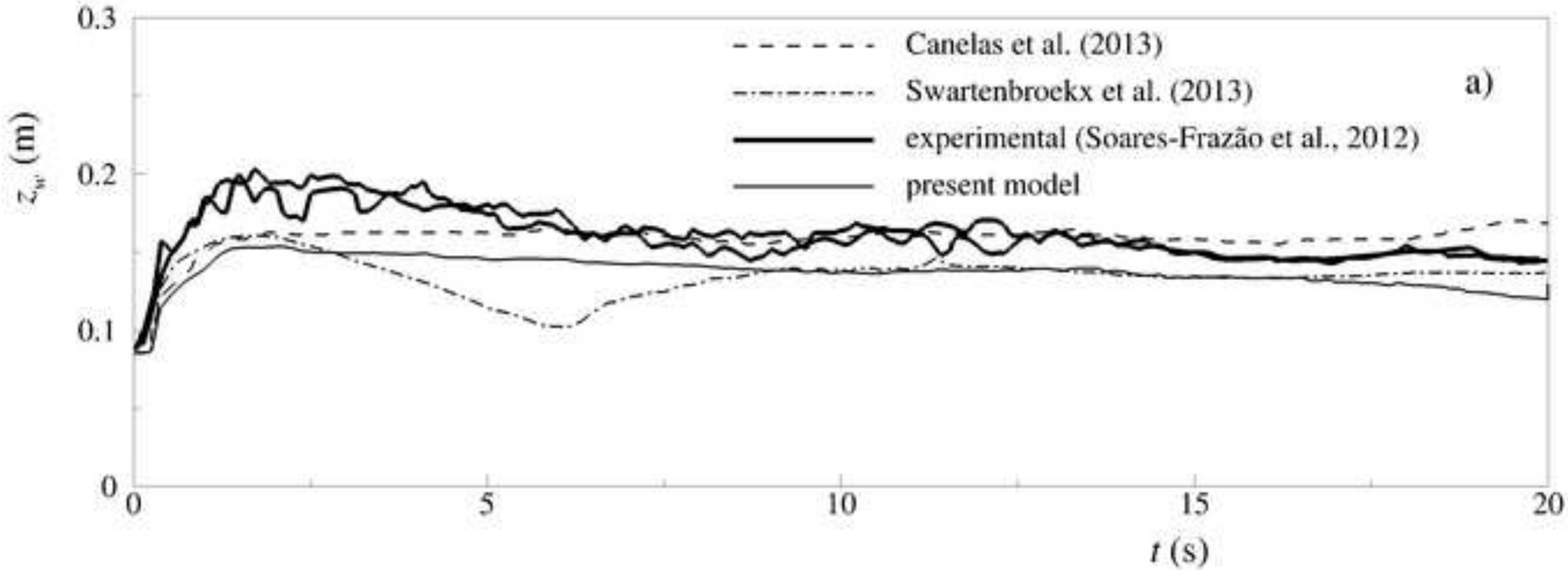

Figure
Click here to download high resolution image

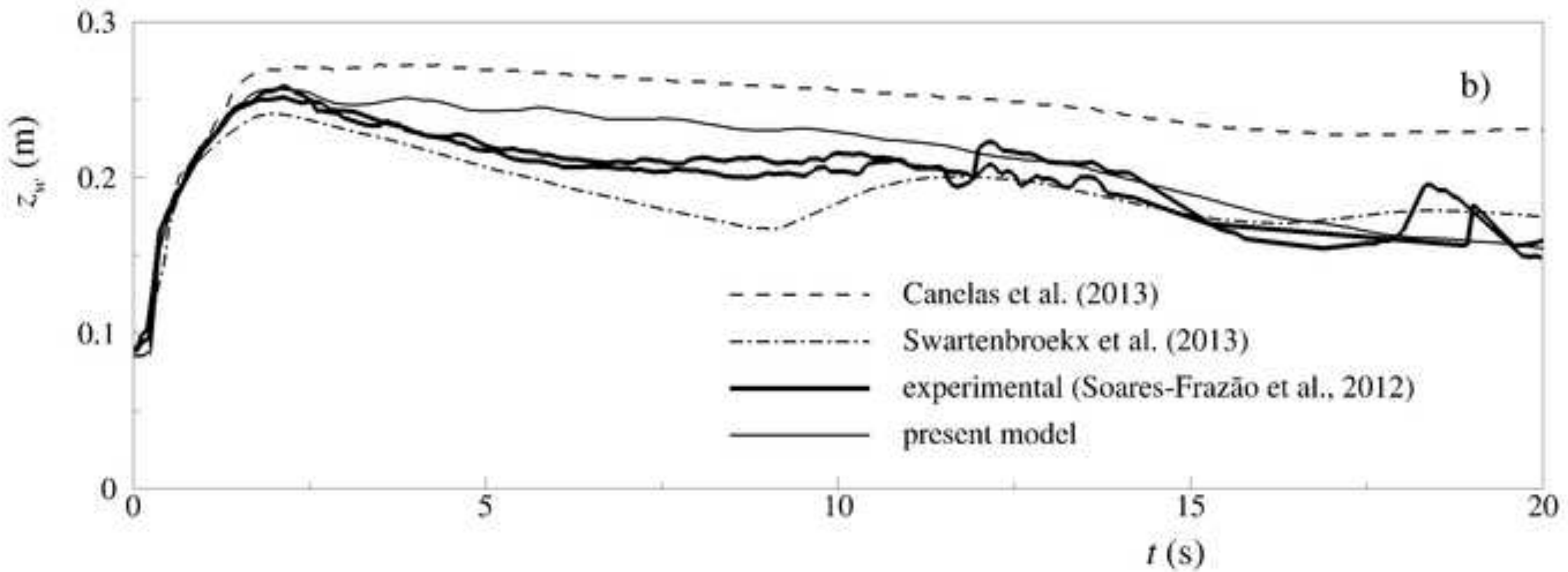

Figure
Click here to download high resolution image

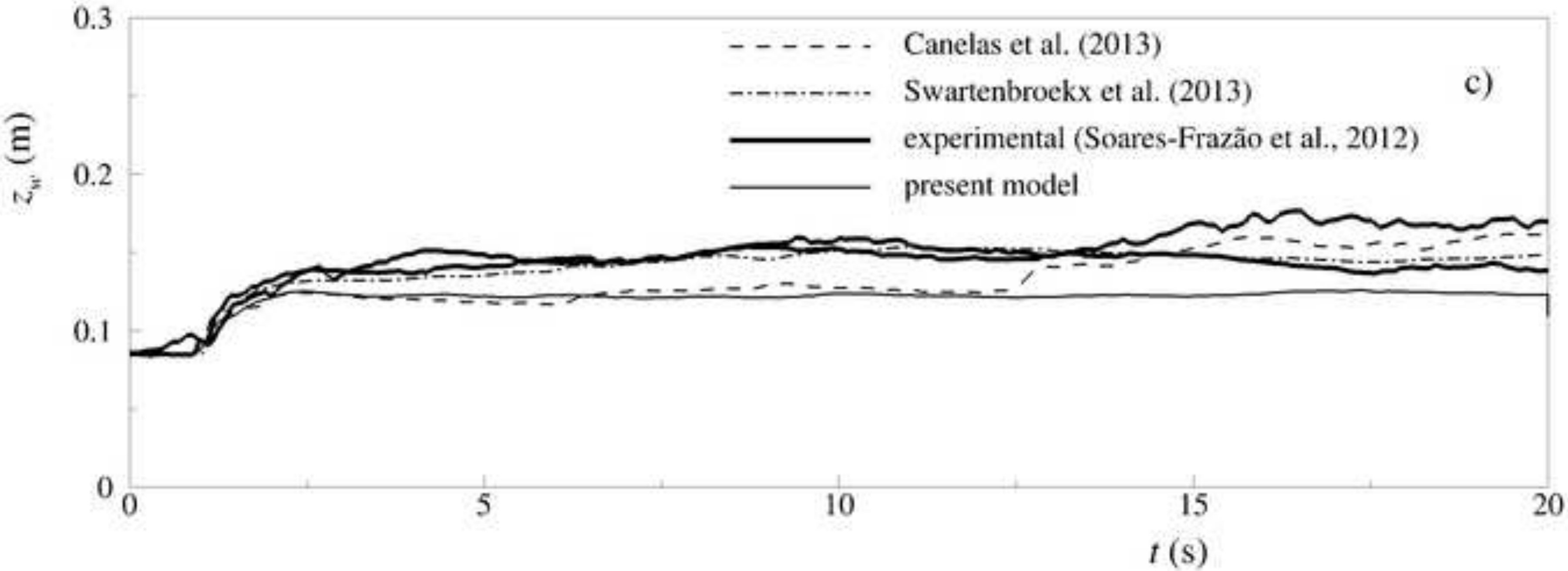

Figure
Click here to download high resolution image

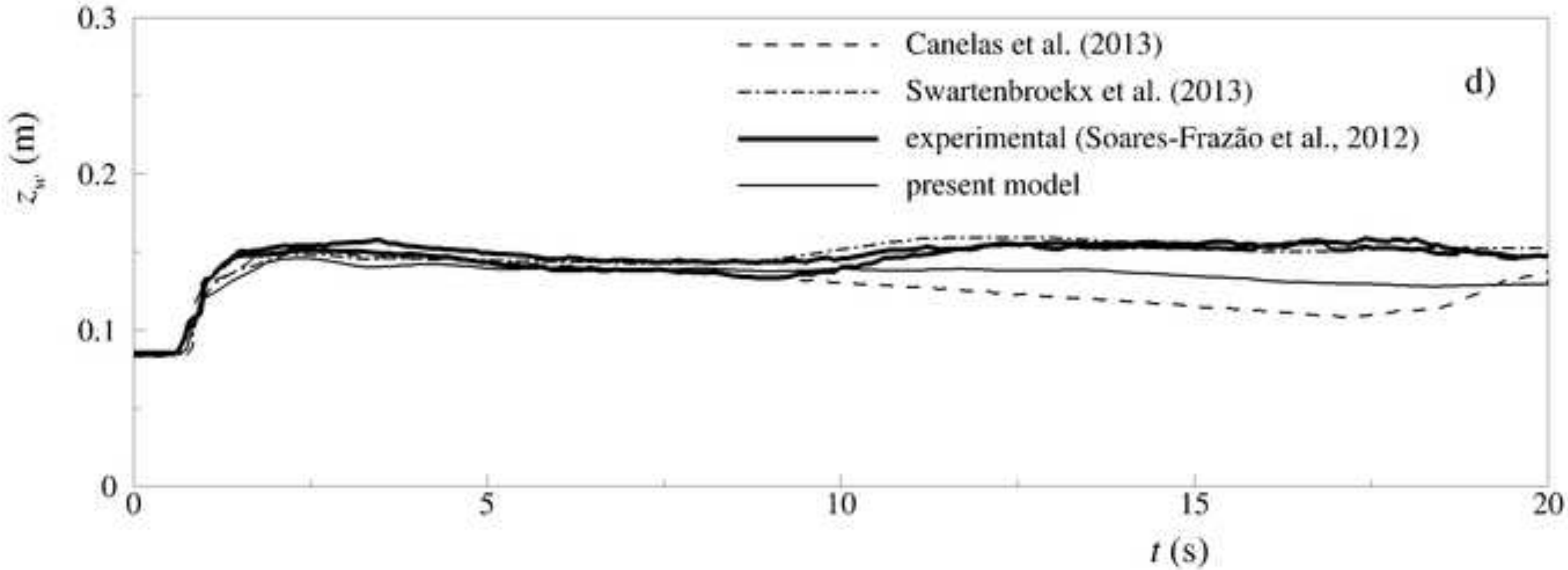

Figure
Click here to download high resolution image

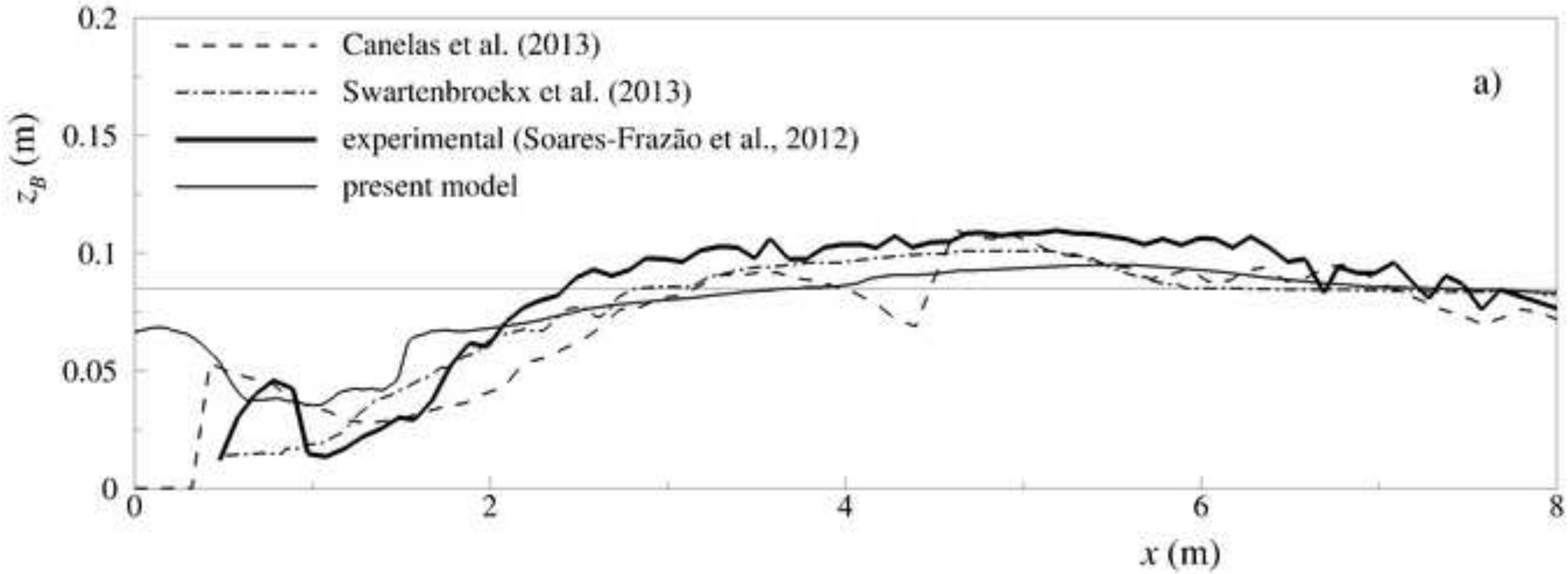

Figure
Click here to download high resolution image

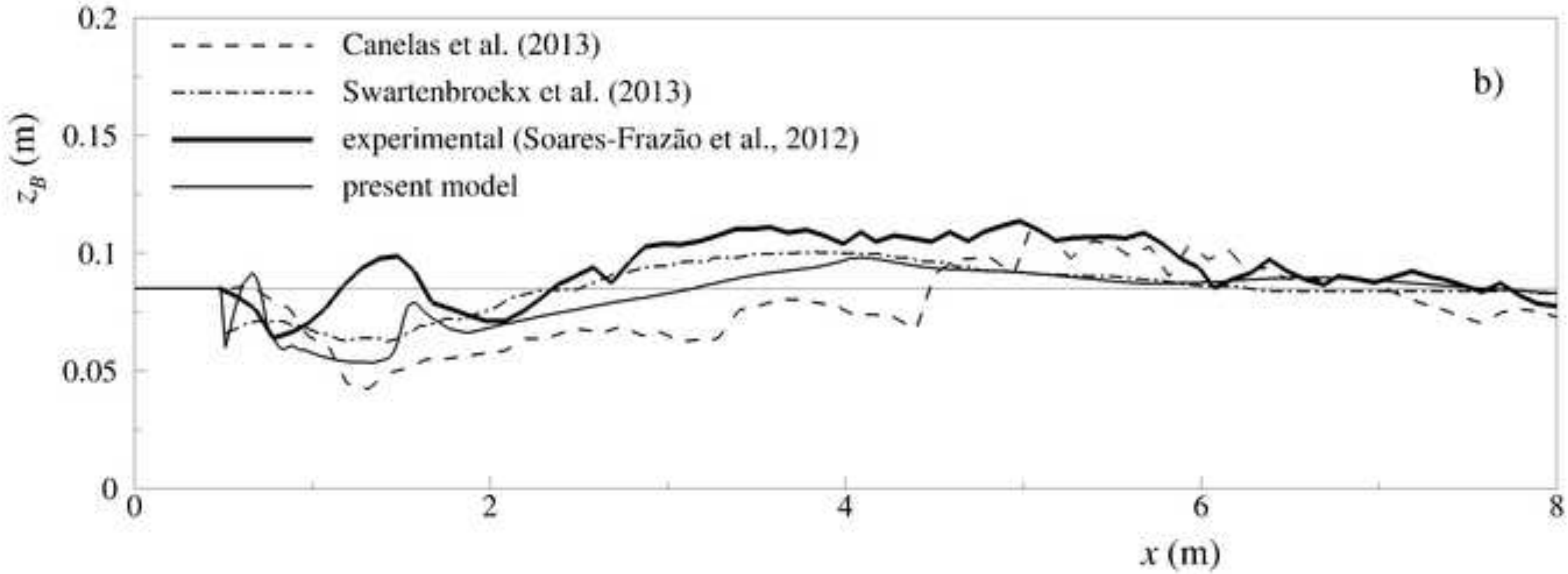

Figure
Click here to download high resolution image

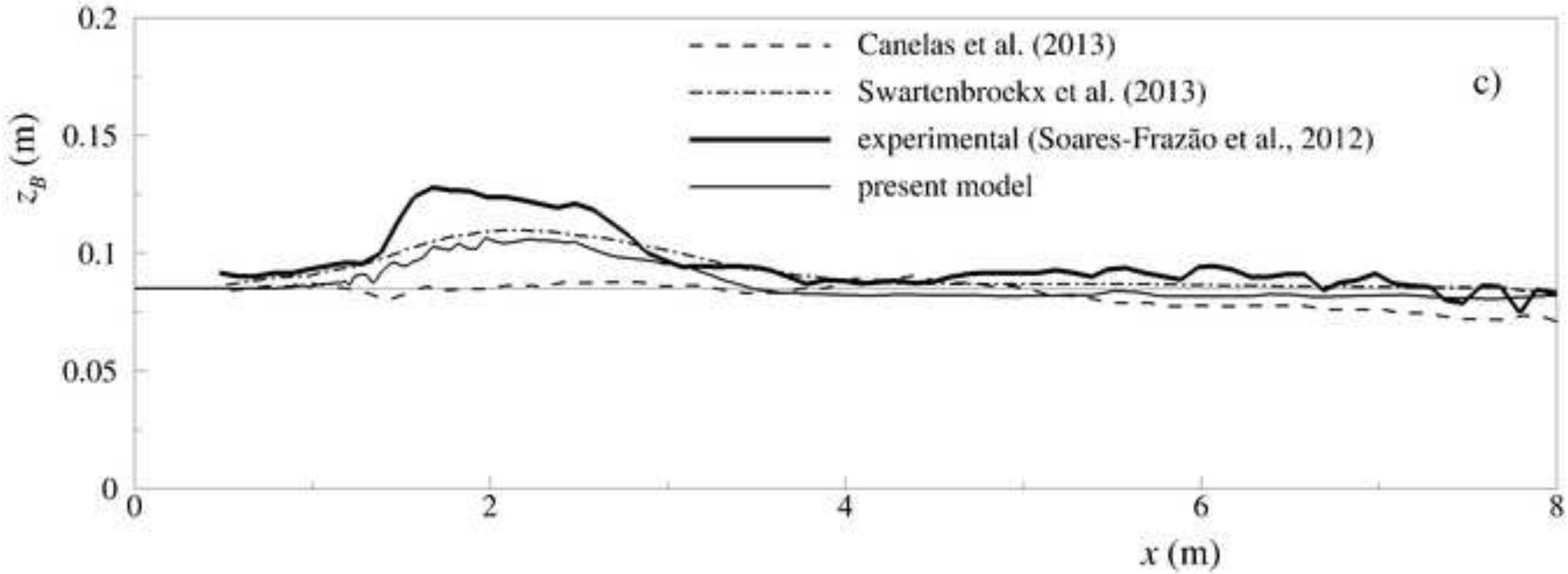

Figure
Click here to download high resolution image

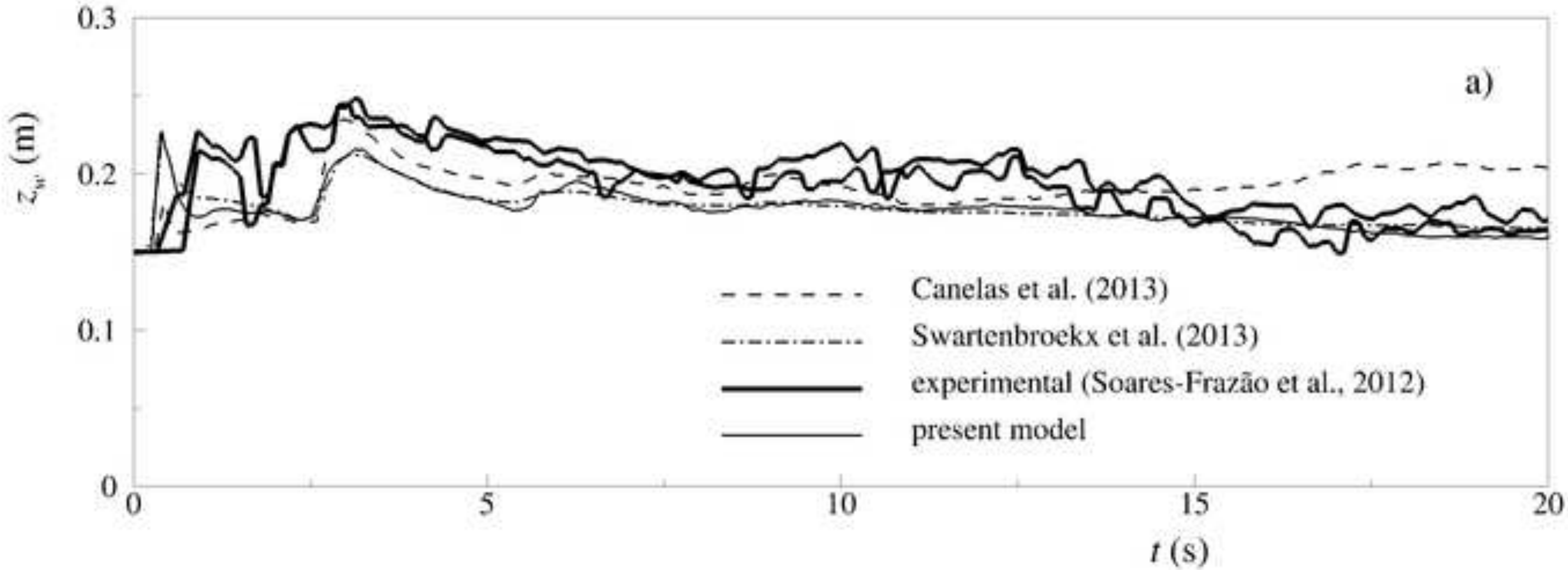

Figure
Click here to download high resolution image

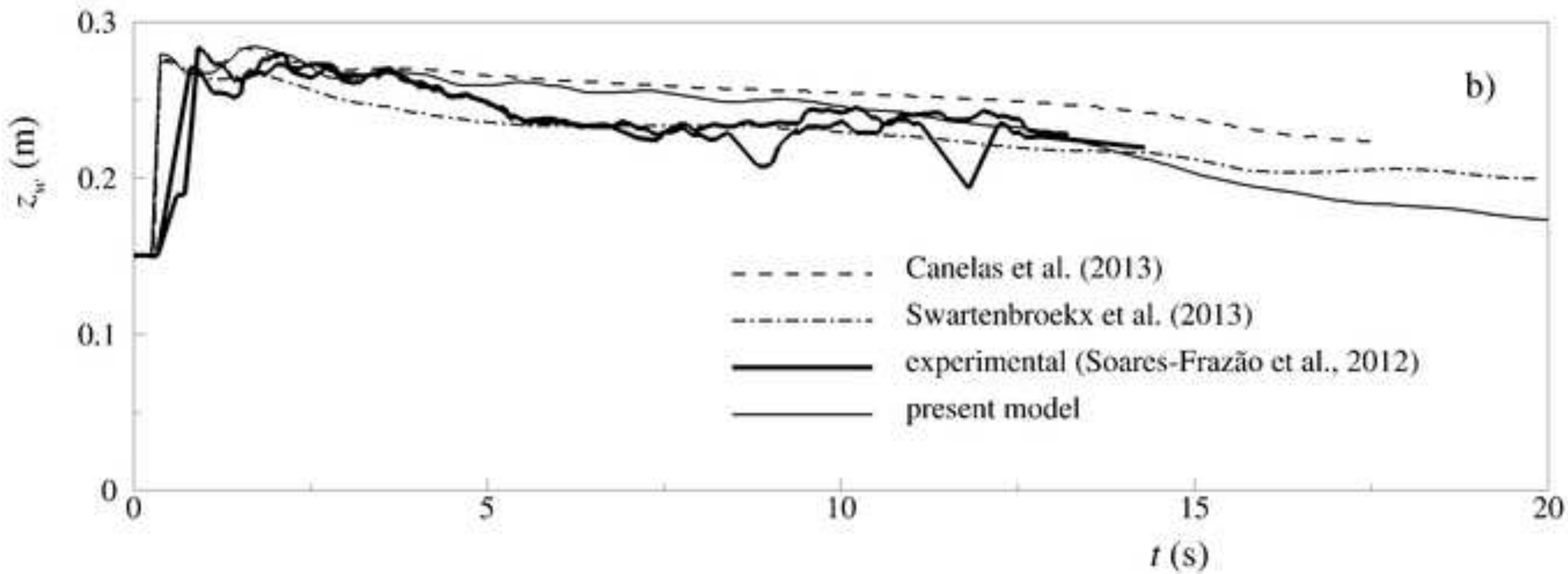

Figure
Click here to download high resolution image

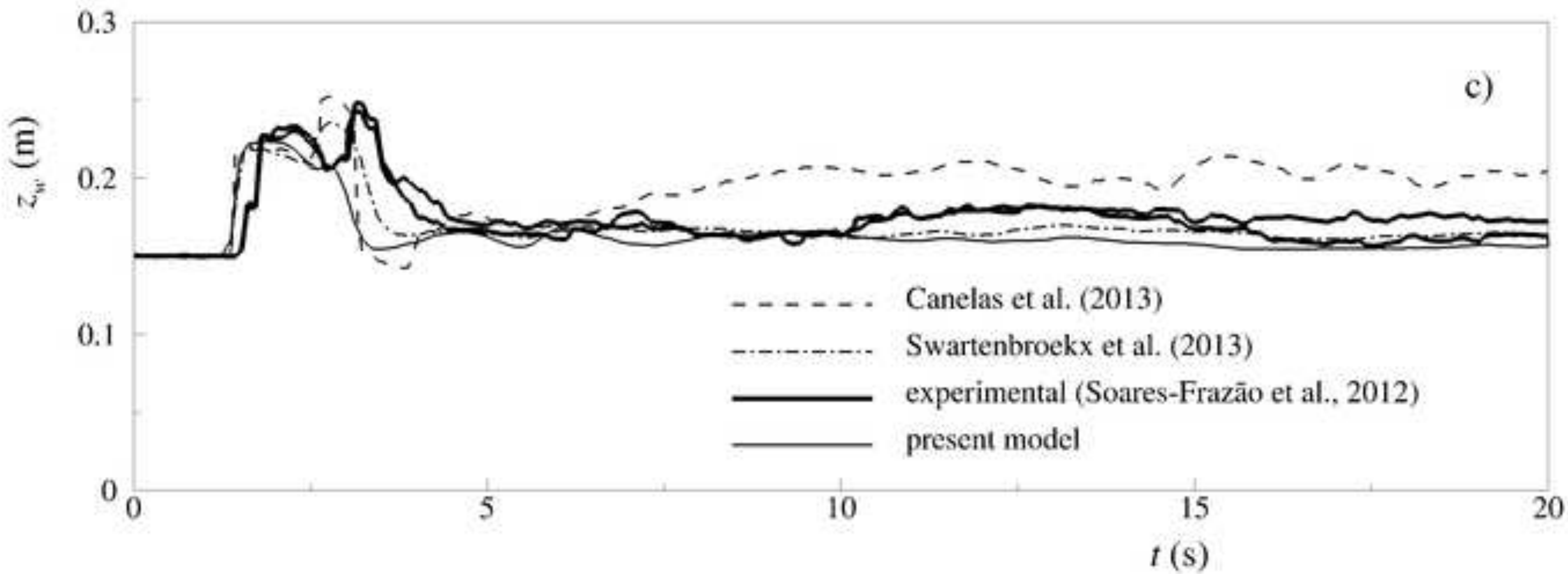

Figure
Click here to download high resolution image

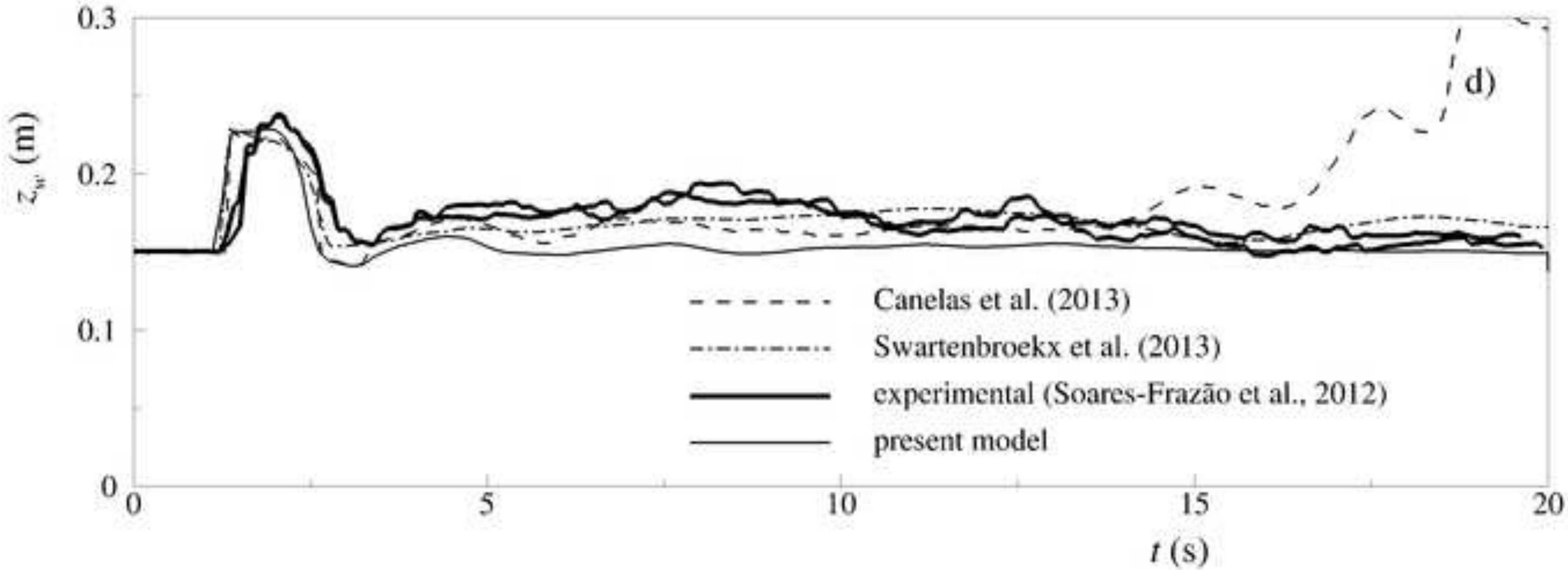

Figure
Click here to download high resolution image

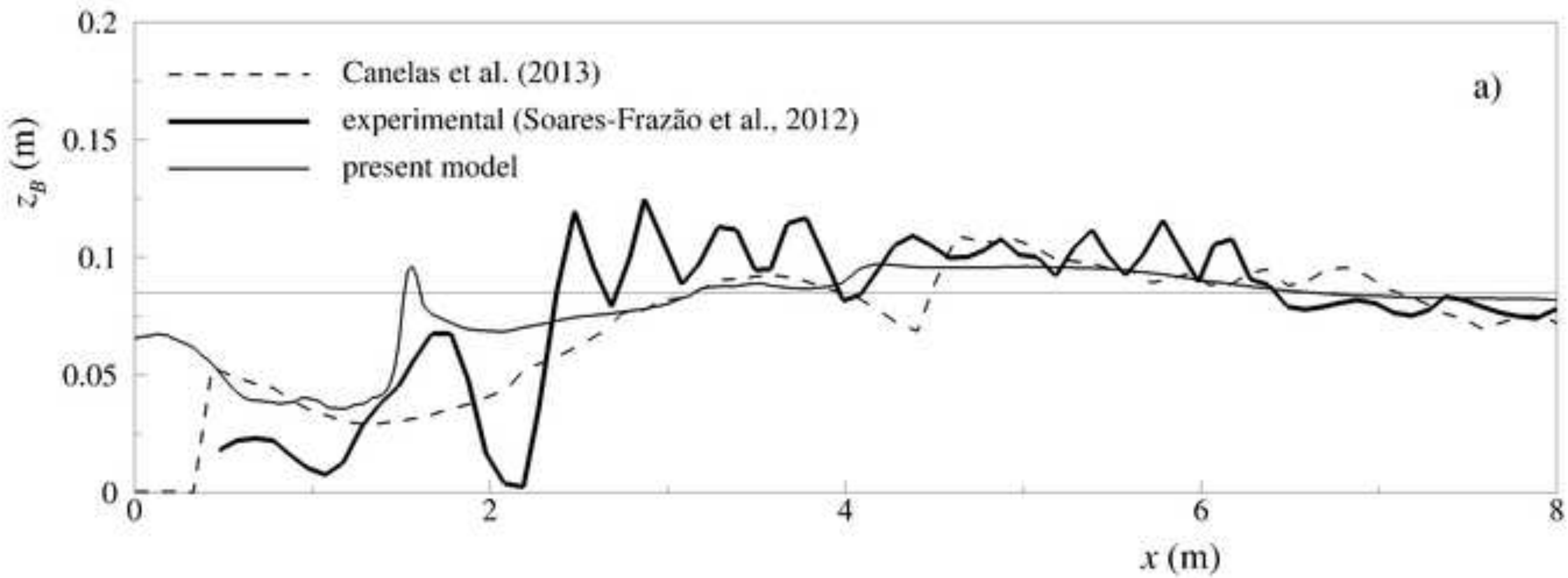

Figure

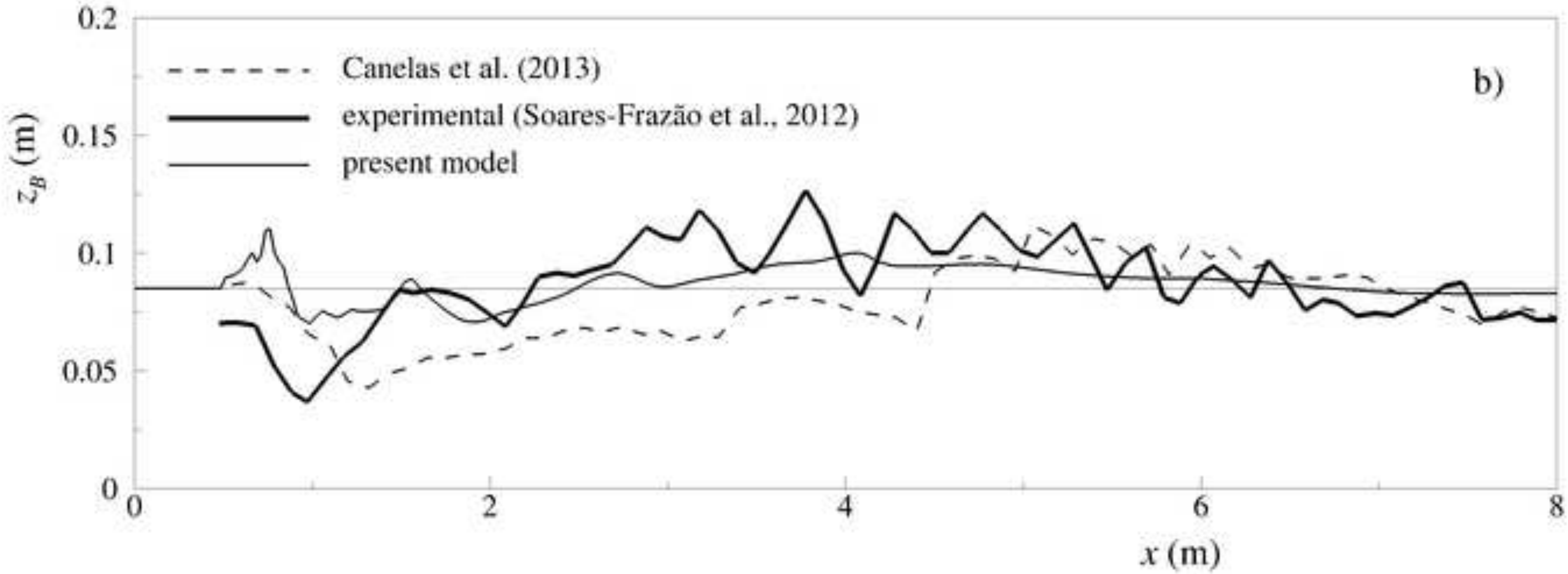

0.2
0.15
0.1
0.05
0
z_B (m)
Canelas et al. (2013)
experimental (Soares-Frazão et al., 2012)
present model
b)
0
2
4
6
8
x (m)

Figure
Click here to download high resolution image

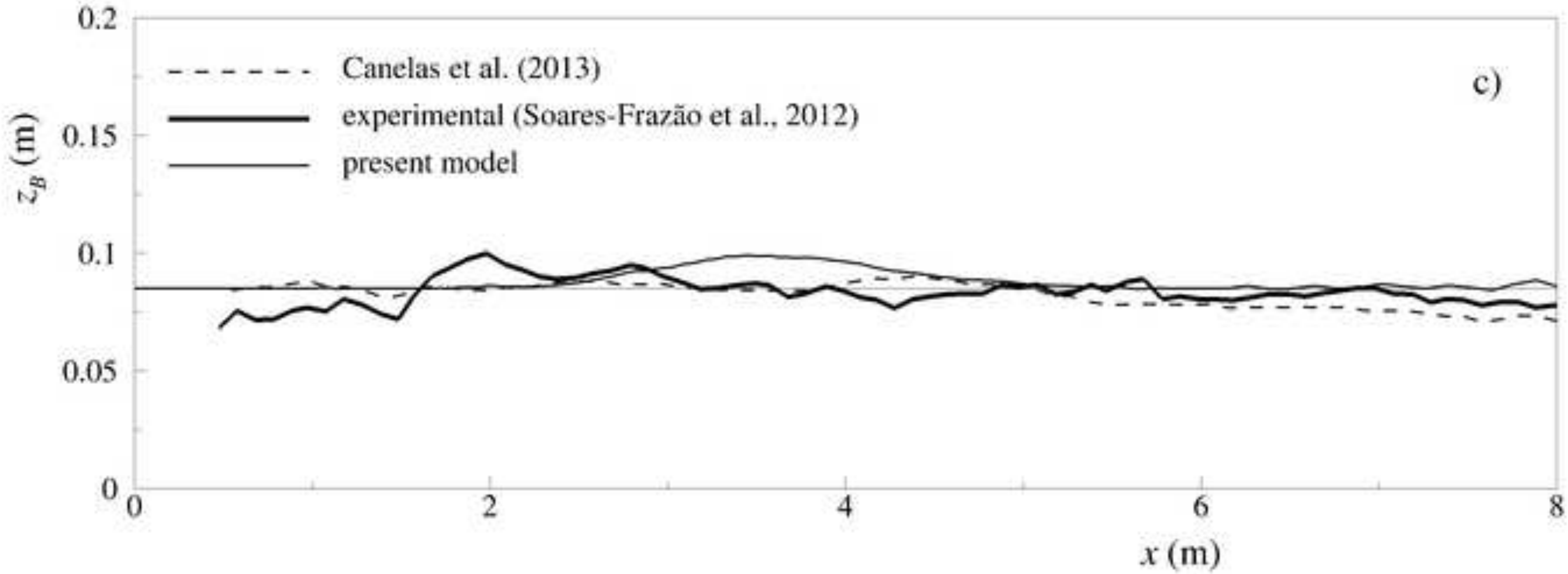

Figure Captions

Figure 1. Comparison between predictions by Eq. (35) and literature data: a) θ_c=0.03; b) θ_c=0.06

Figure 2. 1D Dry-bed test. Measured and computed free-surface and bottom profiles: a) *t*=0.4 s; b) *t*=0.5 s after dam removal

Figure 3. Space-time maps of a) suspended to total solid load ratio; b) bed load thickness to flow depth ratio

Figure 4. NSF-PIRE Benchmark. Scheme of the experimental setup (redrawn from Soares-Frazão et al., 2012)

Figure 5. 2D Dry-bed test. Measured and computed time series of free-surface elevation: a) gauges 1 and 4; b) gauges 2 and 3; c) gauges 5 and 8; d) gauges 6 and 7

Figure 6. 2D dry-bed test. Measured and simulated final bottom profiles: a) *y* = 0.2 m; b) *y* = 0.7 m; c) *y* = 1.45 m

Figure 7. 2D dry-bed test. Velocity vector plot: a) *t* = 2 s; b) *t* = 5 s; c) *t* =20 s after dam removal

Figure 8. 2D dry-bed test. Shields parameter distribution: a) *t* = 2 s; b) *t* = 5 s; c) *t* =20 s after dam removal

Figure 9. 2D dry-bed test. Bed load concentration distribution: a) *t* = 2 s; b) *t* = 5 s; c) *t* =20 s after dam removal

Figure 10. 2D wet-bed test. Measured and computed time series of free-surface elevation: a) gauges 1 and 4; b) gauges 2 and 3; c) gauges 5 and 8; d) gauges 6 and 7

Figure 11. 2D wet-bed test. Measured and simulated final bottom profiles: a) *y* = 0.2 m; b) *y* = 0.7 m; c) *y* = 1.45 m

Figure 12. 2D wet-bed test. Velocity vector plot: a) *t* = 2 s; b) *t* = 5 s; c) *t* =20 s after dam removal

Figure 13. 2D wet-bed test. Shields parameter distribution: a) *t* = 2 s; b) *t* = 5 s; c) *t* =20 s after dam removal

Figure 14. 2D wet-bed test. Bed load concentration distribution: a) *t* = 2 s; b) *t* = 5 s; c) *t* =20 s after dam removal

Figure 15. 1D Dry-bed test. Comparison with results from previous models: bottom and free surface profile: a) *t*=0.4 s; b) *t*=0.5 s after dam removal;

Figure 16. 2D dry-bed test. Time series of free-surface elevation compared with results from previous models: a) gauges 1 and 4; b) gauges 2 and 3; c) gauges 5 and 8; d) gauges 6 and 7

Figure 17. 2D dry-bed test. Final bottom profiles compared with results from previous models: a) *y* = 0.2 m; b) *y* = 0.7 m; c) *y* = 1.45 m

Figure 18. 2D wet-bed test. Time series of free-surface elevation compared with results from previous models: a) gauges 1 and 4; b) gauges 2 and 3; c) gauges 5 and 8; d) gauges 6 and 7

Figure 19. 2D wet-bed test. Final bottom profiles compared with results from previous models: a) *y* = 0.2 m; b) *y* = 0.7 m; c) *y* = 1.45 m

Copyright Agreement

Click here to download Copyright Agreement: journalscta_signed_MG.pdf

ASCE

COPYRIGHT TRANSFER AGREEMENT

Manuscript Number: HYENG-8852R3

Type: Technical Paper

Publication Title: A Two-Dimensional Two-Phase Depth-Integrated Model for Transients over Mobile Bed

Manuscript Authors: Cristiana Di Cristo; Massimo Greco; Michele Iervolino; Angelo Leopardi; Andrea Vacca

Corresponding Author Name and Address: Massimo Greco - Università di Napoli "Federico II" Dipartimento di Ingegneria civile, edile e ambientale - VIA CLAUDIO 21 80125 Napoli - ITALY

This form *must** be returned *with* your final manuscript to: American Society of Civil Engineers, *Journals Production Services Dept.*, 1801 Alexander Bell Drive, Reston, VA 20191-4400.

The author(s) warrant(s) that the above cited manuscript is the original work of the author(s) and has never been published in its present form.

The undersigned, with the consent of all authors, hereby transfers, to the extent that there is copyright to be transferred, the exclusive copyright interest in the above-cited manuscript (subsequently called the "work"), in this and all subsequent editions of this work, and in derivatives, translations, or ancillaries, in English and in foreign translations, in all formats and media of expression now known or later developed, including electronic, to the American Society of Civil Engineers subject to the following.

- The undersigned author and all coauthors retain the right to revise, adapt, prepare derivative works, present orally, or distribute the work provided that all such use is for the personal noncommercial benefit of the author(s) and is consistent with any prior contractual agreement between the undersigned and/or coauthors and their employer(s).

- In all instances where the work is prepared as a "work made for hire" for an employer, the employer(s) of the author(s) retain(s) the right to revise, adapt, prepare derivative works, publish, reprint, reproduce, and distribute the work provided that such use is for the promotion of its business enterprise and does not imply the endorsement of ASCE.

- No proprietary right other than copyright is claimed by ASCE.

- An author who is a U.S. Government employee and prepared the above-cited work does not own copyright in it. If at least one of the authors is not in this category, that author should sign below. If all the authors are in this category, check here ❑ and sign here: ______________________. Please return this form by mail.

SIGN HERE FOR COPYRIGHT TRANSFER [Individual Author or Employer's Authorized Agent (work made for hire)]

Print Author's Name: Massimo Greco   Signature of Author (in ink): Massimo Greco

Print Agent's Name and Title: Signature of Agency Rep (in ink):

Date: 21/01/2015

Note: If the manuscript is not accepted by ASCE or is withdrawn prior to acceptance by ASCE, this transfer will be null and void and the form will be returned to the author.

*Failure to return this form *will* result in the manuscript's not being published.

Editor in Chief

Thank you for submitting your revised article to the Journal of Hydraulic Engineering (JHE), ASCE. I have now received the Associate Editor's comments along with the reviews of your manuscript, which are attached/enclosed for your reference. I appreciate the effort by the reviewers and the AE handling this manuscript.

Please pay attention to the assessments of the reviewers and the Associate Editor. It is important that all the remarks of the referees are accounted for when revising the paper and/or discussed in your rebuttal document.

Based on these evaluations, I find that your manuscript may be suitable for publication after undergoing some revisions focused on the comments provided by the AE and reviewer #1.

I have reviewed myself the paper and I see an expansion of the current work in comparison to the River flow conference paper published in 2014, therefore there is not an issue there. In addition, the authors must provide a comparison between a single phase model and their model using a case example. Please remove unsubstantiated claims that may overstate the merit of the present model and modify the title per AE's recommendation.

We thank the Editor in Chief for having himself reviewed the manuscript and for having recognized its novelty respect to the paper presented at the River Flow 2014 conference.
Moreover, in this new re-revised version we have complied with all the further requests by the AE and the Reviewers, as specified in the following notes.
As requested the English writing has been thoroughly improved.

AE Report: This paper has been gone through three rounds of reviewing, but this revision is not yet good enough. Two reviewers have kindly reviewed it again, and given important comments.

I agrees with Reviewer 1 on that this paper still needs improvements. It is better to remove "with variable bed-load concentration" from the title.

Following the AE indication the title has been changed. The new title is “A Two-Dimensional Two-Phase Depth-Integrated Model for Transients over Mobile Bed”.

The authors should clearly state the advantages and disadvantages of the present model against the single-phase models. It seems that the present model's results are not significantly better than those of the single-phase models. The authors need to convince the readers what is the true value of the present model.

We agree with both the Reviewer 1 and the AE that in the previous version of the manuscript the comparison between the present model and the single phase ones was not deeply discussed. In order to comply with this request, a new sub-section “Comparison with literature models” has been included in the Results paragraph of the revised version. A detailed comparison between the present model and two literature single-phase ones has been carried out, in terms of numerical complexity, model parameters’ estimate and capability in reproducing experimental tests. In particular, for the one dimensional test-case, the comparison has been performed against the mixture single-phase model by Wu and Wang (2007), while the model by Canelas et al. (2013) has been considered for the two-dimensional test-cases. Moreover, for sake of completeness, in such a sub-section also two more complex models, i.e. the two-phase model of Greco et al. (2012a) and the two-layer one of Swartenbroekx et al. (2013), have been considered for the one-dimensional and the two-dimensional test cases, respectively.

I also support Reviewer 1's comment on the authors' claim that the present model relies on only one free parameter. This claim may overstate the merit of the present model. The authors should test the model in more cases and prove the choice and evaluation of this free parameter is not case dependent. A field test case is normally needed to support this kind of statement.

Following the AE request, a sensitivity analysis on the free parameter value has been carried out even for the two-dimensional dam-break test cases. Indeed, the results dependence on the free parameter value has been checked for three different test cases. Moreover, in the revised version of the manuscript the text has been changed in order to avoid any overestimation of the present model's merit.

Reviewer 2 questions what is difference between the present paper and that published in River Flow 2014. The authors have to clarify whether the present paper is original.

As recognized by the EC himself, the present manuscript represents a significant extension of the paper published in RF2014 proceedings. Therefore as suggested by EC this is not an issue.

Finally, I strongly suggest the authors find some help from an English writing expert to improve the article's writing.

English has been improved.

Reviewer #1: The manuscript has been modified, in response to the review comments.

We thank the reviewer for appreciating our efforts.

Yet I am not yet sufficiently convinced and thus recommend that a further revision be submitted.

[1] My major concern relates to the comparison between the present two-phase model and a traditional single-phase model (e.g., Wu and Wang 2007). As I stated last time, detailed mechanisms can be incorporated in two-phase models than in single-phase models. But more parameters are involved in two-phase models, and the computational costs are much higher (if not doubled). I have suggested that a comparison between the present two-phase model and a typical single-phase model are included (listing the parameters, computational costs and the deviations of the modeling results from observed data), so that the readers and end-users of the models are clear about the advantages and disadvantages. Unfortunately, the authors' reply is far from adequate.

We apologize with the reviewer if we did not fully comply with his suggestion in the last review round. In order to comply in a more adequate manner his request, the new sub-section "Comparison with literature models" has been included in the revised version of the manuscript. In particular, a detailed comparison between the present model and the single phase models by Wu and Wang

(2007) and by Canelas et al. (2013) has been performed, in terms of numerical complexity, model parameters' estimate and capability in reproducing experimental tests.

Especially, in this connection, the authors claim that with only a single free parameter c1, the model leads to agreement with observed data (Figs 2 c, d) and the effects of the free parameter c1 on the results are limited. This gives the impression that the present model is almost universally applicable. I am so concerned with this point.

The revised version of the manuscript has been changed in order to avoid such an impression. However, prompted by the reviewer suggestion we have performed a sensitivity analysis of the results on the c1 parameter even for the two-dimensional dam-break cases. The results are included in the revised version. Actually, in all the three test cases presented in the manuscript the sensitivity of the results to c1 has been found to be modest. Of course, it is not guaranteed that this result is valid in all the possible situations, so, in agreement with the reviewer, we have modified the conclusion to avoid the impression of an "universally applicable" model.

[2] Once again, it is not justified to flag out the "variable bed-load concentration" in the title. It is has been widely recognized that sediment concentration is certainly variable in time and space, and actually this is fully incorporated in most single-phase models. To me, the words "with variable bed-load concentration" can be deleted in the title.

Following the Reviewer and AE indication the title has been changed. The new title is "A Two-Dimensional Two-Phase Depth-Integrated Model for Transients over Mobile Bed".

[3] The English language usage throughout the manuscript needs to be greatly improved. At the best, a native speaker is invited to make it.

English has been improved.

Given the above, a further revision is necessary before it could be accepted to publication in JHE.

We are confident that the revised version of the manuscript will comply with all the reviewer requests.

Reviewer 2:

The revised manuscript addresses my comments.

We thank the reviewer for appreciating our efforts.

However, I still don't believe that the model has been well calibrated and tested (especially in comparison to the original model of Greco et al., 2012).

We partially disagree with the reviewer. The proposed model has been tested against three different experiments, similarly to Greco et al. (2012). For each of them, in the revised version of the manuscript, the influence on the results quality of the c_1 parameter has been thoroughly investigated. Moreover, the comparison with the Greco et al. (2012) model has been discussed in revised version in terms of numerical complexity, model parameters' estimate and capability in reproducing experimental tests.

Moreover, shown in the attached file, the present model and some of the results have been recently published in a book (proceedings of the River Flow 2014, Taylor and Francis Group). Thus, the Journal of Hydraulic Engineering may not consider the article as an original and new contribution that advances knowledge in hydraulic engineering.

As recognized by the EC himself, the submitted manuscript represents a significant extension of the paper published in the River Flow 2014 proceedings. The number of differences is witnessed by the length of the manuscript, which is at least three times larger than that of the River Flow 2014 paper. However, prompted by the reviewer suggestion, the River Flow 2014 paper has been cited, as a preliminary study.